EVALUATION OF CHERT PATINATION AS A DATING TECHNIQUE: A CASE STUDY FROM FORT HOOD, TEXAS

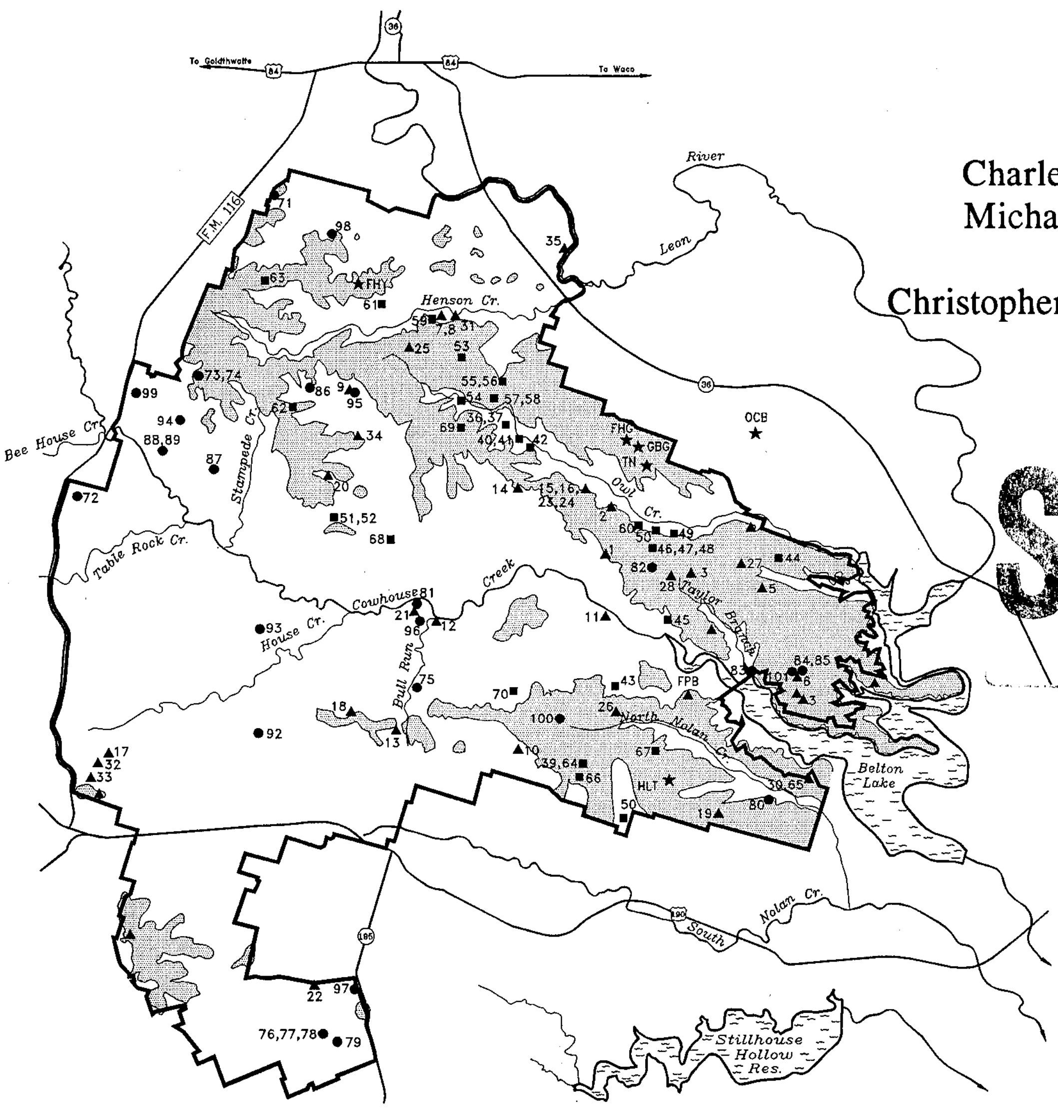

by

Charles D. Frederick
Michael D. Glascock
Hector Neff
Christopher M. Stevenson

UNITED STATES ARMY FORT HOOD
ARCHEOLOGICAL RESOURCE MANAGEMENT SERIES
RESEARCH REPORT NO. 32

1994

EVALUATION OF CHERT PATINATION AS A DATING TECHNIQUE: A CASE STUDY FROM FORT HOOD, TEXAS

by

Charles D. Frederick
Michael D. Glasscock
Hector Neff
Christopher M. Stevenson

UNITED STATES ARMY FORT HOOD
ARCHEOLOGICAL RESOURCE MANAGEMENT SERIES
RESEARCH REPORT NO. 32

1994

EVALUATION OF CHERT PATINATION AS A DATING TECHNIQUE: A CASE STUDY FROM FORT HOOD, TEXAS

prepared for

Directorate of Engineering and Housing
Environmental Management Office
Fort Hood

by

MARIAH ASSOCIATES, INC.
Austin, Texas

in partial fulfillment of
Contract DAKF48-91-D-0058
Delivery Order #16

October 1994

unclassified
SECURITY CLASSIFICATION OF THIS PAGE

REPORT DOCUMENTATION PAGE

Form Approved OMB No. 0704-0188

1a. REPORT SECURITY CLASSIFICATION Unclassified	1b. RESTRICTIVE MARKINGS none
2a. SECURITY CLASSIFICATION AUTHORITY n/a	3. DISTRIBUTION/AVAILABILITY OF REPORT Public Access Unlimited Distribution
2b. DECLASSIFICATION/DOWNGRADING SCHEDULE n/a	
4. PERFORMING ORGANIZATION REPORT NUMBER(S) 662-16	5. MONITORING ORGANIZATION REPORT NUMBER(S) n/a
6a. NAME OF PERFORMING ORGANIZATION Mariah Associates, Inc. 6b. OFFICE SYMBOL *(If applicable)* Austin, Texas	7a. NAME OF MONITORING ORGANIZATION Department of the Army - Fort Hood Directorate of Engineering and Housing
6c. ADDRESS *(City, State, and ZIP Code)* 3939 Bee Caves Road, Suite C-100, Austin TX 78746	7b. ADDRESS *(City, State, and ZIP Code)* Environmental Management Office, Bldg. 4468 Fort Hood, Texas, 77594
8a. NAME OF FUNDING/SPONSORING ORGANIZATION Department of the Army - Fort Hood Directorate of Engineering and Housing 6b. OFFICE SYMBOL *(If applicable)*	9. PROCUREMENT INSTRUMENT IDENTIFICATION NUMBER DAKF48-91-D-0058; Delivery Order Number 16
8c. ADDRESS *(City, State, and ZIP Code)* Environmental Management Office, Bldg. 4468 Fort Hood, Texas, 77594	10. SOURCE OF FUNDING NUMBERS PROGRAM ELEMENT NO. / PROJECT NO. / TASK NO. / WORK UNIT ACCESSION NO.

11. TITLE *(Include Security Classification)*
Evaluation of Chert Patination as a Dating Technique: A Case Study from Fort Hood, Texas

12. PERSONAL AUTHOR(S)
Charles D. Frederick, Michael D. Glasscock, Hector Neff, and Christopher M. Stevenson

13a. TYPE OF REPORT	13b. TIME COVERED	14. DATE OF REPORT *(Year, Month, Day)*	15. PAGE COUNT
Final	From 92 Sep to 94 Oct	1994 October	44 + appendices

16. SUPPLEMENTARY NOTATION
none

17. COSATI CODES			18. SUBJECT TERMS *(Continue on reverse if necessary and identify by block number)*
FIELD	GROUP	SUB-GROUP	archeology, Fort Hood, Texas, Edwards chert, patination, neutron activation analysis, ultraviolet flourescence, petrography, chronometry

19. ABSTRACT *(Continue on reverse if necessary and identify by block number)*
This paper reports the results of a controlled study of chert weathering at Fort Hood, Texas. Petrographic examination and measurement of the white patina associated with 105 archaeological artifacts from three temporal groups forms the basis for evaluating the rate and extent of chert patination in the upland environments of the Edwards Plateau, Central Texas. Artifacts of Late Prehistoric, Archaic, and Paleoindian age recovered from stable upland environments were examined. Controls for artifact age, burial history, edaphic environment, and parent material composition were involved in the selection and evaluation process. The florescence response to short and long wave ultraviolet radiation of all 105 artifacts and representative specimens of all currently known varieties of Edwards Group Chert cropping out at Fort Hood were observed and regarded by those most familiar with the method. All but one was found to be consistent with the known response of Edwards material. Instrumental

20. DISTRIBUTION/AVAILABILITY OF ABSTRACT [X] UNCLASSIFIED/UNLIMITED [ ] SAME AS RPT. [ ] DTIC USERS	21. ABSTRACT SECURITY CLASSIFICATION n/a
22a. NAME OF RESPONSIBLE INDIVIDUAL Jack M. Jackson	22b. TELEPHONE *(Include Area Code)* (817) 287-7965 22c. OFFICE SYMBOL AFZF-DE-ENV

unclassified
SECURITY CLASSIFICATION OF THIS PAGE

Neutron Activation Analysis was used to chemically characterize 121 samples of raw chert taken from six known bedrock sources at Fort Hood, and the population of 105 artifacts was subsequently compared to this source data and membership probabilities calculated. The results of this work suggest that the artifact population is relatively homogeneous but that the chemical fingerprint for Edwards Group chert is currently inadequate. Petrographic examination and analysis of the patina measurements demonstrates that patination (the formation of a pseudo-isotropic patina) is a progressive process in both frequency and magnitude and that artifacts assigned to different temporal groups on the basis of morphology exhibit significantly different degrees of patination. However, the use of chert patination as a dating technique or to distinguish temporally different debitage/artifact groups from mixed age assemblages will incur significant errors, especially with respect to unpatinated specimens. Hence, the prospects of using chert patination as a dating method are poor.

ABSTRACT

This paper reports the results of a controlled study of chert weathering at Fort Hood, Texas. Petrographic examination and measurement of the white patina associated with 105 archaeological artifacts from three temporal groups forms the basis for evaluating the rate and extent of chert patination in the upland environments of the Edwards Plateau, Central Texas. Artifacts of Late Prehistoric, Archaic, and Paleoindian age recovered from stable upland environments were examined. Controls for artifact age, burial history, edaphic environment, and parent material composition were involved in the selection and evaluation process. The florescence response to short and long wave ultraviolet radiation of all 105 artifacts and representative specimens of all currently known varieties of Edwards Group Chert cropping out at Fort Hood were observed and regarded by those most familiar with the method. All but one was found to be consistent with the known response of Edwards material. Instrumental Neutron Activation Analysis was used to chemically characterize 121 samples of raw chert taken from six known bedrock sources at Fort Hood, and the population of 105 artifacts was subsequently compared to this source data and membership probabilities calculated. The results of this work suggest that the artifact population is relatively homogeneous but that the chemical fingerprint for Edwards Group chert is currently inadequate. Petrographic examination and analysis of the patina measurements demonstrates that patination (the formation of a pseudo-isotropic patina) is a progressive process in both frequency and magnitude and that artifacts assigned to different temporal groups on the basis of morphology exhibit significantly different degrees of patination. However, the use of chert patination as a dating technique or to distinguish temporally different debitage/artifact groups from mixed age assemblages will incur significant errors, especially with respect to unpatinated specimens. Hence, the prospects of using chert patination as a dating method are poor.

ACKNOWLEDGEMENTS

This study was funded by the U.S. Army, Fort Hood, contract DAKF-48-91-D-0058. We would like to thank Dr. Jack Jackson and Dr. Kimball Smith for access to the Fort Hood collections and for the opportunity and encouragement they provided throughout the duration of this study. Elton Prewitt and Dr. Thomas Hester kindly agreed to examine and type the projectile points used in the study. J. Michael Quigg assisted in the selection and supervised documentation of the artifacts and actively participated in the design of the research program in its early stages. G. Lain Ellis designed and constructed a photo stand and subsequently produced professional quality photographs of each artifact. Lain also served as a dynamic sounding board and advisor during the data analysis stage of this project.

The projectile points were expertly illustrated by Carol Mills and Mike Hilton provided the CAD maps and figures. The study was coordinated with Fort Hood and Mariah by Principal Investigator Dr. Nicholas Trierweiler. Technical editor was Dee Ann Campbell and document production was conducted by debora White.

Dr. Chris Stevenson of Archaeological Services Consultants, Inc. made the thin sections, measured the patina rinds, and willingly and rapidly addressed numerous queries regarding various aspects of the data. Pam Headrick, Marilyn Masson, and Susan Dial examined the UVF response of the 105 artifacts, and together with Dr. Michael B. Collins, openly discussed the relative merits of this technique. Neutron Activation Analysis (NAA) was carried out by Dr. Michael Glascock and Dr. Hector Neff at The Research Reactor Center, University of Missouri with the assistance of Donna M. Glowacki (Graduate Research Assistant) and Sindy J. Hays (Sr. Research Laboratory Technician) who prepared the samples and performed much of the NAA work on these samples. The principal author bears responsibility for any errors of interpretation.

TABLE OF CONTENTS

APPENDICES

LIST OF FIGURES

LIST OF TABLES

1.0 INTRODUCTION

Between August 1991 and June 1993 Mariah Associates, Inc. (Mariah) conducted field work on 571 prehistoric sites at Fort Hood in Bell and Coryell counties, Texas. The primary goal of the work was to evaluate each site with respect to its eligibility for inclusion in the National Register of Historic Places (NRHP). The work was conducted as one component of Fort Hood's ongoing program to comply with provisions of the National Historic Preservation Act and its implementing regulations, as clarified in a Programmatic Agreement (PA) signed in January 1990 between the United States Army, the State Historic Preservation Officer (SHPO) for Texas, and the Advisory Council for Historic Preservation, and as implemented in the current Historic Preservation Plan (HPP) for Fort Hood.

Concurrent with the program of site assessment, Mariah was authorized to conduct several archaeological research studies at Fort Hood. These studies were carefully designed to facilitate and enhance the ability of Fort Hood to make meaningful and cost-effective NRHP eligibility determinations during the next phase of implementing the HPP. Three of these studies have been previously reported (Trierweiler 1994) and are: (1) a review and analysis of the spatial distribution of Edwards chert throughout Central Texas and an assessment of variability in its appearance and composition; (2) an investigation of the potential of land snail shells to assist in site dating and site formation studies; and (3) an investigation of the structural and chronometric variability of burned rock mound features at Fort Hood.

The current study presents the results of an experiment evaluating the dating potential of chert patination for lithic artifacts found on upland surfaces of the Edwards Plateau. Lithic scatters are one of the most ubiquitous types of archaeological sites in settings such as these at Fort Hood, which lies at the eastern edge of the outcrop of the Edwards Group (Figure 1.1).

The Edwards Group comprises one of the largest chert resources on the Great Plains (Frederick and Ringstaff 1994) and expansive outcrops of Edwards Group chert are often accompanied by extensive lithic scatters created during prehistoric raw material procurement. In the absence of aggrading depositional environments which may preserve temporally discrete occupations, lithic procurement sites are problematic cultural resources because dating any observed event or artifact assemblage is impossible in the absence of temporally diagnostic artifacts.

The utility of chert patination as a dating technique has been frequently debated but inadequately tested. However, if chert patination is found to be relatively consistent within a given region, then it may offer a solution to analyzing unsealed archaeological sites associated with lithic procurement activities. Although previous process-based research has indicated that chert patination may be of little use as a dating technique, repeated observation of artifact collections by archaeologists have drawn attention to the apparently progressive nature of patination and suggested that this should be of some utility in evaluating the age of lithic assemblages. No direct, systematic examination of a temporally separated assemblage has been attempted previously.

In this study we examine the rate of chert patination for artifacts collected from stable upland surfaces at Fort Hood, Texas. Direct measurement of the patina on temporally diagnostic artifacts representing three general time periods form the basis for our observations of the extent of chert patination as a function of time.

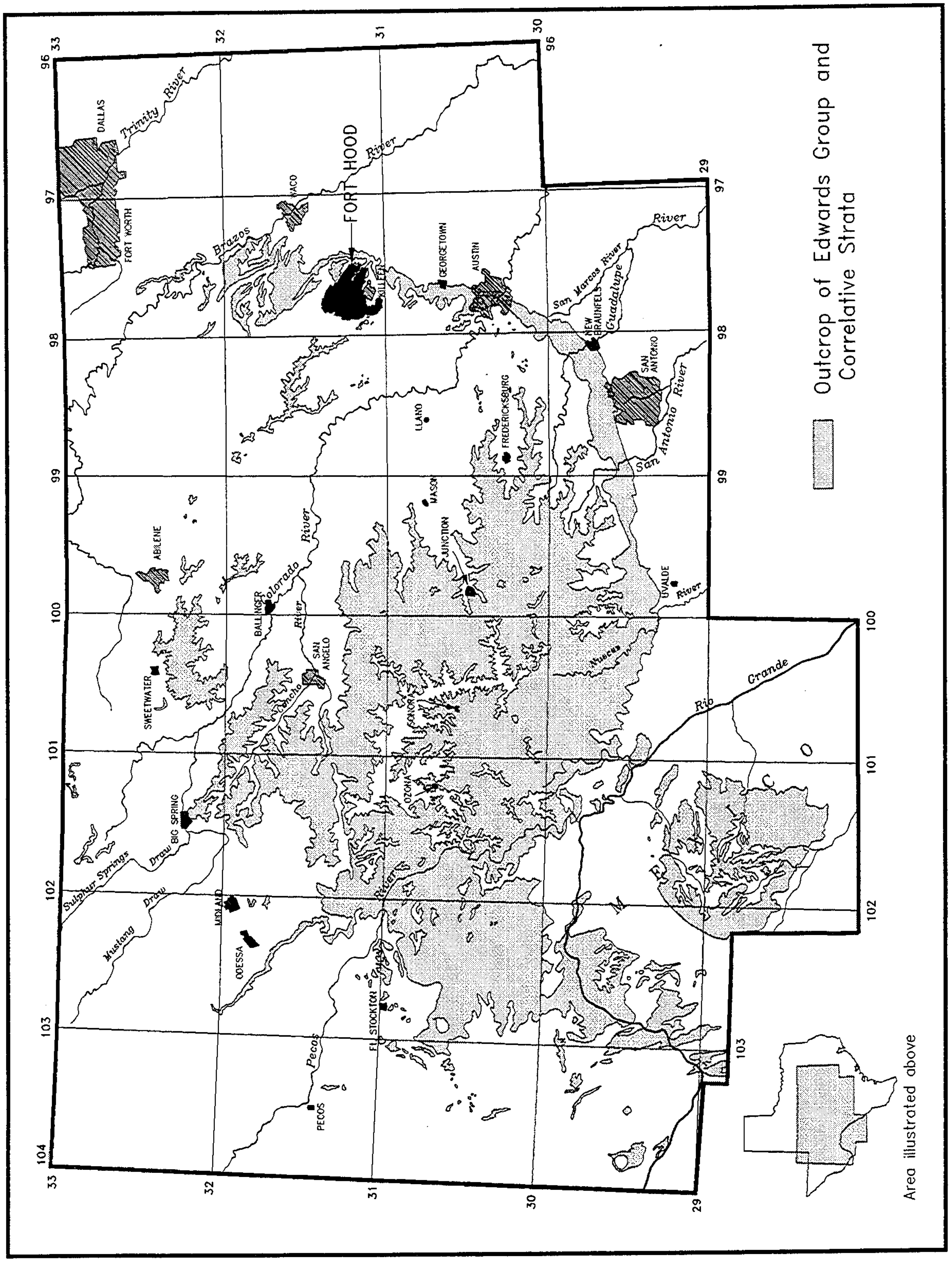

Figure 1.1 Map of Edwards Outcrop, Showing Fort Hood.

Attempts to control for factors that may introduce variability into the rate of patination, such as burial history, parent material composition, and edaphic conditions, have been taken into consideration and evaluated as potentially influential in the patination process. The results are interpreted in terms of the future of patination as a dating technique, especially for unsealed lithic scatters such as those that are common components of the Fort Hood archaeological inventory.

2.0 PREVIOUS RESEARCH ON PATINATION

The weathering of cryptocrystalline silicate artifacts has long captured the attention of archaeologists but unfortunately, a wide variety of different phenomena have been included under the term "patina" (Purdy and Clark 1987; Service 1941; Judd 1887). Some of these phenomena are now known to be the result of additive processes which causes a compound to accumulate on the outside of an artifact or to be incorporated into the structure of the raw material (e.g. desert varnish or mineral crusts). Other phenomena are subtractive processes which result in the net removal of material from the artifact (e.g. white patina). The term patina may have originally referred to tarnish, but has since come to be used as a general term for a light colored weathering rind (Purdy and Clark 1987). Three types of patina are widely discussed in the patination literature: white, brown, and glossy.

Previously, most attention has been devoted to white patinas, whereas the other two classes are less well understood. White patinas, as the name implies, are bluish white, white or light gray in color, often have a splotchy or mottled appearance, and are, in general, are less transparent and generally of a lighter color than the core of the artifact (VanNest 1985; Schmalz 1960; Hurst and Kelly 1961). In thin section, white patinas may be white or pale brown and often appear to be composed of a "very finely dispersed isotropic mineral" under plane polarized light (VanNest 1985), a phenomenon known as pseudo-isotropism (Schmalz 1960; VanNest 1985). A common characteristic of pseudo-isotropic patinas is that, upon addition of an immersion oil with an index of refraction similar to quartz ($n=1.550$), the patina becomes virtually indistinguishable from the unaltered core. White patinas are widely accepted to be the product of selective leaching and result from the scattering of light in the leached areas where there is an increased number of reflective surfaces in the form of grain boundaries and etching pits (Judd 1887; Curwen 1940; Goodwin 1960; Hurst and Kelly 1961; VanNest 1985; Purdy and Clark 1987). The specifics of this process are frequently debated and are still not resolved, but the subtractive nature is widely accepted. Both basic and acidic solutions are known to cause this type of patination in laboratory experiments (Rottländer 1975a; Schmalz 1960).

Brown or dark patinas are weathering rinds that form near the surface of an artifact that are "some shade of brown darker than the core" (Hurst and Kelly 1961) in hand specimen and may also exhibit pseudo-isotropism (Schmalz 1960). This type of patina is not very well understood. Purdy and Clark (1987:229) describe the occurrence of brown patinas that increase in extent with increasing age for artifacts derived from the Santa Fe River and conclude that this form of patina is an additive process and owes to staining by iron oxides (e.g. goethite, hematite, and limonite) and oxides of manganese. Conversely, Rottländer (1975b) has noted that brown patinas are not indicative of an iron concentration near the artifact surface, but rather the result of iron oxidation in this location. Alternatively, others believe brown patinas to be white patinas which have been stained brown with either humic or ferrous compounds (Leudtke 1992:109). Unfortunately, the supporting data for each of the hypotheses is lacking. Therefore, at this point in time, it is not clear if brown patinas are the result of an additive process, a subtractive process, an in situ chemical change such as oxidation, or a combination of these.

Glossy patina is a term applied to artifacts exhibiting an extreme surface luster and has been described as glossy and fully transparent (Rottländer 1975b). Given that some cryptocrystalline silicates have significant lusters prior to patination, the actual occurrence of this type of patination is probably underreported. It is most easily observed by comparing the luster of

newly fractured surfaces with those believed to exhibit a glossy patina. Few studies have examined this type of patina, which is presently believed to be a byproduct of dissolution. Rottländer (1975b:109) has argued that glossy patina forms from the preferential dissolution of crystal edges and corners and the concomitant deposition of silica in fissures that together reduce the effectiveness of the solution process and result in a surface that appears similar to one that has been mechanically polished.

In this paper, the term "patina" refers to the weathering rind visible in petrographic thin sections under transmitted plane-polarized light as a brown, finely dispersed isotropic mineral and identical to that described by (VanNest 1985:331). In general, this type of patina appears white or light gray to the unaided eye and is synonymous with white patina. However, if an artifact exhibited a definable pseudo-isotropic weathering rind, it was measured regardless of the appearance of the patina in hand specimen.

Factors believed to be influential in the patination process have been succinctly summarized by VanNest (1985:328) and may be separated into environmental variables and various attributes of the parent material. Ambient environmental factors include: (1) edaphic conditions such as soil pH, chemistry, permeability, amount and rate of subsurface water exposure, the size of the ions in solution, the presence of alkaline salts and organic acids, temperature (especially cycling across the freezing point) and exposure to ultraviolet and infrared radiation; and (2) very localized conditions restricted to specific artifacts such as lichen growth or intentional patination by cultural placement in springs known to produce accelerated patination (Benedict 1992). Parent material characteristics that may affect patination include mineralogy (composition), structure, porosity, permeability, thermal alteration, and the quantity and type of nonsilica impurities (VanNest 1985:328; Purdy and Clark 1979).

2.1 UTILITY OF PATINATION AS A DATING TOOL

The literature regarding the efficacy of patination as a dating tool is divided, in part the result of very different perspectives of the phenomenon. Repeated observations by archaeologists working with artifact collections has led many to believe that chert patination is indeed progressive and of considerable promise as a dating method. Some of the most directed research on patination has been associated with artifacts made from Knife River Flint (see VanNest 1985 for complete discussion). These studies suggest that: (1) factors other than time influence patination; (2) artifacts exposed on the ground surface may patinate more quickly than buried artifacts; (3) patination may occur in subsurface as well as above ground; (4) moderately to heavily patinated artifacts are more likely to be older than 1,500 years; (5) patination is progressive, occurring more frequently on older artifacts than on younger ones; and (6) patination may be used to examine the taphonomic history of an artifact assemblage. The most optimistic voices have argued that by making measurements of patina thickness for a large number of artifacts from a single occupation of known age at one site, then the mean and standard deviation of the weathering constant for chert may be calculated, thereby making age estimates on the basis of patina thickness possible (Purdy and Clark 1987).

Strident opposition has been raised by those who argue that the large number of factors potentially influencing patination effectively negate the possibility of obtaining useable temporal information from patina observations. Opinions range from extremes such as "the thickness of a patina layer is no guide to the date of the manufacture of a flint artifact" (Rottländer 1975b:109) to general but widespread cautionary statements that recount the potential problems (e.g. Péwé 1954:55; Hester et al. 1982:32; Rosenfeld 1965:212).

The purpose of this paper is to directly test the utility of chert patination as a dating technique,

with regard to the use of patination in separating unburied lithic assemblages found upon limestone surfaces in Central Texas into temporally meaningful groups. We intend to use as a point of departure, information in the literature regarding factors influencing patination and have tried to minimize factors that could introduce noise and therefore interfere with observations directed toward establishing the rate of patination. To do this we have attempted to control for parent material, burial history, and age, and have gathered data on other factors such as soil pH that will allow us to evaluate what, if any, role this may have in the patination process.

3.0 METHODS

To make temporally significant observations, we sampled artifacts from three temporal groups assuming that the existing stone tool typology accurately reflects artifact age, and that the artifacts included in the sample were manufactured during the period established for each artifact type. Three temporal classes were selected, Late Prehistoric, Middle Archaic, and Paleoindian, and a single type of temporally diagnostic projectile point was selected to represent the two youngest temporal groups. Due to the lower frequency of Paleoindian points of all classes in the Fort Hood collection, artifacts of this age included three different diagnostic point types.

Scallorn arrow points, the youngest artifact type in the sample, are common components of Austin Phase archaeological sites and are currently believed to have been manufactured between 1,250 to 750 years B.P. [A.D. 700 to A.D. 1200] (Turner and Hester 1993:230; Jelks 1993:11). Pedernales darts are one of the most frequently recovered projectile points at Fort Hood (e.g. Callister et al. 1994) and represent the Middle Archaic stage in our sample. These dart points have been dated to the period about 3,950 to 3,150 years B.P. (2000 to 1200 B.C.) (Turner and Hester 1993). Three types of Paleoindian projectile points comprise the oldest artifact class in our study. The youngest and best represented point in this category, Angostura, is considered to be of late Paleoindian age and has been recently dated to about 8,805 years B.P. (6855 B.C.) at the Richard Beene site (Turner and Hester 1993:73; Thoms 1993:23), and occurs in deposits dating between about 8,800 and 8,100 years B.P. at the Wilson Leonard site in Williamson County, Texas (Collins et al. 1993; C. Britt Bousman, personal communication 1994). A few Golondrina points, generally associated with the period between 9,180 to 8,780 years B.P. (7230 to 6830 B.C.), are also included in the Paleoindian temporal class (Hester 1983; Turner and Hester 1993:126). The oldest points in the Paleoindian category, and perhaps taxonomically most problematic, are Plainview or Barber-Plainview types that elsewhere in this paper are simply referred to as Plainview. Plainview type points have been recovered from sites dating about 10,000 years B.P. [8,150 to 8,000 B.C.] (Turner and Hester 1993:175; Holliday 1987:23) and at the Wilson Leonard site, points similar to Barber occur in strata as young as 8,800 years B.P. (C. Britt Bousman, personal communication 1994). Therefore we consider the age of the artifacts in this category to be between about 10,200 and 8,800 years B.P. [ca. 8,250 and 6850 B.C.]. Examples of each of the artifact types used in this study are illustrated in Figure 3.1.

Initially, a large number of specimens were pulled from the existing Fort Hood collections. From this group only, artifacts which were collected from stable, upland landscapes were selected for further typological examination (Figure 3.2). All of the points meeting this criteria were independently type classed by two acknowledged authorities (Elton Prewitt and Dr. Thomas Hester) and previously mis-identified or problematic artifacts excluded. Thirty-five specimens were selected from each temporal class (Late Prehistoric, Middle Archaic, and Paleoindian). These 105 artifacts were subsequently drawn, measured and photographed. Next, thin sections were prepared from small samples removed from the point bases and stems, which in general were less likely to have been affected by reuse activities and therefore yield patination measurements that best reflect the full period of time that has elapsed since the artifact was manufactured.

If differential patination was apparent, five measurements of the pseudo-isotropic patina from each side of the artifact were made using an optical micrometer. If differential patination was not apparent, only five measurements were taken from a single side of the artifact.

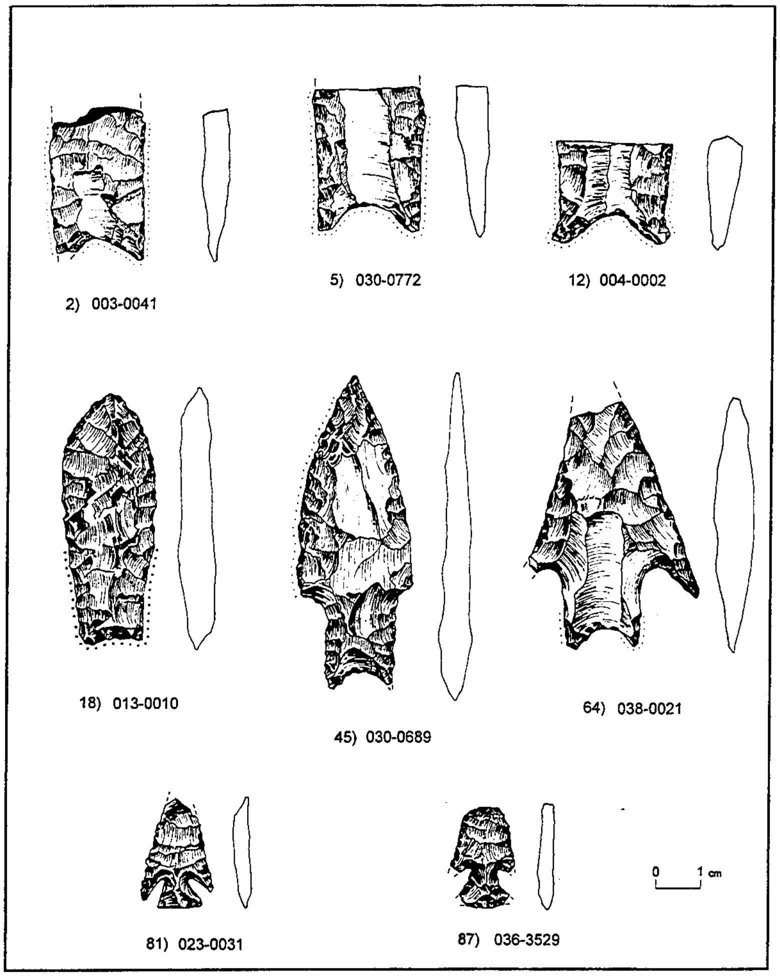

Figure 3.1 Illustration of Point Types Used in the Study.

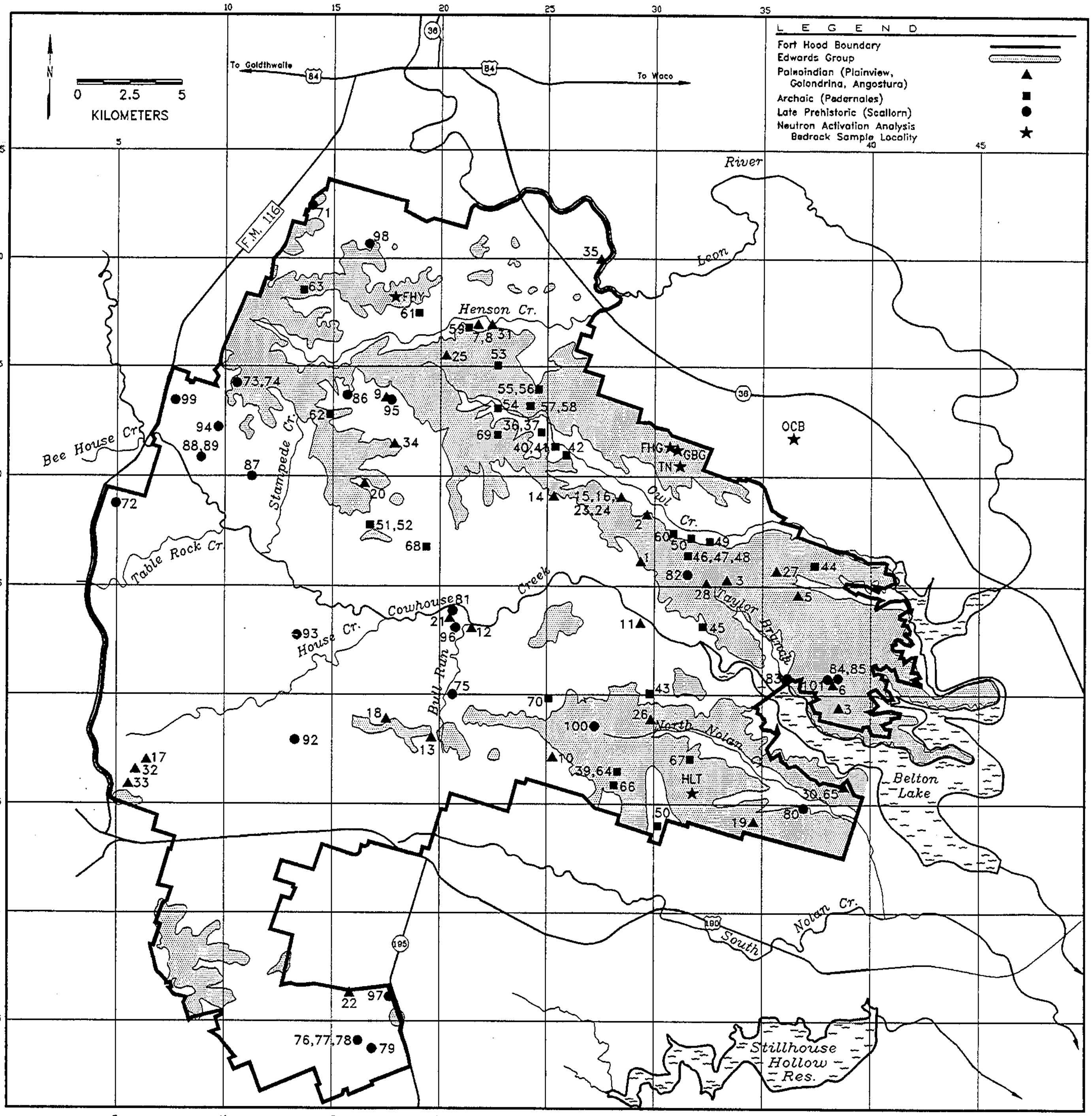

Figure 3.2 Collection Location of the Points Used in the Study, and the Bedrock Chert Samples Examined by INAA.

Readings were made at a magnification of 40x, and if no patina rim was apparent at low power, further inspection at 200x or 800x was used to determine if smaller rims were present. After the thin sections had been made, the remaining portions of the artifacts were sent to the Missouri University Research Reactor (MURR) for instrumental neutron activation analysis. A diamond trim saw was used to remove a portion of each artifact for analysis, and the remaining artifacts were returned to the Fort Hood collection.

To evaluate the role of soil pH in the patination process, the collection sites for 56 artifacts were revisited and one or more soil samples taken and subsequently analyzed for pH. For identification purposes, the artifacts were rank ordered according to temporal class, from oldest to youngest. A cross-reference of the artifact number used in this study with the Fort Hood accession number, the MURR lab number, the thin section identification number, and the artifact class is presented in Table 3.1.

Table 3.1 Listing of Artifact Type, Fort Hood Accession Number, MURR Lab Number, ASC Lab Number, and Descriptive Statistics for the Patina Observations.

					Descriptive Statistics								
					All Measurements			Descriptive Stats Side A			Descriptive Stats Side B		
Specimen Number	Accession Number	MURR Lab No.	Thin Section Number	Point Type	Mean	Std. Dev.	Range	Mean	Std. Dev.	Range	Mean	Std. Dev.	Range
1	03-0028	CDF002	DL-93-487	Plainview	0.50	0.16	0.50	0.62	0.09	0.24	0.38	0.12	0.32
2	03-0041	CDF003	DL-93-480	Plainview	0.53	0.17	0.46	0.52	0.19	0.45	0.55	0.17	0.43
3	30-0403	CDF007	DL-93-499	Plainview	0.31	0.04	0.15	0.32	0.06	0.15	0.29	0.01	0.04
4	30-0444	CDF008	DL-93-469	Plainview	0.18	0.13	0.31	0.28	0.01	0.01	0.25	0.04	0.10
5	30-0772	CDF009	DL-93-498	Plainview	0.42	0.12	0.37	0.48	0.14	0.33	0.35	0.04	0.10
6	30-1559	CDF010	DL-93-488	Plainview	0.14	0.04	0.14	0.16	0.03	0.09	0.12	0.04	0.10
7	35-2881	CDF011	DL-93-481	Plainview	0.16	0.10	0.25	0.16	0.10	0.25	0.00	0.00	0.00
8	35-2882	CDF012	DL-93-471	Plainview	0.47	0.13	0.40	0.53	0.16	0.40	0.40	0.05	0.12
9	36-3107	CDF013	DL-93-486	Plainview	0.00	0.00	0.00	0.00	0.00	0.00	0.00	0.00	0.00
10	44-0553	CDF014	DL-93-493	Plainview	0.06	0.01	0.03	0.06	0.01	0.03	0.00	0.00	0.00
11	03-0026	CDF001	DL-93-496	Golondrina	0.83	0.33	0.77	1.12	0.17	0.36	0.54	0.04	0.11
12	04-0002	CDF004	DL-93-492	Golondrina	0.52	0.14	0.37	0.53	0.15	0.37	0.50	0.15	0.33
13	13-0014	CDF005	DL-93-500	Golondrina	0.00	0.00	0.00	0.00	0.00	0.00	0.00	0.00	0.00
14	02-0223	CDF015	DL-93-497	Angostura	0.00	0.00	0.00	0.00	0.00	0.00	0.00	0.00	0.00
15	03-0042	CDF016	DL-93-477	Angostura	0.53	0.19	0.44	0.53	0.19	0.44	0.00	0.00	0.00
16	03-0043	CDF017	DL-93-491	Angostura	0.31	0.10	0.32	0.38	0.08	0.17	0.24	0.06	0.16
17	1-1286-001	CDF038	DL-93-501	Angostura	0.17	0.04	0.09	0.17	0.04	0.09	0.00	0.00	0.00
18	13-0010	CDF018	DL-93-478	Angostura	0.14	0.07	0.20	0.14	0.07	0.20	0.00	0.00	0.00
19	2-821-001	CDF035	DL-93-502	Angostura	0.00	0.00	0.00	0.00	0.00	0.00	0.00	0.00	0.00
20	21-0020	CDF019	DL-93-475	Angostura	0.00	0.00	0.00	0.00	0.00	0.00	0.00	0.00	0.00
21	21-0037	CDF020	DL-93-479	Angostura	1.94	0.20	0.00	1.94	0.20	0.00	0.00	0.00	0.00
22	23-0003	CDF022	DL-93-482	Angostura	0.46	0.12	0.37	0.50	0.14	0.37	0.41	0.08	0.22
23	25-0035	CDF023	DL-93-495	Angostura	0.00	0.00	0.00	0.00	0.00	0.00	0.00	0.00	0.00
24	25-0041	CDF024	DL-93-474	Angostura	0.42	0.13	0.40	0.45	0.15	0.37	0.39	0.11	0.25
25	25-0139	CDF025	DL-93-484	Angostura	0.37	0.10	0.26	0.37	0.10	0.26	0.00	0.00	0.00
26	30-0007	CDF026	DL-93-476	Angostura	0.43	0.07	0.16	0.43	0.07	0.16	0.00	0.00	0.00

					Descriptive Statistics								
					All Measurements			Descriptive Stats Side A			Descriptive Stats Side B		
Specimen Number	Accession Number	MURR Lab No.	Thin Section Number	Point Type	Mean	Std. Dev.	Range	Mean	Std. Dev.	Range	Mean	Std. Dev.	Range
27	30-0484	CDF027	DL-93-473	Angostura	0.27	0.09	0.29	0.28	0.12	0.29	0.26	0.04	0.12
28	30-439	CDF028	DL-93-489	Angostura	0.21	0.06	0.17	0.25	0.04	0.10	0.16	0.02	0.04
29	33-0018	CDF029	DL-93-490	Angostura	0.32	0.11	0.26	0.32	0.11	0.26	0.00	0.00	0.00
30	33-0045	CDF030	DL-93-494	Angostura	0.84	0.13	0.33	0.84	0.13	0.33	0.00	0.00	0.00
31	35-0178	CDF031	DL-93-472	Angostura	0.33	0.07	0.23	0.37	0.06	0.16	0.29	0.03	0.08
32	40-0982	CDF032	DL-93-483	Angostura	0.27	0.15	0.48	0.36	0.15	0.38	0.18	0.05	0.13
33	40-1025	CDF033	DL-93-485	Angostura	0.38	0.09	0.29	0.43	0.09	0.23	0.32	0.06	0.17
34	40-1043	CDF034	DL-93-470	Angostura	0.42	0.12	0.41	0.42	0.08	0.21	0.41	0.16	0.41
35	54-0005	CDF037	DL-93-503	Angostura	0.00	0.00	0.00	0.00	0.00	0.00	0.00	0.00	0.00
36	05-0048	CDF039	DL-93-573	Pedernales	0.00	0.00	0.00	0.00	0.00	0.00	0.00	0.00	0.00
37	05-0050	CDF040	DL-93-522	Pedernales	0.00	0.00	0.00	0.00	0.00	0.00	0.00	0.00	0.00
38	05-0051	CDF041	DL-93-571	Pedernales	0.00	0.00	0.00	0.00	0.00	0.00	0.00	0.00	0.00
39	11-0006	CDF042	DL-93-517	Pedernales	0.09	0.01	0.03	0.09	0.01	0.03	0.00	0.00	0.00
40	25-0010	CDF043	DL-93-512	Pedernales	0.27	0.04	0.12	0.30	0.03	0.07	0.25	0.01	0.04
41	25-0018	CDF044	DL-93-509	Pedernales	0.09	0.02	0.05	0.09	0.02	0.05	0.00	0.00	0.00
42	25-0023	CDF045	DL-93-507	Pedernales	0.56	0.29	0.68	0.83	0.05	0.12	0.29	0.05	0.12
43	30-0073	CDF046	DL-93-508	Pedernales	0.00	0.00	0.00	0.00	0.00	0.00	0.00	0.00	0.00
44	30-0533	CDF047	DL-93-506	Pedernales	0.10	0.06	0.15	0.12	0.07	0.15	0.07	0.02	0.05
45	30-0689	CDF048	DL-93-505	Pedernales	0.00	0.00	0.00	0.00	0.00	0.00	0.00	0.00	0.00
46	30-1997	CDF049	DL-93-504	Pedernales	0.11	0.05	0.13	0.15	0.02	0.06	0.07	0.02	0.04
47	30-1999	CDF050	DL-93-572	Pedernales	0.45	0.05	0.15	0.47	0.05	0.14	0.43	0.03	0.08
48	30-2000	CDF051	DL-93-514	Pedernales	0.04	0.01	0.01	0.04	0.01	0.01	0.00	0.00	0.00
49	30-2012	CDF052	DL-93-521	Pedernales	0.31	0.05	0.19	0.33	0.03	0.08	0.29	0.05	0.14
50	30-2090	CDF053	DL-93-523	Pedernales	0.09	0.01	0.04	0.10	0.02	0.03	0.09	0.01	0.03
51	35-2204	CDF054	DL-93-520	Pedernales	0.00	0.00	0.00	0.00	0.00	0.00	0.00	0.00	0.00
52	35-2205	CDF055	DL-93-526	Pedernales	0.00	0.00	0.00	0.00	0.00	0.00	0.00	0.00	0.00
53	35-2384	CDF056	DL-93-511	Pedernales	0.38	0.04	0.13	0.40	0.03	0.08	0.37	0.05	0.12
54	35-2391	CDF057	DL-93-518	Pedernales	0.00	0.00	0.00	0.00	0.00	0.00	0.00	0.00	0.00
55	35-2392	CDF058	DL-93-531	Pedernales	0.18	0.05	0.11	0.18	0.05	0.11	0.00	0.00	0.00
56	35-2395	CDF059	DL-93-529	Pedernales	0.00	0.00	0.00	0.00	0.00	0.00	0.00	0.00	0.00
57	35-2647	CDF060	DL-93-515	Pedernales	0.00	0.00	0.00	0.00	0.00	0.00	0.00	0.00	0.00
58	35-2652	CDF061	DL-93-533	Pedernales	0.13	0.02	0.08	0.14	0.03	0.07	0.13	0.02	0.04
59	35-2884	CDF062	DL-93-528	Pedernales	0.09	0.05	0.12	0.12	0.03	0.07	0.05	0.01	0.02
60	36-3001	CDF063	DL-93-513	Pedernales	0.26	0.07	0.18	0.26	0.07	0.18	0.00	0.00	0.00
61	36-3642	CDF108	DL-93-510	Pedernales	0.00	0.00	0.00	0.00	0.00	0.00	0.00	0.00	0.00
62	36-3883	CDF064	DL-93-519	Pedernales	0.00	0.00	0.00	0.00	0.00	0.00	0.00	0.00	0.00
63	37-0669	CDF065	DL-93-516	Pedernales	0.13	0.02	0.06	0.13	0.02	0.06	0.00	0.00	0.00
64	38-0021	CDF066	DL-93-532	Pedernales	0.00	0.00	0.00	0.00	0.00	0.00	0.00	0.00	0.00
65	38-0098	CDF067	DL-93-524	Pedernales	0.73	0.22	0.56	0.93	0.02	0.05	0.53	0.11	0.22
66	38-0733	CDF068	DL-93-525	Pedernales	0.00	0.00	0.00	0.00	0.00	0.00	0.00	0.00	0.00
67	38-0816	CDF069	DL-93-530	Pedernales	0.00	0.00	0.00	0.00	0.00	0.00	0.00	0.00	0.00

Specimen Number	Accession Number	MURR Lab No.	Thin Section Number	Point Type	Descriptive Statistics: All Measurements Mean	Std. Dev.	Range	Descriptive Stats Side A Mean	Std. Dev.	Range	Descriptive Stats Side B Mean	Std. Dev.	Range
68	44-1253M	CDF070	DL-93-527	Pedernales	0.24	0.07	0.17	0.24	0.07	0.17	0.00	0.00	0.00
69	44-1443M	CDF071	DL-93-534	Pedernales	0.05	0.02	0.05	0.06	0.02	0.05	0.04	0.01	0.01
70	44-1614M	CDF072	DL-93-535	Pedernales	0.00	0.00	0.00	0.00	0.00	0.00	0.00	0.00	0.00
71	02-0154	CDF073	DL-93-549	Scallorn	0.00	0.00	0.00	0.00	0.00	0.00	0.00	0.00	0.00
72	02-0203	CDF074	DL-93-548	Scallorn	0.00	0.00	0.00	0.00	0.00	0.00	0.00	0.00	0.00
73	03-0007	CDF075	DL-93-547	Scallorn	0.00	0.00	0.00	0.00	0.00	0.00	0.00	0.00	0.00
74	03-0008	CDF076	DL-93-546	Scallorn	0.00	0.00	0.00	0.00	0.00	0.00	0.00	0.00	0.00
75	13-0060	CDF077	DL-93-545	Scallorn	0.00	0.00	0.00	0.00	0.00	0.00	0.00	0.00	0.00
76	2-348-001	CDF103	DL-93-566	Scallorn	0.00	0.00	0.00	0.00	0.00	0.00	0.00	0.00	0.00
77	2-348-006	CDF105	DL-93-567	Scallorn	0.00	0.00	0.00	0.00	0.00	0.00	0.00	0.00	0.00
78	2-348-007	CDF106	DL-93-569	Scallorn	0.00	0.00	0.00	0.00	0.00	0.00	0.00	0.00	0.00
79	2-384-001	CDF104	DL-93-570	Scallorn	0.00	0.00	0.00	0.00	0.00	0.00	0.00	0.00	0.00
80	22-D	CDF107	DL-93-540	Scallorn	0.00	0.00	0.00	0.00	0.00	0.00	0.00	0.00	0.00
81	23-0031	CDF078	DL-93-539	Scallorn	0.00	0.00	0.00	0.00	0.00	0.00	0.00	0.00	0.00
82	30-0465	CDF079	DL-93-541	Scallorn	0.00	0.00	0.00	0.00	0.00	0.00	0.00	0.00	0.00
83	30-1024	CDF080	DL-93-550	Scallorn	0.00	0.00	0.00	0.00	0.00	0.00	0.00	0.00	0.00
84	30-1646	CDF081	DL-93-542	Scallorn	0.00	0.00	0.00	0.00	0.00	0.00	0.00	0.00	0.00
85	30-1647	CDF082	DL-93-544	Scallorn	0.00	0.00	0.00	0.00	0.00	0.00	0.00	0.00	0.00
86	36-3518	CDF083	DL-93-565	Scallorn	0.00	0.00	0.00	0.00	0.00	0.00	0.00	0.00	0.00
87	36-3529	CDF084	DL-93-564	Scallorn	0.00	0.00	0.00	0.00	0.00	0.00	0.00	0.00	0.00
88	36-3936	CDF085	DL-93-563	Scallorn	0.00	0.00	0.00	0.00	0.00	0.00	0.00	0.00	0.00
89	36-3937	CDF086	DL-93-562	Scallorn	0.00	0.00	0.00	0.00	0.00	0.00	0.00	0.00	0.00
90	38-0475	CDF087	DL-93-561	Scallorn	0.00	0.00	0.00	0.00	0.00	0.00	0.00	0.00	0.00
91	40-0845	CDF088	DL-93-560	Scallorn	0.00	0.00	0.00	0.00	0.00	0.00	0.00	0.00	0.00
92	40-1133	CDF089	DL-93-559	Scallorn	0.00	0.00	0.00	0.00	0.00	0.00	0.00	0.00	0.00
93	40-1283	CDF090	DL-93-558	Scallorn	0.00	0.00	0.00	0.00	0.00	0.00	0.00	0.00	0.00
94	41-0200	CDF091	DL-93-557	Scallorn	0.14	0.03	0.06	0.14	0.03	0.06	0.00	0.00	0.00
95	41-0349	CDF092	DL-93-556	Scallorn	0.00	0.00	0.00	0.00	0.00	0.00	0.00	0.00	0.00
96	41-0385	CDF094	DL-93-555	Scallorn	0.00	0.00	0.00	0.00	0.00	0.00	0.00	0.00	0.00
97	41-0444	CDF093	DL-93-554	Scallorn	0.00	0.00	0.00	0.00	0.00	0.00	0.00	0.00	0.00
98	43-0257	CDF095	DL-93-553	Scallorn	0.30	0.08	0.26	0.36	0.09	0.22	0.24	0.02	0.04
99	44-0030	CDF096	DL-93-552	Scallorn	0.00	0.00	0.00	0.00	0.00	0.00	0.00	0.00	0.00
100	44-0548	CDF097	DL-93-551	Scallorn	0.00	0.00	0.00	0.00	0.00	0.00	0.00	0.00	0.00
101	44-1462M	CDF098	DL-93-538	Scallorn	0.18	0.05	0.15	0.22	0.03	0.09	0.15	0.02	0.06
102	54-0007	CDF099	DL-93-568	Scallorn	0.00	0.00	0.00	0.00	0.00	0.00	0.00	0.00	0.00
103	60-0013	CDF100	DL-93-537	Scallorn	0.00	0.00	0.00	0.00	0.00	0.00	0.00	0.00	0.00
104	60-0014	CDF101	DL-93-536	Scallorn	0.22	0.03	0.10	0.23	0.03	0.08	0.21	0.03	0.06
105	60-0015	CDF102	DL-93-543	Scallorn	0.00	0.00	0.00	0.00	0.00	0.00	0.00	0.00	0.00

4.0 PARENT MATERIAL CHARACTERIZATION

The collection of the artifacts used in this study from Fort Hood strongly favors interpreting all of the artifacts as Edwards chert. As noted previously, Fort Hood lies at the eastern edge of the Edwards Group outcrop (Figure 1.1) and at least 16 physically distinct variants of Edwards chert are currently recognized on or in the immediate vicinity of the base (Frederick and Ringstaff 1994). The Edwards Group and correlative strata crop out in Texas and Mexico and are a lower Cretaceous age limestone which forms one of the most extensive sources of lithic raw material on the North American Great Plains.

Cryptocrystalline silicates associated with the Edwards Group occur in a variety of nodular and bedded forms, and on the whole, are highly variable in appearance. The heterogeneous nature of this material has led to the generalization of the term "Edwards chert" to represent any gray or tan chert found in West Texas and the Southern Plains (Frederick and Ringstaff 1994; Tunnell 1978; Hoffman et al. 1991) and has encouraged discovery of a simple, expedient means of identification. At this point in time there is no single reliable means of identifying Edwards chert.

In order to control for parent material, two techniques were employed; ultraviolet-excited fluorescence (UVF) and instrumental neutron activation analysis (INAA). UVF is widely gaining acceptance as a reliable and expedient means of identifying Edwards chert but it is yet to be fully tested, especially with respect to other cryptocrystalline silicates that crop out in Central Texas. INAA, on the other hand, has been repeatedly demonstrated to be useful in distinguishing morphologically similar cryptocrystalline silicates (e.g. Leudtke 1992; Morrow et al. 1992; Hoard et al. 1993), and is employed here to serve as an independent means of evaluating the artifact assemblage's parent material homogeneity.

4.1 ULTRAVIOLET-EXCITED FLUORESCENCE (UVF)

Previous studies in the midwest U.S. (e.g. Hoffman et al. 1991; Hillsman 1992; Ahler 1991) and ongoing research with Edwards Group chert (Personal communication, Michael B. Collins and Pam Headrick, Texas Archaeological Research Laboratory [TARL]) suggest that UVF may be an inexpensive and expedient means of identification of this source. In an unpublished work, Michael Collins and Pam Headrick have examined 257 specimens of Edwards chert collected from 47 localities across the Edwards outcrop and found that 92 percent fluoresce shades of yellow and orange, the majority of which correspond to colors on Munsell sheets 5Y and 2.5Y (Personal communication, Pam Headrick, 1994). Approximately eight percent of Edwards Group chert examined by Hedrick and Collins exhibited no visible fluorescence. At our request, all of the artifacts in this study, in addition to the 15 bedrock sources recognized by the current Ft. Hood taxonomy, and another 43 bedrock samples collected from across the Edwards outcrop, were inspected for long and short wave UV response by personnel at the Texas Archaeological Research Laboratory (TARL; Pam Headrick, Marilyn Masson, and Susan Dial) with extensive experience with this method. All of the Edwards bedrock sources examined, except one black chert that crops out near Fort Hood (known locally as Owl Creek Black) were found to fluoresce various shades of yellow and orange consistent with the known response of Edwards Group chert. All but three of the artifacts in this study (76, 54, and 40) were also found to fluoresce similar colors and would be classified as Edwards Group chert by this technique. Of the samples failing to fluoresce, one was a black chert similar in general appearance to Owl Creek Black and the remaining two fluoresced faintly and elicited a mixed review from the TARL personnel, but not strong enough to suggest rejecting the specimens as Edwards.

Therefore, on the basis of UVF analysis, the majority of the artifacts in this sample may be inferred to be Edwards Group chert.

4.2 INSTRUMENTAL NEUTRON ACTIVATION ANALYSIS (INAA)

Chemical characterization and evaluation of the parent material heterogeneity of the artifacts was provided by INAA. Previous to this investigation, the only known application of INAA to characterize chert samples from the Edwards Group was reported by McGinley and Schweikert (1979). Based on the relative abundances of nine elements, they were able to classify two chemical types suggesting an elemental inhomogeneity in the Edwards Group. Two recent MURR investigations (Hoard et al. 1992; Hoard et al. 1993) reporting data on 25 to 30 elements established chemical fingerprints for cryptocrystalline silicates from sources located in the northern Great Plains. These included the White River Badlands in southwestern South Dakota, Table Mountain in east-central Wyoming, and Flattop Butte in northeastern Colorado. In addition, the MURR databank contains trace element data on Cobden-Dongola chert from southern Illinois (Morrow et al. 1992), Knife River Flint from west-central North Dakota (Christensen 1991), and unpublished data on the Florence-A chert from Kay County, Oklahoma located in north-central Oklahoma. These latter cryptocrystalline silicates provide a comparative database for examining the application of INAA in the chemical differentiation of cherts in the midcontinental United States.

Since the primary objective in employing INAA in this project was to obtain an independent evaluation of the parent material homogeneity of the artifact population, six bedrock sources of Edwards Group chert previously identified by Dickens (1993) were first analyzed. Following this, the compositional information for the 105 artifacts was compared with the bedrock sources and membership probabilities calculated.

A total of 121 bedrock chert source samples representing the six different chert types were submitted to MURR in December 1993. The samples were assigned analytical sample IDs in accordance with Archaeometry Laboratory procedures requiring six-character alphanumeric names where the first three characters of the are alphabetical (e.g., EFC for Edwards Formation chert) and the last three characters are numeric beginning with the first sample (i.e., EFC001) and extending through the last sample (i.e., EFC121) (Table 4.1).

The mostly fist-sized source samples were washed in deionized water and scrubbed with a soft bristled brush to remove any adhering loose particles or surface dirt. After drying, the samples were crushed between steel plates using a Carver Laboratory Press which created a number of fragments of 50 to 100 mg size. After crushing, the fragments were inspected under a laboratory magnifier to identify and remove fragments containing weathered cortex, crush fractures, or metallic streaks. A few grams of these interior fragments were collected from each sample and placed in clean storage containers prior to being weighed. Careful inspection determined that samples EFC018 and EFC120 contained insufficient interior fragments for our analysis and both were excluded, resulting in 119 source samples for analysis.

The 105 projectile points were assigned analytical IDs using a three-letter prefix of CDF followed by a three-number suffix in accordance with an accompanying shipping log. A cross-reference between MURR's analytical IDs and the Fort Hood Accession Numbers is provided in Table 3.1. Portions of each sample for analysis were removed from each artifact by using a diamond trim saw. As before, these sample portions were placed in plastic bags and crushed between tool steel plates to create several fragments which were weighed in approximately the same amounts as mentioned earlier, using the same types of sample vials.

Table 4.1 Sample ID Numbers assigned by MURR.

Type	Local Name	Sample IDs included
1	Owl Creek Black	EFC001 through EFC021
2	Gray-Brown-Green	EFC022 through EFC042
3	Fort Hood Yellow	EFC043 through EFC062
4	Texas Novaculite	EFC063 through EFC082
5	Heiner Lake Tan	EFC083 through EFC102
6	Fort Hood Gray	EFC103 through EFC121

The next step was to weigh aliquots of the specimens for both the short and long irradiation procedures employed at MURR. For short irradiations, approximately 200 mg of fragments were weighed into the approximately 1 ml high-density polyethylene vials used for short irradiations at MURR. For long irradiations, 800 to 1,000 mg of interior fragments were weighed into high-purity quartz vials. The quartz vials were later sealed with an oxygen torch flame. Standards using the well characterized National Institute of Standards and Technology (NIST) reference materials SRM-1633a Fly Ash and SRM-278 Obsidian Rock were similarly prepared for standardization and quality control, respectively.

Irradiation and Analysis

The samples and standards in polyvials were sequentially irradiated in pairs at MURR using the pneumatic tube irradiation system. Each sample was irradiated for five seconds in a thermal neutron flux of 8 x 10^{13} n/cm^2/s. The samples were allowed to decay for 25 minutes before being counted on a pair of high-resolution germanium detectors for a total of 720 seconds each. On a daily basis, each of the detector systems are capable of measuring three SRM-1633a, three SRM-278 standards, and approximately 30 artifacts. The short-lived elements determined by this procedure are Al, Ca, Dy, K, Mn, Na, and V.

Long irradiation samples and standards were bundled together by wrapping the quartz vials in aluminum foil. Each bundle for irradiation consisted of 30 artifacts, four SRM-1633a standards, and two SRM-278 quality controls. The bundle was placed in an aluminum can for insertion into an in-pool irradiation position at MURR for 70 hours, where the samples were exposed to a flux of 5 x 10^{13} n/cm^2/s. Following irradiation, the samples were permitted to decay for eight days before unwrapping and cleaning the quartz vials in aqua regia. The cleaned vials were loaded on an automatic sample changer and counted for 2,000 seconds each to measure the medium half-life elements including As, Ba, La, Lu, Nd, Sm, U, and Yb. After the medium count was completed, the samples were moved to a storage area and held for four weeks before being reloaded on the sample changer for counts of 10,000 seconds each to determine elements available from the long-lived isotopes. The elements determined from the long measurement include Ce, Co, Cr, Cs, Eu, Fe, Hf, Rb, Sb, Sc, Sr, Ta, Tb, Th, Zn, and Zr.

By comparison to the included analytical standards, concentrations for each of the 31 elements in the unknowns were calculated. For additional information about the procedures for sample preparation and standardization, the reader is referred to Glascock et al. (1988).

Results and Statistical Analysis

Following the calculation of elemental concentrations for all samples, the results were tabulated with the Lotus 1-2-3 spreadsheet program and subsequently exported into a DBASE file where the descriptive information for all specimens could be incorporated. A complete listing of the all element concentrations determined for the 119 source specimens and 105 projectile points is provided in Appendix D-1. Samples with elements at concentrations below our detection limit are reported as zeroes. Finally, the numerical data were converted into GAUSS data sets for statistical treatment using a series of GAUSS language routines written by Neff (1990).

Before treating the six Edwards Formation chert types separately, means and standard deviations for all elements determined in the 119 source samples were computed as shown in Table 4.2. The elements As, Lu, Nd, Yb, Cs, Tb, Ca, Dy, K, and V were found to be below detection in approximately half of the samples making these elements less useful for statistical analysis. Although few elements (e.g., Rb, Sr, Ta, Zn, and Mn) have missing values, for a small number of samples a replacement procedure is possible. Thus, 21 of the 31 measured elements were identified as being potentially useful for treatment by our pattern recognition and statistical procedures.

Intercomparison Between Chert Types Within the Edwards Group

Inspection of the large variations in concentrations listed in Table 4.2 indicates that the Edwards Group chert samples are not very homogeneous and that differences between samples of various types or from different geographic areas within the Edwards Formation are probable. To examine differentiation between types, individual GAUSS data sets were created by grouping the source samples according to the categories listed on the shipping log. After creating the initial groups a log base-10 transformation of the 21 element concentrations (i.e., Ba, La, Sm, U, Ce, Co, Cr, Eu, Fe, Hf, Rb, Sb, Sc, Sr, Ta, Th, Zn, Zr, Al, Mn, and Na) was performed. Log transformation of the concentrations partially counteracts the weighing effect occurring from the fact that element concentrations range from below ppm for some elements to a few percent for others. Also, trace elements tend to approximate a normal distribution more closely following log transformation (Luedtke 1978; Luedtke 1992). Elements with missing values in a few samples were preserved rather than eliminated by applying a GAUSS routine that replaces the missing value with a new concentration value that minimizes the Mahalanobis distance for a specimen from the centroid of its group (Sayre 1975).

In order to examine differentiation between the Edwards Group chert types analyzed in this study, the entire Edwards Group source material data set was subjected to an RQ-mode principal components analysis (PCA). Although PCA is not a group-formation technique, it facilitates recognition of groups by performing a transformation of the data set based on eigenvector methods. The PCA transformation determines the direction and magnitude of maximum variance in the data set in hyperspace (Davis 1986) such that the first principal component (PC) is oriented in the direction of maximum variance. The second PC will be orthogonal to the first PC and be oriented in the direction of maximum remaining variance. This procedure continues until the number of PCs is equal to the number of original dimensions. Thus, the PCA technique provides a new basis for describing the entire distribution of elemental concentrations in the data set. Positions of specimens in the original element concentration space can be converted to their principal component scores (calculated in terms of linear combinations of the original data). Often, inspection of plots of the first few PCs will be adequate to identify the most important partitions in the data set.

Table 4.2 Descriptive Statistics for Chert Source Samples from the Texas Edwards Formation Reported in Parts Per Million.

Element	Mean	St. Dev.	% St. Dev.	No. Obs.	Minimum	Maximum
AS	0.269	0.114	42.522	28	0.110	0.590
BA	18.653	8.740	46.856	119	7.190	48.670
LA	0.605	0.707	116.948	119	0.115	5.318
LU	0.007	0.004	59.155	65	0.001	0.020
ND	0.554	0.651	117.538	90	0.108	3.461
SM	0.146	0.092	63.041	119	0.051	0.459
U	1.632	0.857	52.537	119	0.588	4.017
YB	0.015	0.020	131.989	70	0.002	0.093
CE	0.564	0.481	85.326	119	0.147	3.299
CO	0.017	0.010	56.779	119	0.002	0.054
CR	0.694	0.326	46.962	119	0.163	1.572
CS	0.008	0.005	66.413	85	0.002	0.022
EU	0.007	0.014	204.034	119	0.001	0.089
FE	153.734	124.193	80.784	119	15.500	766.500
HF	0.037	0.021	56.223	119	0.005	0.089
RB	0.285	0.141	49.432	115	0.054	0.655
SB	0.009	0.004	41.121	119	0.003	0.018
SC	0.060	0.030	50.025	119	0.009	0.113
SR	4.952	4.596	92.804	109	0.630	31.660
TA	0.007	0.005	65.715	115	0.001	0.018
TB	0.008	0.011	152.984	64	0.001	0.053
TH	0.066	0.040	60.327	119	0.013	0.157
ZN	0.523	0.417	79.818	117	0.054	2.784
ZR	8.045	3.916	48.672	119	3.165	19.892
AL	1677.519	422.726	25.199	119	1019.700	2828.500
CA	3266.418	4025.909	123.252	56	256.300	20631.000
DY	0.125	0.076	61.038	15	0.047	0.272
K	312.435	114.973	36.799	52	93.400	531.300
MN	1.172	1.732	147.782	111	0.079	9.400
NA	251.536	110.636	43.984	119	102.100	497.400
V	2.236	0.903	40.378	65	0.709	4.957

The RQ-mode PCA procedure provides the advantage of permitting the calculation of object and variable loadings on the same axes (Neff 1994) based on the variance-covariance matrix (note: standard PCA uses the correlation matrix). Examination of the PCA results found that the first three, first four, and first five PCs cumulatively account for greater than 82, 87, and 90 percent, respectively, of the variance in the data set. Elements most heavily loaded on the first PC are Co, Fe, Hf, Sc, Sr, Ta, Th, Zn, and Mn. Elements contributing most to the second PC are La, Sm, Ce, Eu, Sr, and Mn. The RQ-mode PCA procedure also enables generation of RQ-mode plots of the elements and data points (or groups of data points) on the same bivariate diagrams as shown in Figures 4.1 and 4.2 for principal components PC01 vs. PC02 and PC01 vs. PC03, respectively. Confidence ellipses at the 90 percent confidence interval are shown to indicate the level of differentiation achieved. Distances from the plot origin (0,0) to the elements (solid dots) indicate the relative importance of that element's contribution to variance in the two dimensions shown. During the process of group refinement, a number of outlier samples were identified and removed from further consideration. The outliers were also inspected visually and several were found to be visibly dissimilar from other source samples of that type. Samples removed include the following:

Owl Creek Black	EFC003, EFC010, EFC011, and EFC012
Gray-Brown-Green	EFC025 and EFC035
Fort Hood Yellow	EFC050, EFC058, and EFC059 (all visually gray not tan)
Texas Novaculite	EFC070 and EFC073
Heiner Lake Tan	no samples removed
Fort Hood Gray	EFC109

The twelve removed specimens were excluded from the groups plotted in Figures 4.1 and 4.2.

From Figures 4.1 and 4.2 we find that most of the differentiation between the various Edwards Formation chert types is due to the transition metals (Fe, Co, and Zn) and rare earth elements (La, Ce, Sm, and Eu). The Owl Creek Black and Gray-Brown-Green chert types which overlap on PC01 vs. PC03 are primarily differentiated by Mn as shown in Figure 4.2. As seen in the Fe vs. Mn bivariate plot shown in Figure 4.3, concentrations of Fe are adequate to clearly differentiate three Edwards Formation chert types (Owl Creek Black, Gray-Brown-Green, and Tan with high Fe concentrations) from two others (Heiner Lake Tan and Fort Hood Gray). Figure 4.3 also confirms the differentiation of Owl Creek Black from Gray-Brown-Green on the basis of Mn.

The first five principal components which describe more than 90 percent of the variance in the data set were used to calculate the Mahalanobis distances between individual specimens and the group centroids for the six chert types. Probabilities of group membership were derived from these calculations. With the exception of three source samples (two Owl Creek Black and one Gray-Brown-Green) which were chemically assigned to the Fort Hood Yellow chert group, the classifications were very successful.

<u>Comparison of Edwards Group with other Cryptocrystalline Silicates</u>

Compositional data for the Edwards Group and the other cryptocrystalline silicates in our database were compared by performing a PCA on the log transformed data for eight source groups combined (i.e., Table Mountain, White River Badlands, Knife River Flint, Florence-A Chert, Cobden-Dongola Chert, Flattop Butte Chalcedony, Gering Formation Chalcedony, and Edwards Group Chert). The new elemental coordinates derived from the PCA transformation provide a new window through which the differences between chert types can often be viewed more readily. The success of differentiating Edwards Group source materials from the other sources on the basis of PCA is shown in the PC01 versus PC02 plot in Figure 4.4, where 90 percent confidence ellipses surrounding each source material are shown.

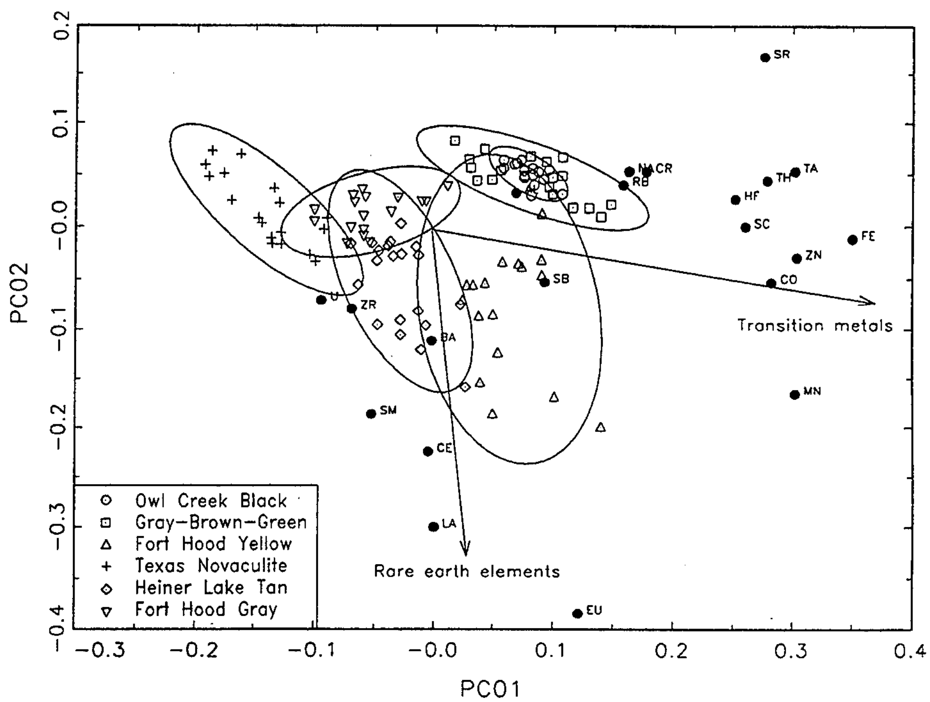

Figure 4.1 RQ-mode Bivariate Plot of the First and Second Principal Components for Six Chert Types Within the Edwards Group.

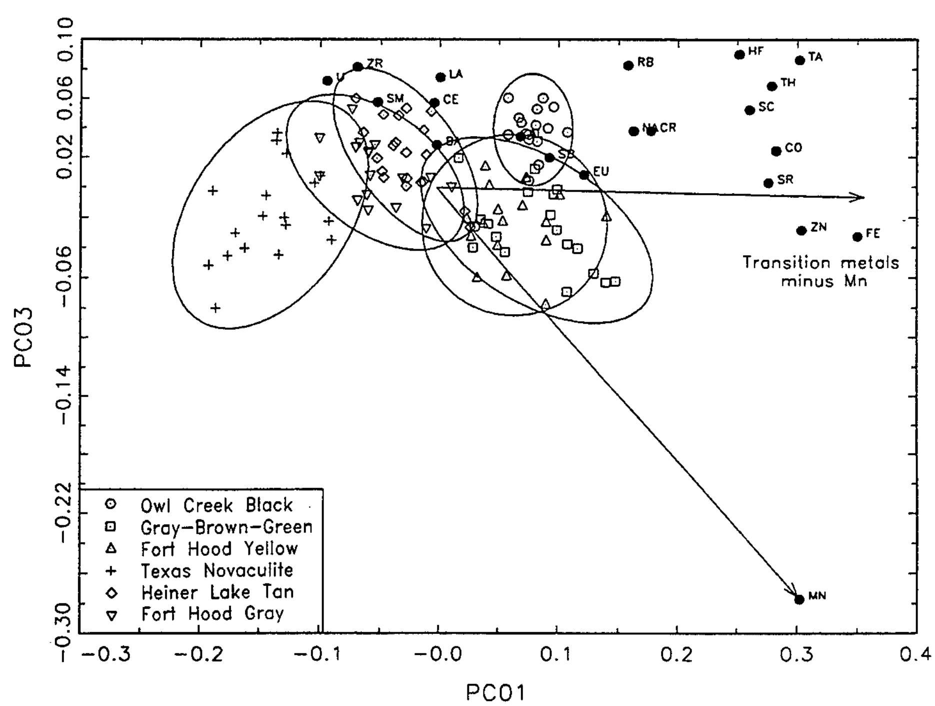

Figure 4.2 RQ-mode Bivariate Plot of the First and Third Principal Components for Six Chert Types Within the Edwards Group.

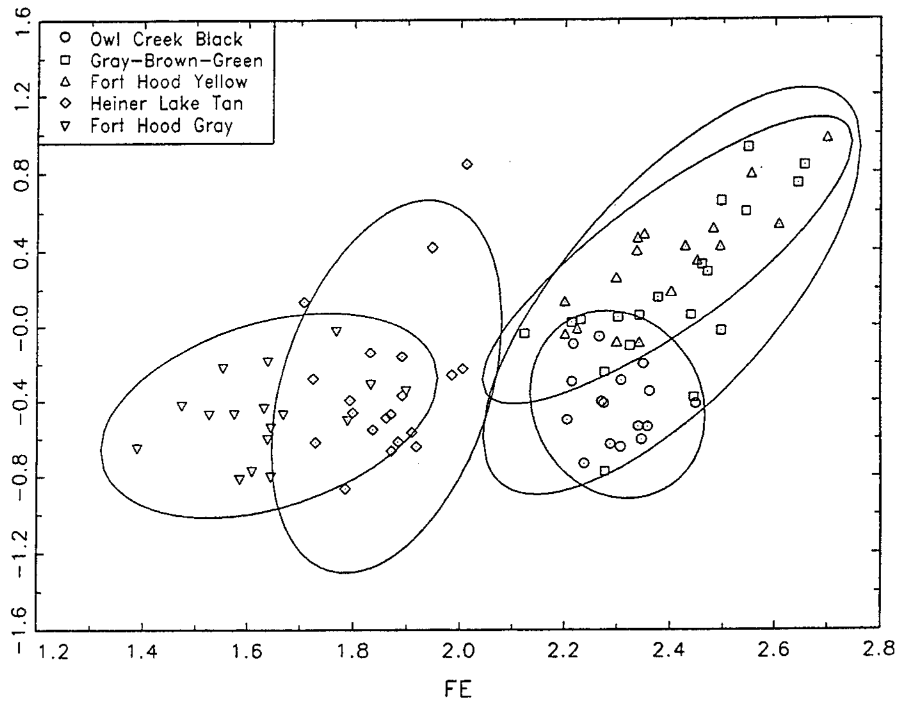

Figure 4.3 Bivariate Plot of Fe versus Mn Showing the Chemical Differences between the Owl Creek Black, Gray-Brown-Green, and Fort Hood Yellow Chert Types, and the Heiner Lake Tan and Fort Hood Gray Chert Types from the Edwards Group.

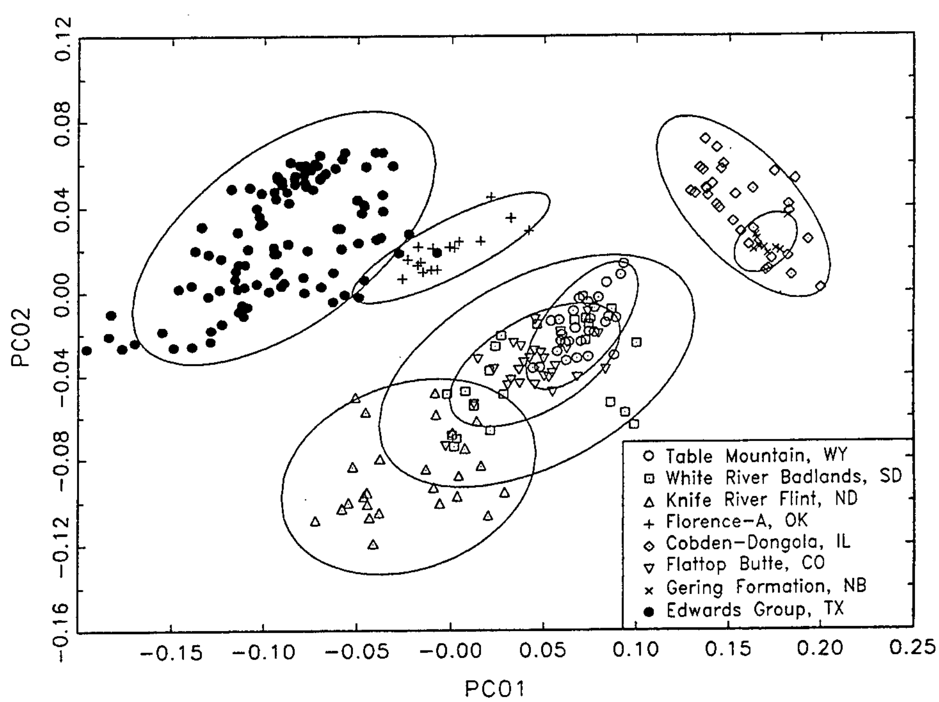

Figure 4.4 Bivariate Plot of the First and Second Principal Components for Several Different Cryptocrystalline Silicates Located in the Midcontinental U.S.

As shown, the compositional fingerprint for Edwards Formation source materials is well separated from six of the seven other types to which it is compared. The cryptocrystalline silicate most similar to the Edwards Formation is the Florence-A chert from Kay County, Oklahoma which is also geographically nearest to the Edwards Formation source area.

Comparison of Projectile Points with Source Types and Membership Probabilities

The PCA transformations derived from the source data mentioned above were applied to the data for the 105 projectile points. The artifacts were then projected against the source data to determine probabilities and "most probable" group classifications for each specimen. Table 4.3 lists the results following application of this procedure. Approximately 25 of the artifacts have membership probabilities greater than five percent but the majority have probabilities below 1 percent. Of the artifacts with membership probabilities greater than five percent, Fort Hood Yellow is the most favored. The general relationship between the artifacts and the six bedrock source groups is illustrated in Figure 4.5. Figure 4.6 compares the 90 percent confidence ellipses for the six Edwards Group bedrock samples as a group, with other cryptocrystalline silicates in the MURR database, and the principal component scores for the 105 artifacts in the study. The latter figure clearly illustrates that a significant number of the artifacts in this study do not fall within the 90 percent confidence ellipse of the presently known Edwards Group. If the UVF analysis is considered to be accurate, then this illustration suggests that additional work is necessary to obtain an adequate chemical fingerprint for Edwards Group chert. The latter result is not surprising since bedrock source sampling for this project was from a very limited region on or near the Fort Hood military base, and represents a small portion of the overall outcrop. Analysis of source samples from a larger, more geographically representative portion of the Edwards outcrop is currently underway.

In general, however, the INAA results indicate that with three possible exceptions (specimens 23, 76, and 80), all of the samples in the population are relatively consistent. About half of the samples fall within the 90 percent confidence ellipse for the examined Edwards Group bedrock samples. It is interesting to note that one of the three outliers identified by INAA, specimen 76, also failed to fluoresce and probably is not Edwards chert. In the absence of the trace element data, the lack of fluorescence response by this specimen would be dismissed because black chert associated with the Edwards Group is known not to fluoresce. On Figure 4.6, this specimen appears to fall within the 90 percent confidence ellipse for Cobden-Dongola chert which is a blue-gray-black chert that crops out in Illinois (Morrow et al. 1992). Without trace element data for other cherts that crop out in Central Texas, especially those associated with the Permian and Pennsylvanian strata, the association of this artifact with Cobden-Dongola is tentative since the similarities in chert color and trace element composition with Cobden-Dongola may simply be coincidental.

Table 4.3 Mahalanobis Distance Calculation and Posterior Classification for Two or More Groups.

Reference groups and numbers of specimens:

1	PC-F1	16
2	PC-F2	19
3	PC-F3	17
4	PC-F4	18
5	PC-F5	20
6	PC-F6	17

Variables used:

PC01 PC02 PC03 PC04 PC05

Probabilities:

ID. NO.	PC-F1	PC-F2	PC-F3	PC-F4	PC-F5	PC-F6	BEST GP.
CDF001	0.000	0.000	0.062	0.040	0.049	0.000	3
CDF002	0.000	0.000	0.000	0.105	0.001	0.000	4
CDF003	0.018	0.001	0.206	0.000	0.003	0.322	6
CDF004	0.004	0.000	0.092	0.005	0.013	0.005	3
CDF005	0.000	0.000	0.000	0.001	0.762	0.000	5
CDF007	0.000	0.000	0.505	0.000	0.009	0.166	3
CDF008	0.000	0.000	5.827	0.012	0.132	0.001	3
CDF009	0.000	0.000	5.398	0.002	0.515	0.000	3
CDF010	0.001	0.000	8.682	0.000	0.020	0.176	3
CDF011	0.000	0.000	0.462	0.003	0.013	0.005	3
CDF012	0.000	0.000	0.002	0.373	3.400	0.008	5
CDF013	0.000	0.000	12.970	0.004	0.058	0.000	3
CDF014	0.002	0.000	11.282	0.013	0.062	0.201	3
CDF015	0.006	0.000	3.943	0.000	0.002	0.027	3
CDF016	0.000	0.000	0.000	0.049	0.046	0.000	4
CDF017	0.000	0.000	0.000	0.015	0.000	0.000	4
CDF018	0.000	0.000	3.687	0.022	0.234	0.001	3
CDF019	0.000	0.000	0.050	0.000	0.000	0.000	3
CDF020	0.000	0.000	0.000	0.164	0.059	0.000	4
CDF022	0.000	0.000	0.000	0.002	0.012	0.000	5
CDF023	0.000	0.000	2.042	0.000	0.000	0.000	3
CDF024	0.000	0.000	0.000	0.909	2.649	0.013	5
CDF025	0.011	0.000	0.037	0.000	0.000	0.003	3
CDF026	0.000	0.000	0.000	0.010	0.000	0.001	4
CDF027	0.000	0.000	0.000	0.988	0.080	0.007	4
CDF028	0.000	0.000	0.044	0.497	6.374	0.001	5
CDF029	0.000	0.000	0.000	0.435	0.096	0.000	4
CDF030	0.000	0.000	0.405	1.026	2.407	0.010	5
CDF031	0.000	0.000	0.000	0.050	0.000	0.000	4
CDF032	0.000	0.000	0.000	0.106	0.075	0.001	4
CDF033	0.000	0.000	0.000	0.155	2.866	0.001	5
CDF034	0.000	0.000	0.000	0.086	0.005	0.000	4
CDF035	0.000	0.000	0.065	0.215	0.232	1.294	6
CDF037	0.000	0.000	6.779	0.057	1.683	0.000	3

ID. NO.	PC-F1	PC-F2	PC-F3	PC-F4	PC-F5	PC-F6	BEST GP.
CDF038	0.000	0.000	0.000	0.016	0.002	0.002	4
CDF039	0.006	0.000	6.376	0.001	0.009	0.007	3
CDF040	0.108	0.005	19.141	0.000	0.016	0.175	3
CDF041	0.000	0.000	0.195	0.002	0.011	0.005	3
CDF042	0.000	0.001	0.000	0.006	0.001	0.001	4
CDF043	0.000	0.000	21.142	0.013	0.155	0.001	3
CDF044	0.000	0.000	0.057	1.336	0.006	0.580	4
CDF045	0.009	0.000	9.424	0.004	0.100	0.096	3
CDF046	0.000	0.000	0.001	2.133	73.099	0.009	5
CDF047	0.000	0.000	0.001	0.032	0.004	0.000	4
CDF048	0.000	0.000	0.000	0.603	0.013	0.003	4
CDF049	0.000	0.000	0.027	0.000	0.000	0.001	3
CDF050	0.000	0.000	0.000	0.121	1.046	0.007	5
CDF051	0.000	0.000	0.006	3.278	14.358	0.068	5
CDF052	0.000	0.000	0.000	0.006	0.007	0.000	5
CDF053	0.004	0.000	1.963	0.000	0.002	0.001	3
CDF054	0.406	0.028	1.016	0.000	0.001	0.048	3
CDF055	0.000	0.000	0.000	0.011	0.047	0.001	5
CDF056	0.002	0.000	9.196	0.001	0.009	0.002	3
CDF057	0.000	0.000	42.159	0.029	1.088	0.000	3
CDF058	0.000	0.000	12.491	0.011	0.217	0.000	3
CDF059	0.000	0.000	0.096	1.782	0.000	0.018	4
CDF060	0.407	0.000	6.964	0.000	0.007	0.506	3
CDF061	0.001	0.000	2.587	0.013	0.016	0.003	3
CDF062	0.005	0.041	0.310	0.025	0.239	0.174	3
CDF063	0.004	0.041	0.175	0.007	1.918	14.405	6
CDF064	0.000	0.000	0.002	12.093	0.013	1.870	4
CDF065	0.002	0.000	21.793	0.013	0.052	0.010	3
CDF066	0.000	0.000	1.716	0.494	0.019	0.051	3
CDF067	0.000	0.001	0.000	0.013	0.002	0.007	4
CDF068	0.000	0.000	0.000	0.540	0.078	0.025	4
CDF069	0.000	0.000	0.000	1.359	5.694	0.007	5
CDF070	0.000	0.000	0.000	0.009	3.721	0.000	5
CDF071	1.730	0.005	1.711	0.000	0.046	1.351	1
CDF072	0.000	0.000	0.000	1.422	3.010	0.008	5
CDF073	0.000	0.000	3.939	0.002	0.016	0.000	3
CDF074	0.000	0.000	1.992	0.000	0.000	0.006	3
CDF075	0.000	0.000	0.000	5.334	0.051	0.614	4
CDF076	0.000	0.000	0.000	0.484	0.054	0.005	4
CDF077	0.000	0.000	0.000	1.486	0.120	0.050	4
CDF078	0.000	0.000	6.817	0.000	0.004	0.011	3
CDF079	0.000	0.000	0.000	4.774	32.734	0.186	5
CDF080	0.000	0.000	36.626	0.003	0.002	0.014	3
CDF081	0.000	0.000	0.000	0.356	2.070	0.003	5
CDF082	0.000	0.000	2.187	0.000	0.001	0.001	3

ID. NO.	PC-F1	PC-F2	PC-F3	PC-F4	PC-F5	PC-F6	BEST GP.
CDF083	0.001	0.000	21.952	0.031	0.239	0.054	3
CDF084	0.000	0.000	4.977	0.240	0.000	0.018	3
CDF085	0.000	0.000	0.001	0.751	18.498	0.000	5
CDF086	0.001	0.000	5.419	0.002	0.000	0.014	3
CDF087	32.353	1.520	0.818	0.000	0.011	0.813	1
CDF088	0.000	0.000	0.000	0.616	1.788	0.007	5
CDF089	0.000	0.000	0.994	0.036	0.380	0.000	3
CDF090	0.000	0.000	0.000	1.278	0.318	0.260	4
CDF091	0.000	0.000	1.669	5.017	0.001	0.796	4
CDF092	0.000	0.000	0.000	0.650	1.154	0.455	5
CDF093	0.000	0.000	0.000	1.325	0.777	0.009	4
CDF094	0.000	0.000	0.001	0.750	2.212	0.406	5
CDF095	0.000	0.000	22.590	0.001	0.009	0.003	3
CDF096	0.000	0.000	0.027	0.588	2.939	0.014	5
CDF097	0.000	0.000	0.000	0.292	0.014	0.000	4
CDF098	0.000	0.000	0.000	0.274	0.155	0.132	4
CDF099	0.000	0.000	75.429	0.008	0.062	0.006	3
CDF100	0.000	0.000	0.005	0.780	43.410	0.003	5
CDF101	0.000	0.000	0.000	1.043	0.029	0.005	4
CDF102	0.000	0.000	0.002	1.024	15.879	0.009	5
CDF103	0.000	0.000	0.004	0.000	0.000	0.000	3
CDF104	0.000	0.000	0.001	0.003	0.002	0.000	4
CDF105	0.000	0.000	0.000	0.468	0.814	0.008	5
CDF106	0.002	0.000	0.086	0.001	0.000	0.000	3
CDF107	0.000	0.000	0.014	0.000	0.000	0.000	3
CDF108	0.000	0.000	0.000	0.005	0.023	0.000	5

Probability Cutoff Values:
Group:

	0.01000	0.10000	1.00000	5.00000	10.00000	20.00000	100.00000
PC-F1	98	2	3	1	0	0	1
PC-F2	101	3	0	1	0	0	0
PC-F3	50	12	9	13	10	4	7
PC-F4	41	22	26	13	2	1	0
PC-F5	36	30	16	15	2	3	3
PC-F6	69	16	16	3	0	1	0

Summary of Best Classification of Projected Specimens: Classified Into Group:

	PC-F1	PC-F2	PC-F3	PC-F4	PC-F5	PC-F6	Total
From Group:							
PC-ARTS 2	0	45	29	26	3	105	
Total	2	0	45	29	26	3	105

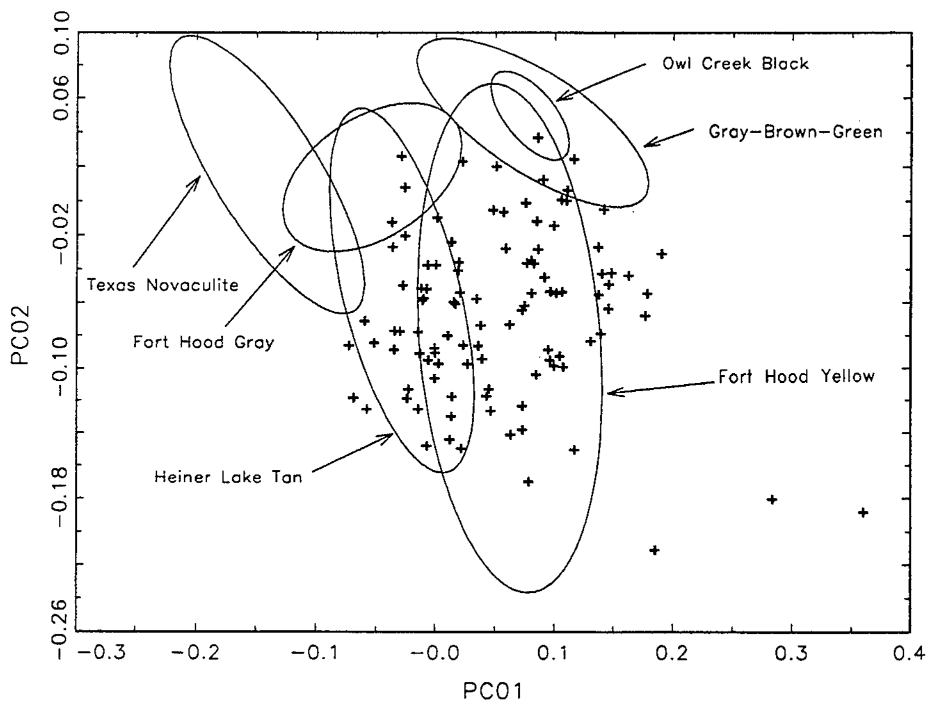

Figure 4.5 Bivariate Plot of the First and Second Principal Components for the Six Edwards Group Bedrock Source (90% Confidence Ellipses) and the 105 Artifacts Examined.

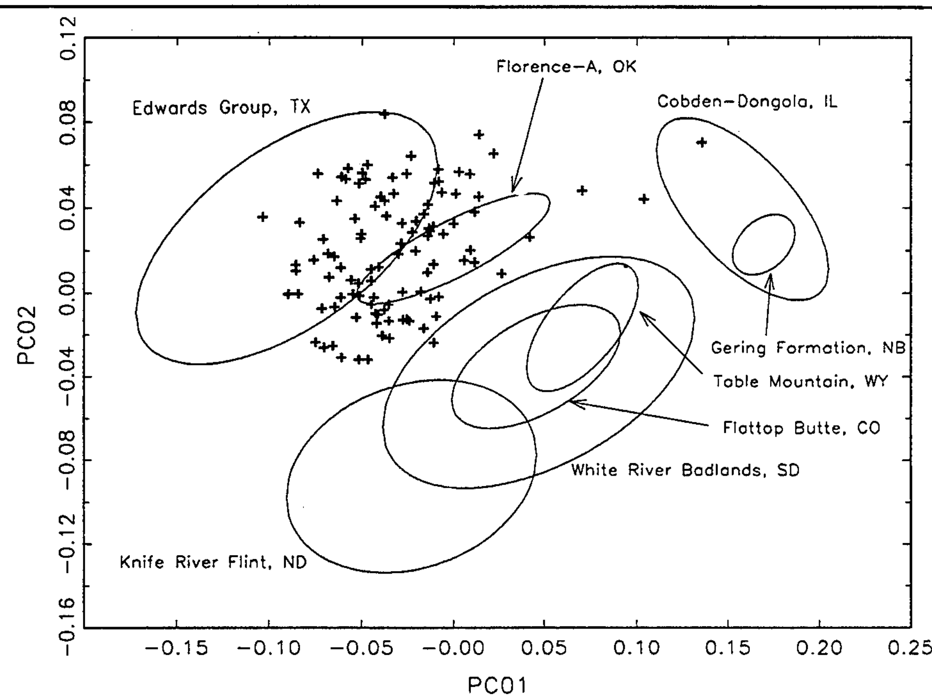

Figure 4.6 Bivariate Plot of the First and Second Principal Components for Several Different Cryptocrystalline Silicates Located in the Midcontinental U.S., and the 105 Artifacts Examined During this Study.

5.0 ANALYSIS OF THE PATINATION RESULTS

The results of the patina measurements for each artifact class are listed on Table 3.1, summarized in Tables 5.1 and 5.2, and are graphically illustrated in Figure 5.1. The raw data used to compile Table 3.1 is provided in Appendix A. The results of these measurements indicate that patination increases in both frequency and depth with time and are best viewed graphically in Figure 5.1. The left half of this figure (Figures 5.1A, 5.1B, and 5.1C) illustrates the mean and standard deviation of the patina thickness for each side of differentially patinated specimens, organized by temporal group. Side A, defined as being the most patinated side, is illustrated with a bold line, whereas side B, the least patinated, is shown with a lighter weight line. If no differential patination was observed, only a single bar is plotted for the specimen, and unpatinated specimens are indicated by an "x" with a patina thickness value of 0.0 mm. The right half, Figures 5.1D, 5.1E, and 5.1F, illustrate the mean and standard deviation for all observations for each artifact, and the group mean and standard deviation (dashed horizontal line and shaded area). In general, the number of patinated specimens within each group increases with group age. Only 11.4 percent of the Late Prehistoric arrows are patinated, whereas 54.3 percent of the Middle Archaic darts and 80 percent of the Paleoindian darts are patinated. This clearly demonstrates that patination is a progressive phenomenon, the older the group of artifacts, the greater the proportion of patinated specimens.

However, not only does the proportion of patinated artifacts within a given population increase with time, but the thickness of the patina increases as well (see Tables 5.1 and 5.2). The mean patina, calculated using all observations (sides A and B grouped), for the Late Prehistoric Scallorn points is 0.02 ± 0.071 mm. The Middle Archaic Pedernales darts exhibit significantly thicker patinas, with a group mean (all observations) of 0.12 ± 0.18 mm. Within the Paleoindian category, Golondrina points exhibited the largest group mean (0.45 ± 0.42 mm), and Plainview the smallest (0.28 ± 0.19 mm) with Angostura falling between the two with a group mean of 0.35 ± 0.41 mm. The mean patina for all Paleoindian projectiles as a group is 0.34 ± 0.36 mm. The impression that older artifacts have thicker patinas is clearly supported.

In order to test if the population means are significantly different, a t-test assuming unequal variances was performed. The results of this test between the mean patina for all observations for all three groups indicates that the group mean in each case is significantly different at the .01 level (Table 5.3) and that the three groups do not represent the same population. Alternatively, t-tests between the different Paleoindian type classes all failed to reject the null hypothesis and indicate that they represent the same populations.

5.1 DIFFERENTIAL PATINATION

The proportion of differentially patinated specimens relative to the number of patinated artifacts in each class is remarkably similar for each temporal group. About 64.5 percent of the patinated Paleoindian darts are differentially patinated, whereas this value is 63.2 percent for the Archaic darts and 75 percent for the Late Prehistoric arrows. In most cases, the degree of patination on Side A overlaps with the observed patina on Side B at one standard deviation, but this is not always the case (see Figure 5.1A-C). Approximately 22 to 25 percent of the differentially patinated specimens in the Archaic and Paleoindian groups exhibit patinas that do not overlap at all, whereas 66 percent of the patinated Late Prehistoric specimens fit this criteria.

Table 5.1 Summary of Descriptive Statistics for all Observations of Patina Thickness in Each Artifact Class.

	Plainview	Golondrina	Angustura	All Paleo	Pedernales	Scallorn
Mean	0.28	0.45	.035	0.34	0.12	0.02
Standard Deviation	0.194	0.419	0.411	0.357	0.179	0.071
Range	0.533	0.830	1.940	1.940	0.733	0.301
Maximum	0.53	0.830	1.94	1.94	0.73	0.30
Minimum	0	0	0	0	0	0
n	10	3	22	35	35	35

Table 5.2 Descriptive Statistics Reflecting Differentially Patinated Specimens.

	Plainview		Golondrina		Angustura		All Paleo		Pedernales		Scallorn	
Side	A	B	A	B	A	B	A	B	A	B	A	B
Mean	0.31	0.26	0.55	0.35	0.37	0.34	0.37	0.314	0.14	0.10	0.03	0.021
Standard Deviation	0.218	0.17	0.561	0.302	0.411	0.41	0.373	0.347	0.224	0.141	0.080	0.061
Range	0.625	0.546	1.121	0.540	1.940	1.940	1.940	1.940	0.934	0.533	0.356	0.245
Maximum	0.625	0.546	1.121	0.54	1.940	1.940	1.940	1.940	0.934	0.53	0.356	0.245
Minimum	0	0	0	0	0	0	0	0	0	0	0	0
n	10	10	3	3	22	22	35	35	35	35	35	35

Note: If no significant difference was observed between Side A and Side B, the value observed for Side A was used to calculate theSide B statistics.

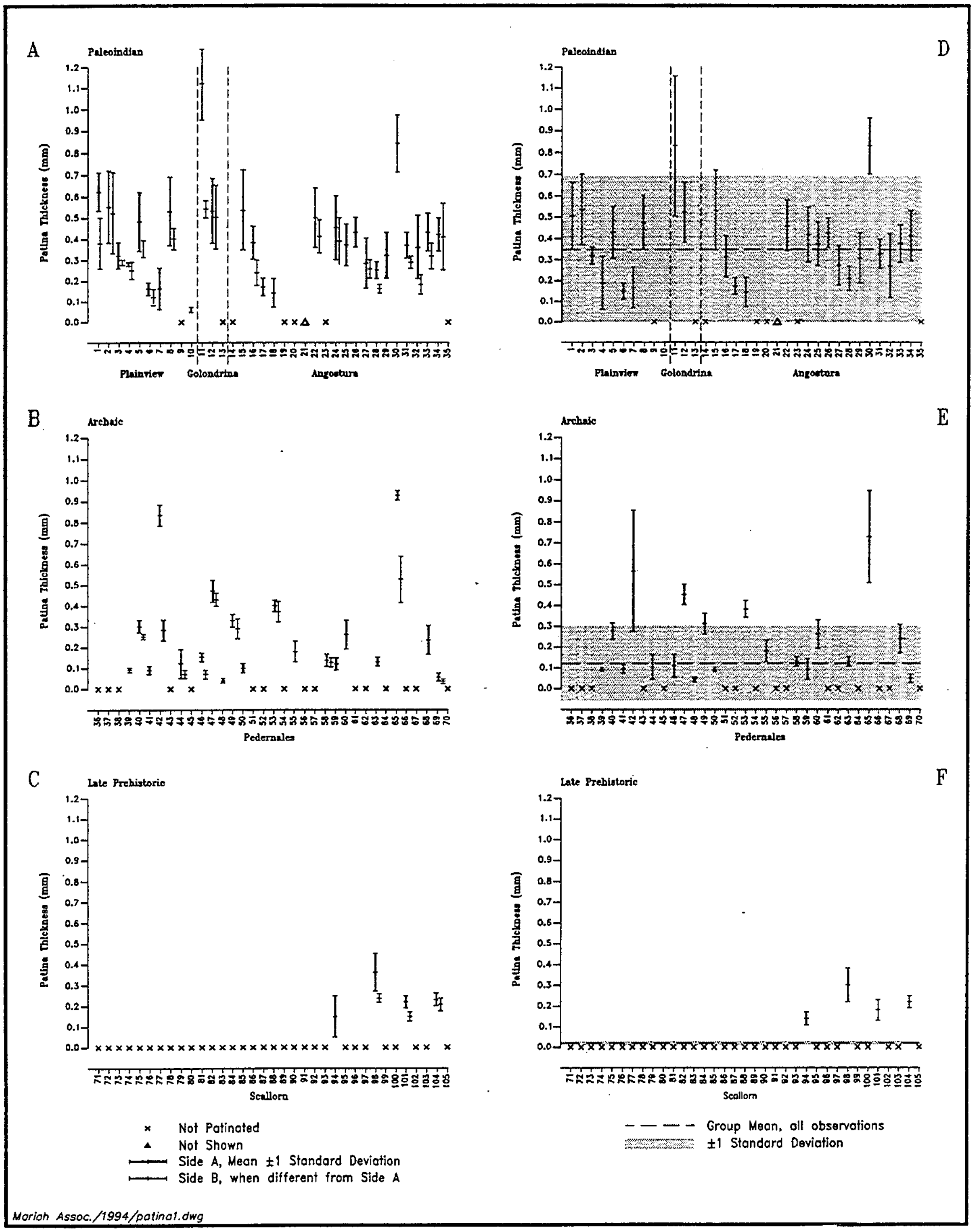

Figure 5.1 Plot Illustrating the Results of Patination by Point Type.

(A-C: In the left column, mean and standard deviation of patina rind thickness for each side of differentially patinated specimens are plotted separately, with side A being a heavier line width. The right side plots the mean of all observations for each artifact. A horizontal dashed line and screen show the group mean and one standard deviation, respectively.) (D-F: Mean patina thickness for side A plotted against mean patina thickness of side B. Side A was defined as the side with the thickest patina. This figure illustrates that although there is a close association between most differentially patinated specimens, significant differences may occur in older specimens (Middle Archaic and Paleoindian).

Table 5.3 t-Test for Two Samples Assuming Unequal Variances, a=0.01.

	Middle Archaic (n=35) mean = 0.1229 variance = 0.319	Late Prehistoric (n=35) mean = 0.0239 variance = 0.0050
Paleoindian (n=35) mean = 0.3403 variance = 0.1271	df = 50.07 t = 3.2243 t Critical two-tail = 2.6777 p(T<=t) two-tail = 0.0022	df = 36.67 t = 5.1484 t Critial two-tail = 2.7194 P(T<=t) two-tail = 9.581 x 10^{-6}
Middle Archaic		df = 44.38 t = 3.0461 t Critical two-tail = 2.6922 P(T<=t) two-tail = 0.0039

	Plainview (n=10) mean = 0.2768 variance = 0.0374	Golondrina (n=3) mean = 0.4496 variance = 0.1759
Angostura (n=22) mean = 0.3543 variance = 0.1692	df = 29.8922 t = -0.7241 t Critical two-tail = 2.7563 P(T<=t) two-tail = 0.4747	df = 2.5549 t = -0.3700 t Critical two-tail = 9.9249 P(T<=t) two-tail = 0.5606
Plainview		df = 2.2616 t = -0.6917 t Critical two-tail = 9.9249 P(T<=t) two-tail = 0.5606

5.2 RATE OF PATINATION

The observed rate of patination for each group, calculated as the group mean patina thickness divided by the upper and lower age bracket for each artifact class, appears to increase with elapsed time (Figure 5.2). The group mean rate of patination for Scallorn arrow points ranged between 1.6 and 2.6 x 10^{-5} mm/year, whereas the observed rate for Middle Archaic darts is nearly double that, with values ranging between 3.04 and 3.81 x 10^{-5} mm/year. There is considerable variation in the observed mean rate for each Paleoindian artifact class. The mean rate of patination for Angostura points falls between 3.97 and 4.32 x 10^{-5} mm/year, whereas Plainview ranges between 2.74 and 3.18 x 10^{-5} mm/year, and Golondrina exhibits the greatest variation with the observed rate falling between 5.12 to 10.9 x 10^{-5} mm/year. The exceptionally high observed rate of patination for Golondrina artifacts is probably unduly influenced by the small sample size for this artifact class. Taken as a whole, the mean rate of patination within the Paleoindian class overlaps with, but slightly exceeds, the Middle Archaic rate, with values falling between 3.3 and 4.19 x 10^{-5} mm/year.

If the rate of patination for each artifact is calculated in a similar manner and is considered in absence of nonpatinated specimens, it is clear that the rate of patination for artifacts in each class decreases with time. For instance, the four patinated Scallorn arrow points exhibit rates between 10 x 10^{-5} and 40 x 10^{-5} mm/year which overlaps with, but in general is far in excess of, the rate of patination observed in either the Middle Archaic or Paleoindian classes.

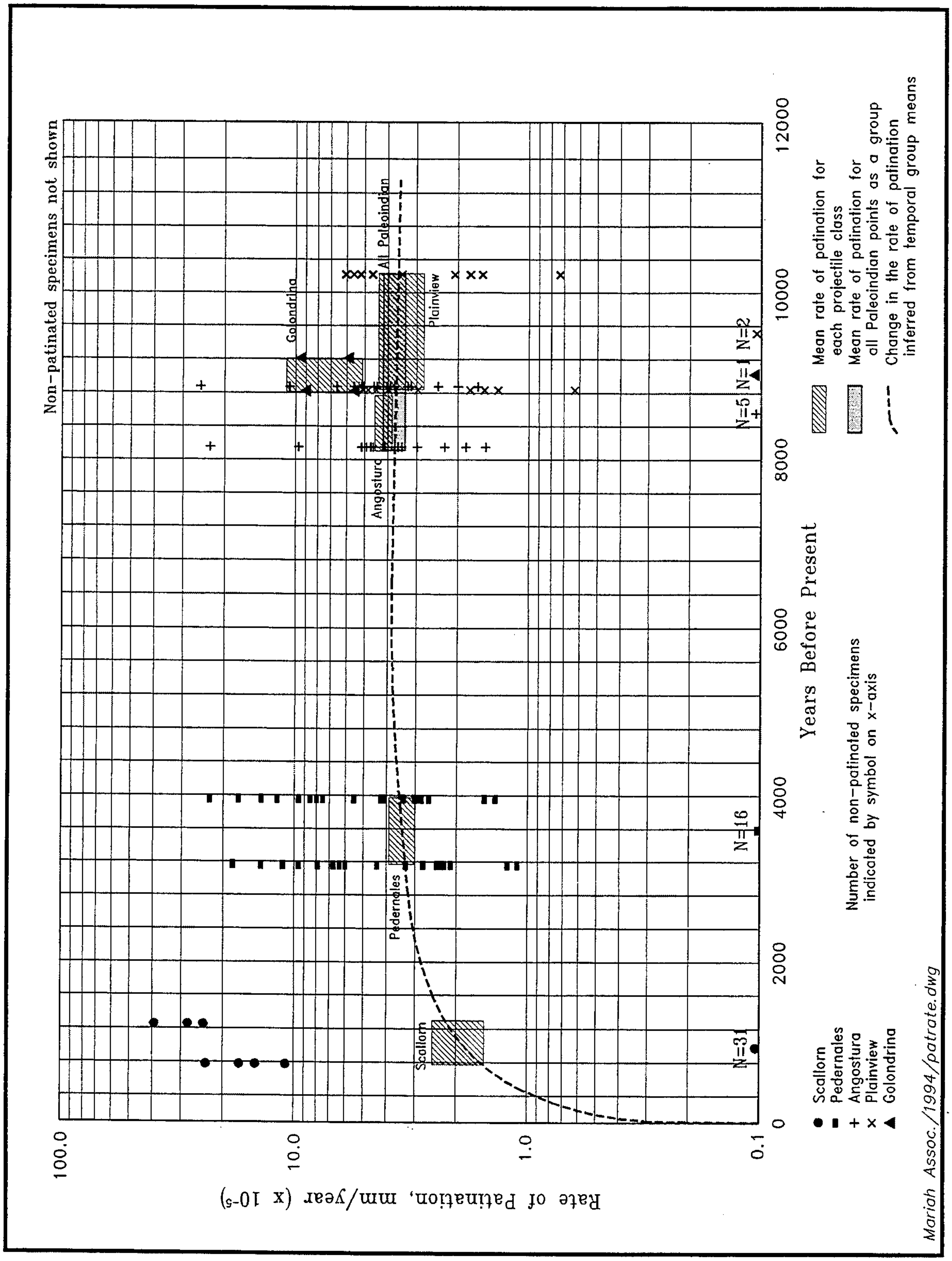

Figure 5.2 Plot of Mean Rate of Patination for Each Artifact Class (Boxes) and the Rate of Patination Calculated for Each Patinated Artifact in Each Class (Symbols).

These latter two classes exhibit ranges between 1.11 and 23 x 10^{-5} mm/year and 0.6 and 23 x 10^{-5} mm/year. Together, these data indicate that the change in patination rate is most rapid during the first millennium, and then decreases through time. The patination rate calculated for each temporal group, however, actually increases through time but there is considerable overlap in rate between Archaic and Paleoindian specimens.

5.3 INFLUENCE OF PARENT MATERIAL UPON PATINATION

The parent material characterization studies support the assumption that the majority of the artifacts are manufactured of Edwards Group chert. However, as mentioned previously, chert associated with the Edwards Group is highly heterogeneous, even within a relatively small region such as Fort Hood (see Frederick and Ringstaff 1994). During other work at Fort Hood, we began to notice that translucent varieties of Edwards chert appeared to patinate faster and more heavily than opaque varieties.There are sound reasons to suspect that translucent chert may patinate differently than opaque chert. For one, it is also widely accepted that chalcedony is more readily soluble in water than other varieties of quartz (Heaney and Post 1992:443; Leudtke 1992:109). Recently, Heaney and Post (1992) have observed that most cherts, chalcedony in particular, contain significant quantities of a relatively unknown quartz polymorph known as moganite and that moganite, is significantly more soluble than quartz in water. They further speculated that the apparently increased solubility of chalcedony is in part due to its moganite component. Leudtke (1992:6) notes that "most, if not all, cherts made up of chalcedony are indeed translucent" but that the converse is not necessarily true. If translucent cherts found in the Edwards Group contain a large proportion of chalcedony, then the rate and extent of patination for translucent chert may be greater than opaque cherts. In order to test this observation we decided to pose it as a hypothesis stating that translucent chert artifacts within the same temporal group are significantly more patinated than opaque cherts artifacts. The null hypothesis states that there is no significant difference between the two groups.

As part of the artifact documentation process, the translucency of each artifact was measured according to the technique outlined in Leudtke (1992:68) where the artifact is held a constant distance from a 75 watt light bulb and the point at which the artifact becomes opaque is measured. For this analysis we arbitrarily identified a translucent chert as those exhibiting measurements >2 mm. Previous examination of bedrock sources at Fort Hood indicated that translucency values range between <1 mm and about 15 mm, but all of the clearly translucent cherts have values >2 mm (Frederick and Ringstaff 1994).

We subsequently compared the overall mean patina values between the opaque and translucent artifacts in two temporal groups (Archaic and Paleoindian). Of the Paleoindian artifacts made from translucent chert (specimens 8,10, 13, 17, 20, 21, 24, 27, 31, and 32), 80 percent are patinated and the mean observed patina for this group is 0.39 mm, which is slightly greater than the group mean (0.34 mm). Likewise, the mean patina for Pedernales darts made from similarly translucent chert (specimens 39, 40, 44, 47, 52, 59, 61, 65, and 68) is 0.21 mm, or nearly double the group mean of 0.12 mm. In the case of the Middle Archaic darts, 78 percent of the translucent chert artifacts are patinated, whereas only 54 percent of the total population of Pedernales darts are patinated. A t-test assuming unequal variances between the translucent and opaque groups for both temporal classes indicates that for an $\alpha = .05$, neither of the means are significantly different and the null hypothesis cannot be rejected. Therefore we find no significant difference in the degree of patination between opaque and translucent chert. However, given that 24 percent more of the Pedernales darts made of translucent material are patinated, it appears that translucent materials may patinate more quickly. Given that the presence of a white patina may interfere with obtaining a true

translucency value for patinated artifacts, a better test of this hypothesis may be accomplished by measuring the patina thickness induced on flakes of known translucency by exposure to a caustic solution for a set period of time.

5.4 RELATIONSHIP OF SOIL pH AND PATINATION

In order to evaluate what, if any, relationship exists between soil pH and the extent of patination, we revisited the point of collection for 56 artifacts in the examined group that were found in the maneuver areas at Fort Hood (and therefore easily accessible). At each location we collected one or more soil sample that represented the full range of soil variability at that site and then measured the pH of a 1:1 soil-to-water paste after a 24 hour period with a Corning Checkmate portable pH meter. Where more than one sample was collected, the pH values were averaged. The results demonstrate that the examined surface soils range from slightly above neutral (7.03) to slightly alkaline (8.29), with the mean value being 7.75. Correlation of soil pH and the total mean patina values reveals that there is no systematic relationship present ($r=-0.032$). It is possible that edaphic environments exhibiting a wider range of pH or a more uniformly alkaline pH may indeed influence the patination process, but within the examined population, soil pH appears to have no influence on the observed degree of patination.

6.0 CONCLUSIONS

Although previous research has cast doubt on the existence of measurable or consistent temporal component to chert patination, the results of this study clearly demonstrate that at a population level, the formation of white patina is progressive in both frequency and magnitude through time. It is also clear that the lack of a patina on any individual artifact is virtually meaningless, since more than 20 percent of all of the artifacts examined in each temporal class were unpatinated. Comparison of the mean patinas between groups demonstrated that each group is significant at the .01 level.

Previous researchers have concluded that this form of patination is a selective leaching process which is diffusion controlled, and have suggested that the rate of leaching should decrease with time (Purdy and Clark 1987:215). Our results indicate that the rate of patination (leaching) for a population actually increases with time, and therefore may not be simply a diffusion-controlled process, although when only patinated specimens are considered, the rate of patination does decrease with time. There is no evidence to support the assertion that more translucent artifacts patinate more deeply than opaque artifacts of the same age, but the significantly greater proportion of patinated artifacts among the Pedernales artifacts made of translucent chert suggests that translucent material may patinate more quickly.

The parent material controls employed in this study suggest that the majority of the artifacts are made of Edwards Group chert. However, the INAA bedrock source data base used in this study to identify Edwards chert is in need of refinement. The bedrock assemblage characterized for this study includes only 37.5 percent of the known varieties of Edwards chert that occur on Fort Hood (cf. Frederick and Ringstaff 1994), and the taxonomy presented by Frederick and Ringstaff is known to underestimate the actual physical variability of Edwards chert in this region and is itself in need of refinement. With respect to the parent material influence on the patination process, Edwards Group chert is more heterogeneous in appearance than most other cryptocrystalline silicates and therefore the properties influencing patination are more variable as well. Hence, some of the noise observed may be attributable to the parent material properties of the individual artifact. In specific, porosity and mineralogy may hold considerable promise in understanding the variable nature of chert patination.

It is well established that silica (both quartz and amorphous silica) are more soluble in solutions with elevated pH (>8), and numerous previous studies have suggested that edaphic conditions such as soil pH may strongly influence the rate of patination. Our observations indicate that there is no correlation between soil pH and the extent or rate of patination. It is possible that the pH of soil water and groundwater may deviate from the soil pH, but we cannot comment on this relationship. However, the complete lack of correlation of soil pH, and patination implies that other factors, besides time and soil pH are responsible for the observed variability in patination.

So what are the prospects of applying patination as a tool in separating mixed-age debitage assemblages into temporally meaningful groups for analysis? In order to do this one must first define age groups on the basis of patina thickness, and then have an expedient means of measuring the patina. Although the latter is not currently available, we can model the results of such an experiment using the data presented in Table 3.1. For this example, we will assume that Late Prehistoric artifacts are unpatinated, Archaic artifacts will exhibit a patina between 0 and 0.15 mm, and Paleoindian artifacts will exhibit patinas >0.15 mm. If we then reclassify the artifacts in each temporal group using these criteria, we can evaluate the success of such an analysis (Table 6.1).

Table 6.1 Predictive Accuracy of Projectile Point Age Based on Patina Thickness, All Artifacts.

Date Based on Morphology	Point Type	Date Based on Patina Thickness: Paleoindian (>.15 mm)	Archaic (0-.15 mm)	Late Prehistoric (0 mm)	Total
Late Prehistoric	Scallorn	3	1	31	35
Archaic	Pedernales	9	10	16	35
Paleoindian	Plainview, Angostura, Golondrina	25	3	7	35
Total		37	14	54	105

In the Paleoindian class, 29 percent would be misidentified, and 70 percent of the those artifacts (n=7) would fall in the Late Prehistoric patina group. Nearly three quarters of the Archaic artifacts are misclassified by this approach, with 25.7 percent identified as Paleoindian and 45.7 percent classified as Late Prehistoric. All but 11.4 percent of the late Prehistoric artifacts would be classified correctly, but of the four artifacts that patinated, three would be placed into the Paleoindian category.

If we modify the strategy to only examine patinated artifacts, the numbers change a little Table 6.2. Using the same group thresholds, but reducing the population to include only patinated artifacts in each group, 89.3 percent of the Paleoindian artifacts are correctly classified and the remainder are misidentified as Archaic. Approximately half (52.6%) of the patinated Pedernales darts would be assigned an Archaic age and 47.4 percent would be identified as Paleoindian. Since we defined the Late Prehistoric category as unpatinated, the error in misclassification remains the same.

Obviously the relative error is going to change as a function of the threshold assumed for the boundary between the Paleoindian and Archaic classes. It is also possible that the errors incurred by applying this technique on a single site may be somewhat smaller since the artifact parent material and environmental factors will probably be more uniform than the sampled population used in this model. However, just using the relative degree of patination to separate mixed age assemblage of debitage into different "age" classes will be more accurate for patinated specimens than unpatinated ones, since about 33 percent of the artifacts in the two categories we have considered to be "patinated" (Paleoindian and Middle Archaic) were not.

In summary, the results of this study suggest that it is unlikely that chert patination will ever develop into a reliable dating method. The observed variability effectively negates the significant temporal component of the patination process which is present in the data. Factors previously recognized as influential in patination, specifically parent material mineralogy and porosity, may explain much of the variability observed in this experiment, and should be investigated further. We find that Rottländer's (1975b) assertion that a patina says nothing about an artifact's age misleading, since time and patination are clearly related. His statement might be better reworded to say that the lack of a patina says nothing about an artifact's age.

Table 6.2 Predictive Accuracy of Projectile Point Age Based on Patina Thickness, Patinated Artifacts Only.

		Date Based on Patina Thickness			
Date Based on Morphology	Point Type	Paleoindian (>.15 mm)	Archaic (0-.15 mm)	Late Prehistoric (0 mm)	Total
Late Prehistoric	Scallorn	3	1	na	4
Archaic	Pedernales	9	10	na	19
Paleoindian	Plainview, Angostura, Golondrina	25	3	na	28
Total		37	14	na	51

7.0 REFERENCES CITED

Ahler, Stanley A.
1991 U.V. Fluorescence as a Relative Age Indicator in Knife River Flint Artifacts. Paper presented at the 49th Plains Anthropological Conference, Lawrence, Kansas. Manuscript in the possession of the Authors.

Benedict, James B.
1992 Sacred Hot Springs, Instant Patinas. *Plains Anthropologist* 37(138):1-6.

Callister, Kathleen, Jay Peck, and J. Michael Quigg
1994 Analysis and Variation in Fort Hood Projectile Points. In Archeological Investigations on 571 Prehistoric Sites at Fort Hood, Bell and Coryell Counties, Texas, edited by W. Nicholas Trierweiler. *Fort Hood Archeological Resource Management Series No. 31*, pp 294-318.

Christensen, R. C.
1991 *Instrumental Neutron Activation Analysis of Knife River Flint from the Primary Source Area: Phase I: Elemental Description and Statement of Variability*. Masters Thesis, Department of Sociology and Anthropology, University of Mississippi, 176 pages.

Collins, Michael B., C. Britt Bousman, Paul Goldberg, Paul R. Takac, Jan C. Guy, Jose Luis Lanata, Thomas W. Stafford, and Vance T. Holliday
1993 The Paleoindian Sequence at the Wilson-Leonard Site, Texas. *Current Research in the Pleistocene* 10:10-12.

Curwen, Cenil E.
1940 The White Patination of Black Flint. *Antiquity* 14:435-437.

Davis, J. C.
1986 *Statistics and Data Analysis in Geology*. 2nd edition, John Wiley and Sons: New York.

Dickens, William
1993 Lithic Analysis, In *Archaeological Investigations in Bull Branch: Results of the 1990 Summer Archaeological Field School*, edited by D. L. Carlson, pp. 79-116. Archaeological Management Series Research Report Number 19. United States Army, Fort Hood, Texas.

Frederick, Charles D., and Christopher Ringstaff
1994 Lithic Resources at Fort Hood: Further Investigations. In Archeological Investigations on 571 Prehistoric Sites at Fort Hood, Bell and Coryell Counties, Texas, edited by W. Nicholas Trierweiler. *Fort Hood Archeological Resource Management Series No. 31*, pp 125-181.

Glascock, M. D., J. M. Elam, and R. H. Cobean
1988 Differentiation of Obsidian Sources in Mesoamerica. In *Archaeometry '88*, edited by R. M. Farquhar, R. G. V. Hancock, and L. A. Pavlish, pp. 245-251. University of Toronto.

Goodwin, A. J. H.
1960 Chemical Alteration (Patination) of Stone. In *The Application of Quantitative Methods in Archaeology*, edited by R. F. Heizer and S. F. Cook, pp. 300-323. Viking Fund Publications in Archaeology 28. New York: Wenner Gren Foundation.

Heaney, Peter J., and Jeffrey E. Post
1992 The Widespread Distribution of a Novel Silica Polymorph in Microcrystalline Quartz Varieties. *Science* 255:441-443.

Hester, Thomas R., Harry J. Shafer, Thomas C. Kelly, and Giancarlo Ligabue
1982 Observations on the Patination Process and the Context of Antiquity: a Fluted Projectile Point from Belize, Central America. *Lithic Technology* 11(2):29-34.

Hester, Thomas R.
1983 Late Paleo-Indian Occupations at Baker Cave, Southwestern Texas. *Bulletin of the Texas Archaeological Society* 53:101-119.

Hillsman, Matthew J.
1992 *Evaluation of Visible and Ultraviolet-excited Attributes of Some Texas and Macroscopically Similar New Mexico Cherts*. Unpublished Masters thesis, Eastern New Mexico University.

Hoard, R. J., S. R. Holen, M. D. Glascock, H. Neff, and J. M. Elam
1992 Neutron Activation Analysis of Stone from the Chadron Formation and a Clovis Site on the Great Plains. *Journal of Archaeological Science* 19:655-665.

Hoard, R. J., J. R. Bozell, S. R. Holen, M. D. Glascock, H. Neff, and J. M. Elam
1993 Source Determination of White River Group Silicates from Two Archaeological Sites in the Great Plains. *American Antiquity* 58:698-710.

Hoffman, Jack L., Lawrence C. Todd, and Michael B. Collins
1991 Identification of Central Texas Edwards Chert at the Folsom and Lindenmeier Sites. *Plains Anthropologist* 36:297-308.

Holliday, Vance T.
1987 Cultural Chronology. In *Lubbock Lake: Late Quaternary Studies on the Southern High Plains*, edited by Eileen Johnson, pp. 22-25. College Station, Texas, Texas A & M University Press.

Hurst, Vernon J., and A. R. Kelley
1961 Patination of Cultural Flints. *Science* 134(3474):251-256.

Jelks, Edward b.
1993 Observations on the Distributions of Certain Arrow-point Types in Texas and Adjacent Regions. *Lithic Technology* 18:9-15.

Judd, J. W.
1887 On the Unmaking of Flints. *Proceedings of the Geological Association* 10:217-226.

Luedtke, B. E.
1978 Chert Sources and Trace Element Analysis. *American Antiquity* 43:413-423.

Luedtke, B. E.
1992 *An Archaeologist's Guide to Chert and Flint*. Institute of Archaeology, University of California, Los Angeles. 172 pages.

McGinley, A. N. and E. A. Schweikert
1979 Neutron Activation Analysis of Flints from the Edwards Formation. *Journal of Radioanalytical Chemistry* 52:101-110.

Morrow, C. A., J. M. Elam, and M. D. Glascock
1992 The Use of Blue-grey Chert in Midwestern Prehistory: The Need for Baseline Data. *Midcontinental Journal of Archaeology* 17:166-197.

Neff, H.
1990 A Series of Routines Written in GAUSS Language. Unpublished programs. Missouri University Research Reactor.

Neff, H.
1994 RQ-Mode Principal Components Analysis of Ceramic Compositional Data. *Archaeometry* 36:115-130.

Péw,, Troy L
1954 The Geological Approach to Dating Archaeological Sites. *American Antiquity* 20:51-61.

Purdy, Barbara A., and David E. Clark
1978 Weathering Studies of Chert: A Potential Solution to the Chronology Problem in Florida. *Proceedings of the 18th International symposium on Archaeometry and Archaeological Prospection*, Bonn, pp. 440-450.

Purdy, Barbara A., and David E. Clark
1987 Weathering of Inorganic Materials: Dating and Other Applications. *Advances in Archaeological Method and Theory*, Vol. 11, pp. 211-253.

Rosenfeld, Andrée
1965 *The Inorganic Raw Materials of Antiquity*. New York: Frederick A. Praeger, 245 p.

Rottländer, R.
1975a Some Aspects of the Patination of Flint. In *Staringia No. 3, Second International Symposium on Flint*, pp. 54-56.

Sayre, E.V.
1975 Brookhaven Procedures for Statistical Analyses of Multivariate Archaeometric Data. Brookhaven National Laboratory Report BNL-23128. New York (unpublished).

Schmalz, Robert F.
1960 Flint and the Patination of Flint Artifacts. *Proceedings of the Prehistoric Society* 26(3):44-49.

Service, E.
1941 Lithic Patina as an Age Criterion. *Papers of the Michigan Academy of Science, Arts and Letters* 27:553-557.

Thoms, Alston V.
1993 Knocking Sense from Old Rocks: Typologies and the Narrow Perspective of the Angostura Point Type. *Lithic Technology* 18:16-27.

Trierweiler, W. Nicholas (editor)
1994 Archeological Investigations on 571 Prehistoric Sites at Fort Hood, Bell and Coryell Counties, Texas. *Fort Hood Archeological Resource Management Series, No. 31.*

Tunnell, Curtis
1978 *The Gibson Lithic Cache from West Texas*. Office of the State Archaeologist, Texas Historical Commission, Office of the State Archaeologist Report 30, Austin, Texas.

Turner, Ellen Sue, and Thomas R. Hester
1993 *A Field Guide to Stone Artifacts of Texas Indians*, second edition. Gulf Publishing Company, Houston, Texas.

VanNest, Julieann
1985 Patination of Knife River Flint artifacts. *Plains Anthropologist* 30-110:325-339.

APPENDIX A

Sample Identification Cross List and Raw Data for Patination and Soil pH Observations

Table A-1 Sample Identification Cross List and Raw Data for Patination and Soil pH Observations.

			Raw Data Side A (mm)					Raw Data Side B (mm)									
Sample Rank	Accession Number	Point Type	1	2	3	4	5	1	2	3	4	5	Soil pH	Ass'd Min Age	Calc Min Rate	Ass'd Max Age	Calc Max Rate min
1	03-0028	Plainview	0.506	0.671	0.744	0.584	0.618	0.329	0.242	0.399	0.351	0.565	nd	8800	4.91	10200	5.69
2	03-0041	Plainview	0.393	0.719	0.697	0.528	0.267	0.725	0.587	0.643	0.478	0.298	nd	8800	5.23	10200	6.06
3	30-0403	Plainview	0.348	0.289	0.298	0.264	0.419	0.287	0.292	0.320	0.289	0.284	7.98	8800	3.03	10200	3.51
4	30-0444	Plainview	0.278	0.287	0.000	0.000	0.000	0.222	0.315	0.225	0.267	0.219	7.78	8800	1.78	10200	2.06
5	30-0772	Plainview	0.444	0.579	0.677	0.382	0.343	0.320	0.362	0.331	0.309	0.413	7.49	8800	4.08	10200	4.73
6	30-1559	Plainview	0.118	0.160	0.205	0.163	0.157	0.163	0.104	0.065	0.121	0.129	8.29	8800	1.36	10200	1.57
7	35-2881	Plainview	0.065	0.053	0.157	0.213	0.301	nd	nd	nd	nd	nd	nd	8800	1.55	10200	1.79
8	35-2882	Plainview	0.270	0.590	0.514	0.624	0.666	0.472	0.396	0.382	0.416	0.348	nd	8800	4.59	10200	5.31
9	36-3107	Plainview	nd	nd	nd	nd	nd	nd	nd	nd	nd	nd	7.90	8800	0.00	10200	0.00
10	44-0553	Plainview	0.053	0.079	0.076	0.065	0.048	nd	nd	nd	nd	nd	7.90	8800	0.63	10200	0.73
11	03-0026	Golondrina	1.216	1.258	1.264	0.907	0.958	0.545	0.607	0.514	0.494	0.539	nd	8780	9.05	9180	9.46
12	04-0002	Golondrina	0.486	0.632	0.295	0.596	0.663	0.657	0.601	0.365	0.559	0.331	nd	8780	5.65	9180	5.91
13	13-0014	Golondrina	nd	nd	nd	nd	nd	nd	nd	nd	nd	nd	nd	8780	0.00	9180	0.00
14	02-0223	Angostura	nd	nd	nd	nd	nd	nd	nd	nd	nd	nd	nd	8100	0.00	8800	0.00
15	03-0042	Angostura	0.351	0.315	0.548	0.685	0.750	nd	nd	nd	nd	nd	nd	8100	6.02	8800	6.54
16	03-0043	Angostura	0.435	0.475	0.396	0.301	0.315	0.315	0.281	0.242	0.152	0.208	nd	8100	3.54	8800	3.85
17	1-1286-001	Angostura	0.202	0.208	0.118	0.152	0.160	nd	nd	nd	nd	nd	7.97	8100	1.91	8800	2.07
18	13-0010	Angostura	0.152	0.048	0.124	0.129	0.247	nd	nd	nd	nd	nd	nd	8100	1.59	8800	1.73
19	2-821-001	Angostura	nd	nd	nd	nd	nd	nd	nd	nd	nd	nd	8.01	8100	0.00	8800	0.00
20	21-0020	Angostura	nd	nd	nd	nd	nd	nd	nd	nd	nd	nd	7.81	8100	0.00	8800	0.00
21	21-0037	Angostura	nd	nd	nd	nd	nd	nd	nd	nd	nd	nd	nd	8100	22.05	8800	23.95
22	23-0003	Angostura	0.576	0.517	0.548	0.258	0.624	0.522	0.388	0.396	0.306	0.421	7.29	8100	5.18	8800	5.62
23	25-0035	Angostura	nd	nd	nd	nd	nd	nd	nd	nd	nd	nd	nd	8100	0.00	8800	0.00
24	25-0041	Angostura	0.663	0.531	0.292	0.390	0.374	0.492	0.520	0.326	0.354	0.267	nd	8100	4.78	8800	5.19
25	25-0139	Angostura	0.404	0.334	0.419	0.483	0.219	nd	nd	nd	nd	nd	nd	8100	4.23	8800	4.59
26	30-0007	Angostura	0.407	0.528	0.368	0.388	0.475	nd	nd	nd	nd	nd	7.80	8100	4.92	8800	5.35
27	30-0484	Angostura	0.154	0.236	0.197	0.444	0.365	0.208	0.264	0.233	0.326	0.275	7.76	8100	3.07	8800	3.34
28	30-439	Angostura	0.261	0.272	0.312	0.208	0.216	0.138	0.174	0.163	0.169	0.143	7.28	8100	2.34	8800	2.54
29	33-0018	Angostura	0.455	0.362	0.191	0.368	0.228	nd	nd	nd	nd	nd	nd	8100	3.65	8800	3.96
30	33-0045	Angostura	0.896	0.871	0.952	0.860	0.618	nd	nd	nd	nd	nd	7.89	8100	9.54	8800	10.36
31	35-0178	Angostura	0.382	0.317	0.315	0.376	0.472	0.326	0.295	0.275	0.242	0.289	nd	8100	3.74	8800	4.06
32	40-0982	Angostura	0.233	0.371	0.618	0.264	0.315	0.138	0.138	0.174	0.267	0.166	7.35	8100	3.05	8800	3.31
33	40-1025	Angostura	0.514	0.478	0.281	0.390	0.466	0.343	0.326	0.402	0.323	0.228	7.09	8100	4.26	8800	4.63
34	40-1043	Angostura	0.360	0.463	0.534	0.441	0.323	0.688	0.315	0.275	0.393	0.365	7.86	8100	4.72	8800	5.13
35	54-0005	Angostura	nd	nd	nd	nd	nd	nd	nd	nd	nd	nd	nd	8100	0.00	8800	0.00
36	05-0048	Pedernales	nd	nd	nd	nd	nd	nd	nd	nd	nd	nd	nd	3150	0.00	3950	0.00
37	05-0050	Pedernales	nd	nd	nd	nd	nd	nd	nd	nd	nd	nd	nd	3150	0.00	3950	0.00
38	05-0051	Pedernales	nd	nd	nd	nd	nd	nd	nd	nd	nd	nd	nd	3150	0.00	3950	0.00
39	11-0006	Pedernales	0.104	0.079	0.101	0.081	0.084	nd	nd	nd	nd	nd	7.87	3150	2.27	3950	2.85
40	25-0010	Pedernales	0.331	0.337	0.267	0.281	0.267	0.258	0.222	0.247	0.256	0.247	nd	3150	6.87	3950	8.61
41	25-0018	Pedernales	0.090	0.079	0.098	0.115	0.067	nd	nd	nd	nd	nd	nd	3150	2.28	3950	2.85
42	25-0023	Pedernales	0.902	0.823	0.837	0.795	0.787	0.348	0.272	0.250	0.340	0.225	nd	3150	14.12	3950	17.71
43	30-0073	Pedernales	nd	nd	nd	nd	nd	nd	nd	nd	nd	nd	8.12	3150	0.00	3950	0.00

			Raw Data Side A (mm)					Raw Data Side B (mm)									
Sample Rank	Accession Number	Point Type	1	2	3	4	5	1	2	3	4	5	Soil pH	Ass'd Min Age	Calc Min Rate	Ass'd Max Age	Calc Max Rate min
44	30-0533	Pedernales	0.053	0.073	0.087	0.208	0.191	0.053	0.067	0.076	0.053	0.107	7.54	3150	2.45	3950	3.08
45	30-0689	Pedernales	nd	nd	nd	nd	nd	nd	nd	nd	nd	nd	nd	3150	0.00	3950	0.00
46	30-1997	Pedernales	0.140	0.118	0.143	0.180	0.163	0.062	0.059	0.096	0.053	0.076	7.80	3150	2.76	3950	3.46
47	30-1999	Pedernales	0.472	0.542	0.466	0.399	0.461	0.427	0.402	0.433	0.396	0.480	8.26	3150	11.33	3950	14.21
48	30-2000	Pedernales	0.051	0.042	0.039	0.039	0.048	nd	nd	nd	nd	nd	7.90	3150	1.11	3950	1.39
49	30-2012	Pedernales	0.303	0.320	0.331	0.388	0.315	0.289	0.312	0.340	0.306	0.199	nd	3150	7.86	3950	9.85
50	30-2090	Pedernales	0.110	0.087	0.090	0.087	0.121	0.101	0.081	0.093	0.101	0.076	7.84	3150	2.40	3950	3.01
51	35-2204	Pedernales	nd	nd	nd	nd	nd	nd	nd	nd	nd	nd	nd	3150	0.00	3950	0.00
52	35-2205	Pedernales	nd	nd	nd	nd	nd	nd	nd	nd	nd	nd	nd	3150	0.00	3950	0.00
53	35-2384	Pedernales	0.379	0.368	0.402	0.407	0.447	0.435	0.393	0.331	0.320	0.354	nd	3150	9.71	3950	12.18
54	35-2391	Pedernales	nd	nd	nd	nd	nd	nd	nd	nd	nd	nd	nd	3150	0.00	3950	0.00
55	35-2392	Pedernales	0.242	0.219	0.143	0.135	0.140	nd	nd	nd	nd	nd	nd	3150	4.45	3950	5.58
56	35-2395	Pedernales	nd	nd	nd	nd	nd	nd	nd	nd	nd	nd	nd	3150	0.00	3950	0.00
57	35-2647	Pedernales	nd	nd	nd	nd	nd	nd	nd	nd	nd	nd	nd	3150	0.00	3950	0.00
58	35-2652	Pedernales	0.124	0.152	0.185	0.129	0.118	0.112	0.110	0.121	0.135	0.149	nd	3150	3.38	3950	4.24
59	35-2884	Pedernales	0.129	0.115	0.152	0.143	0.084	0.051	0.053	0.042	0.045	0.037	nd	3150	2.15	3950	2.70
60	36-3001	Pedernales	0.213	0.275	0.166	0.281	0.348	nd	nd	nd	nd	nd	7.64	3150	6.50	3950	8.15
61	36-3642	Pedernales	nd	nd	nd	nd	nd	nd	nd	nd	nd	nd	nd	3150	0.00	3950	0.00
62	36-3883	Pedernales	nd	nd	nd	nd	nd	nd	nd	nd	nd	nd	nd	3150	0.00	3950	0.00
63	37-0669	Pedernales	0.138	0.112	0.171	0.121	0.129	nd	nd	nd	nd	nd	7.98	3150	3.40	3950	4.26
64	38-0021	Pedernales	nd	nd	nd	nd	nd	nd	nd	nd	nd	nd	7.78	3150	0.00	3950	0.00
65	38-0098	Pedernales	0.949	0.921	0.919	0.966	0.913	0.598	0.629	0.607	0.424	0.407	7.93	3150	18.57	3950	23.28
66	38-0733	Pedernales	nd	nd	nd	nd	nd	nd	nd	nd	nd	nd	7.94	3150	0.00	3950	0.00
67	38-0816	Pedernales	nd	nd	nd	nd	nd	nd	nd	nd	nd	nd	7.65	3150	0.00	3950	0.00
68	44-1253M	Pedernales	0.292	0.250	0.205	0.146	0.312	nd	nd	nd	nd	nd	nd	3150	6.10	3950	7.65
69	44-1443M	Pedernales	0.045	0.048	0.034	0.067	0.081	0.045	0.039	0.039	0.048	0.034	nd	3150	1.22	3950	1.52
70	44-1614M	Pedernales	nd	nd	nd	nd	nd	nd	nd	nd	nd	nd	nd	3150	0.00	3950	0.00
71	02-0154	Scallorn	nd	nd	nd	nd	nd	nd	nd	nd	nd	nd	8.08	750	0.00	1250	0.00
72	02-0203	Scallorn	nd	nd	nd	nd	nd	nd	nd	nd	nd	nd	7.65	750	0.00	1250	0.00
73	03-0007	Scallorn	nd	nd	nd	nd	nd	nd	nd	nd	nd	nd	nd	750	0.00	1250	0.00
74	03-0008	Scallorn	nd	nd	nd	nd	nd	nd	nd	nd	nd	nd	nd	750	0.00	1250	0.00
75	13-0060	Scallorn	nd	nd	nd	nd	nd	nd	nd	nd	nd	nd	nd	750	0.00	1250	0.00
76	2-348-001	Scallorn	nd	nd	nd	nd	nd	nd	nd	nd	nd	nd	7.31	750	0.00	1250	0.00
77	2-348-006	Scallorn	nd	nd	nd	nd	nd	nd	nd	nd	nd	nd	7.31	750	0.00	1250	0.00
78	2-348-007	Scallorn	nd	nd	nd	nd	nd	nd	nd	nd	nd	nd	7.31	750	0.00	1250	0.00
79	2-384-001	Scallorn	nd	nd	nd	nd	nd	nd	nd	nd	nd	nd	7.56	750	0.00	1250	0.00
80	22-D	Scallorn	nd	nd	nd	nd	nd	nd	nd	nd	nd	nd	7.52	750	0.00	1250	0.00
81	23-0031	Scallorn	nd	nd	nd	nd	nd	nd	nd	nd	nd	nd	nd	750	0.00	1250	0.00
82	30-0465	Scallorn	nd	nd	nd	nd	nd	nd	nd	nd	nd	nd	7.85	750	0.00	1250	0.00
83	30-1024	Scallorn	nd	nd	nd	nd	nd	nd	nd	nd	nd	nd	7.85	750	0.00	1250	0.00
84	30-1646	Scallorn	nd	nd	nd	nd	nd	nd	nd	nd	nd	nd	7.83	750	0.00	1250	0.00
85	30-1647	Scallorn	nd	nd	nd	nd	nd	nd	nd	nd	nd	nd	7.92	750	0.00	1250	0.00
86	36-3518	Scallorn	nd	nd	nd	nd	nd	nd	nd	nd	nd	nd	7.86	750	0.00	1250	0.00
87	36-3529	Scallorn	nd	nd	nd	nd	nd	nd	nd	nd	nd	nd	7.92	750	0.00	1250	0.00

Sample Rank	Accession Number	Point Type	Raw Data Side A (mm) 1	2	3	4	5	Raw Data Side B (mm) 1	2	3	4	5	Soil pH	Ass'd Min Age	Calc Min Rate	Ass'd Max Age	Calc Max Rate min
88	36-3936	Scallorn	nd	nd	nd	nd	nd	nd	nd	nd	nd	nd	7.80	750	0.00	1250	0.00
89	36-3937	Scallorn	nd	nd	nd	nd	nd	nd	nd	nd	nd	nd	7.21	750	0.00	1250	0.00
90	38-0475	Scallorn	nd	nd	nd	nd	nd	nd	nd	nd	nd	nd	8.18	750	0.00	1250	0.00
91	40-0845	Scallorn	nd	nd	nd	nd	nd	nd	nd	nd	nd	nd	7.69	750	0.00	1250	0.00
92	40-1133	Scallorn	nd	nd	nd	nd	nd	nd	nd	nd	nd	nd	8.07	750	0.00	1250	0.00
93	40-1283	Scallorn	nd	nd	nd	nd	nd	nd	nd	nd	nd	nd	7.61	750	0.00	1250	0.00
94	41-0200	Scallorn	0.154	0.101	0.107	0.157	0.166	nd	nd	nd	nd	nd	7.87	750	10.97	1250	18.28
95	41-0349	Scallorn	nd	nd	nd	nd	nd	nd	nd	nd	nd	nd	8.15	750	0.00	1250	0.00
96	41-0385	Scallorn	nd	nd	nd	nd	nd	nd	nd	nd	nd	nd	nd	750	0.00	1250	0.00
97	41-0444	Scallorn	nd	nd	nd	nd	nd	nd	nd	nd	nd	nd	7.03	750	0.00	1250	0.00
98	43-0257	Scallorn	0.315	0.309	0.404	0.486	0.267	0.244	0.267	0.253	0.222	0.239	7.72	750	24.04	1250	40.07
99	44-0030	Scallorn	nd	nd	nd	nd	nd	nd	nd	nd	nd	nd	8.10	750	0.00	1250	0.00
100	44-0548	Scallorn	nd	nd	nd	nd	nd	nd	nd	nd	nd	nd	7.77	750	0.00	1250	0.00
101	44-1462M	Scallorn	0.180	0.197	0.219	0.267	0.239	0.138	0.121	0.154	0.146	0.180	7.65	750	14.72	1250	24.53
102	54-0007	Scallorn	nd	nd	nd	nd	nd	nd	nd	nd	nd	nd	nd	750	0.00	1250	0.00
103	60-0013	Scallorn	nd	nd	nd	nd	nd	nd	nd	nd	nd	nd	nd	750	0.00	1250	0.00
104	60-0014	Scallorn	0.197	0.205	0.275	0.236	0.216	0.177	0.191	0.230	0.236	0.208	nd	750	17.37	1250	28.95
105	60-0015	Scallorn	nd	nd	nd	nd	nd	nd	nd	nd	nd	nd	nd	750	0.00	1250	0.00

APPENDIX B

Plates Illustrating Points Used in Study Grouped by Type

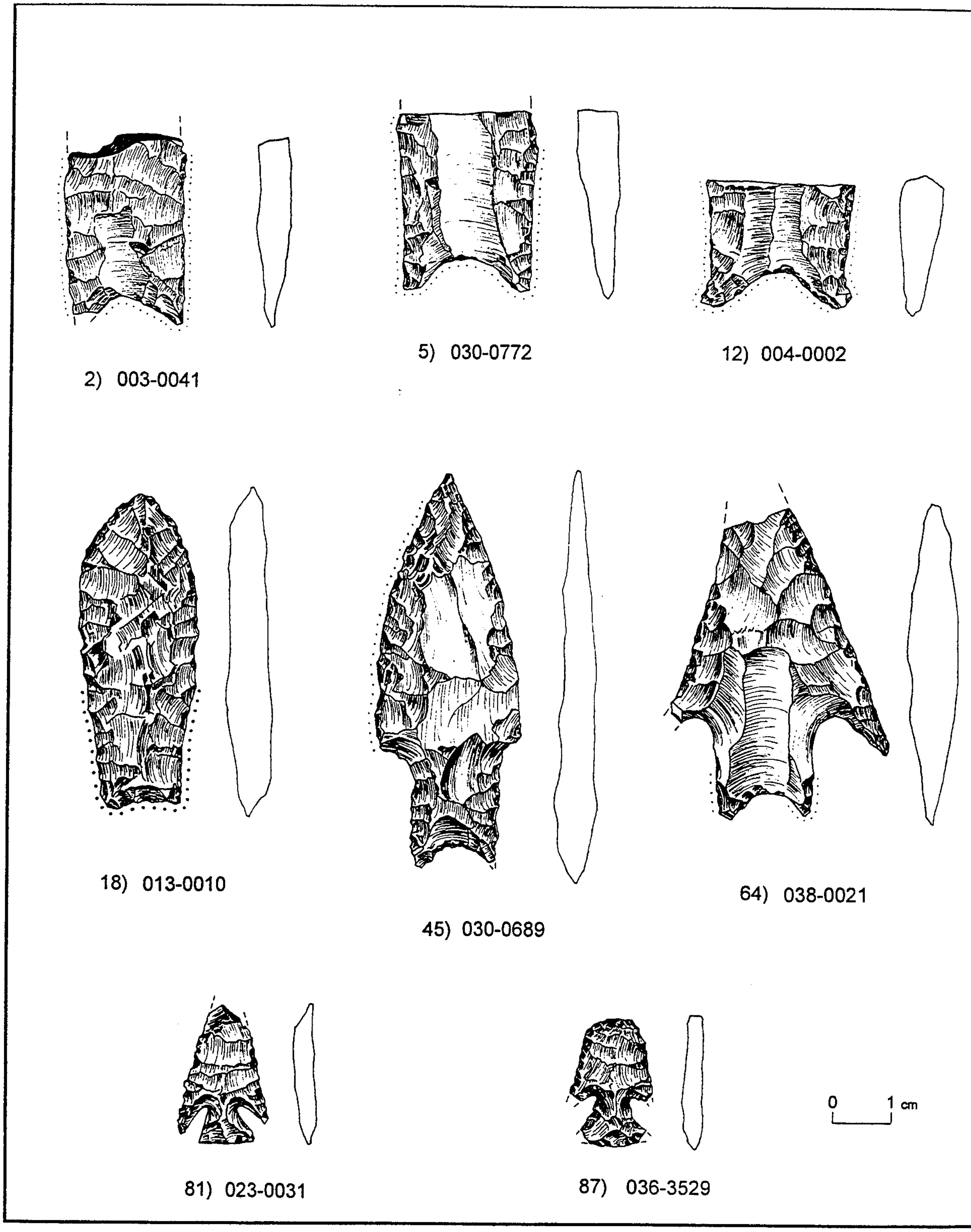
2) 003-0041
5) 030-0772
12) 004-0002
18) 013-0010
45) 030-0689
64) 038-0021
81) 023-0031
87) 036-3529
0 1 cm

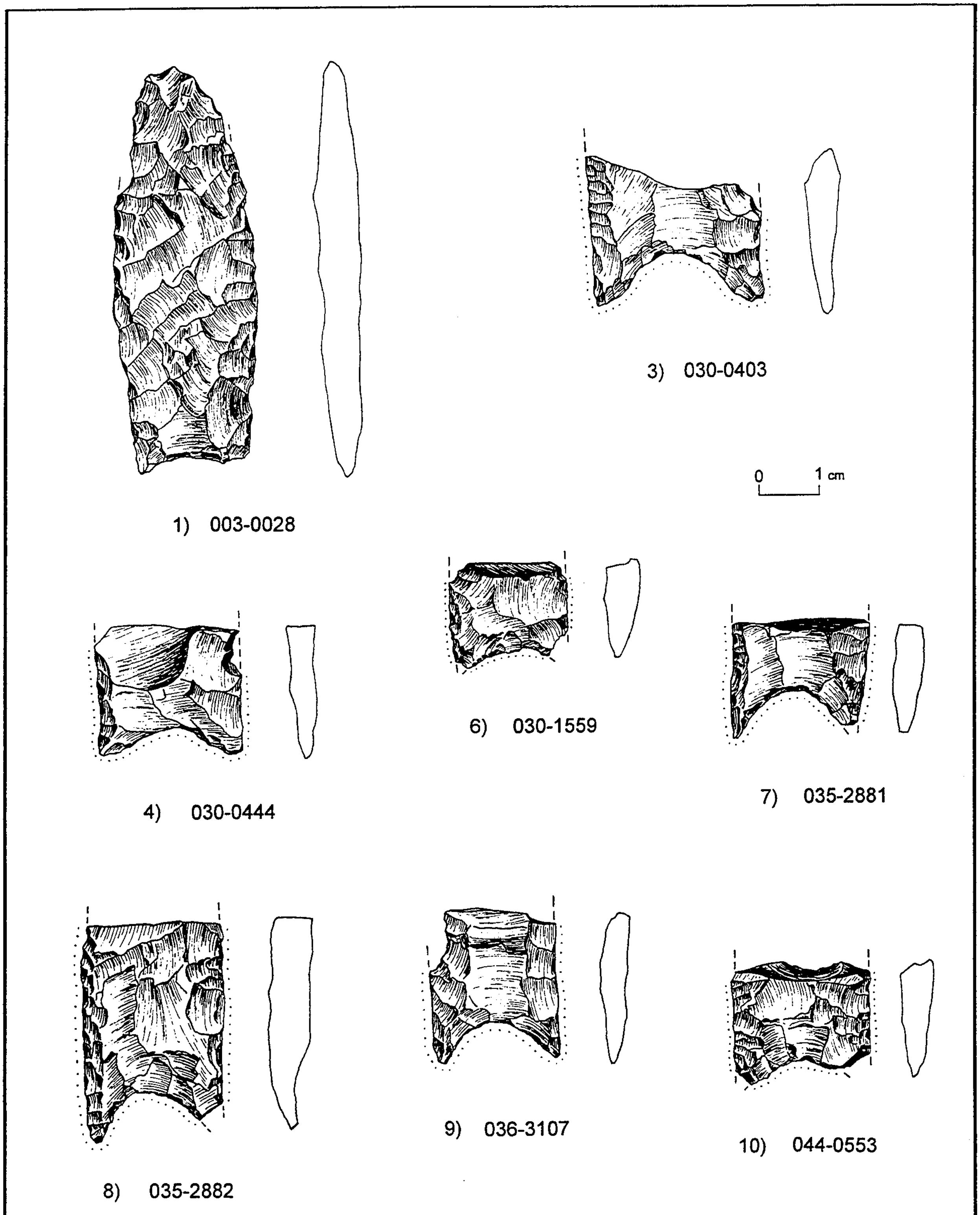
1) 003-0028
3) 030-0403
0 1 cm
6) 030-1559
4) 030-0444
7) 035-2881
8) 035-2882
9) 036-3107
10) 044-0553

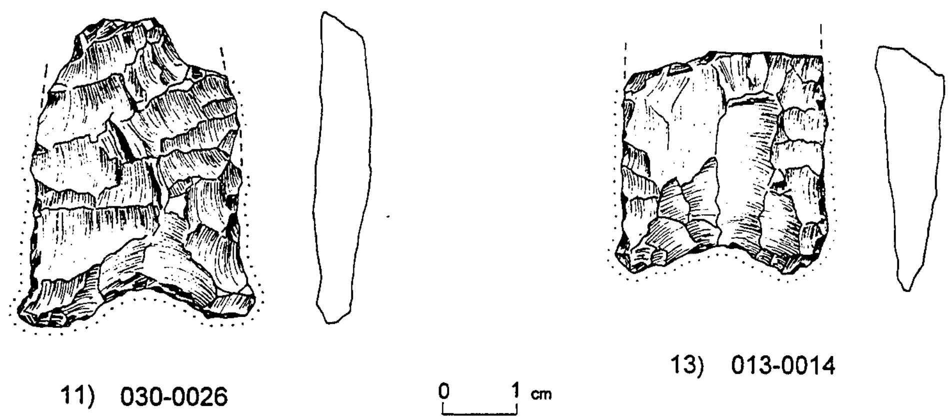

11) 030-0026

13) 013-0014

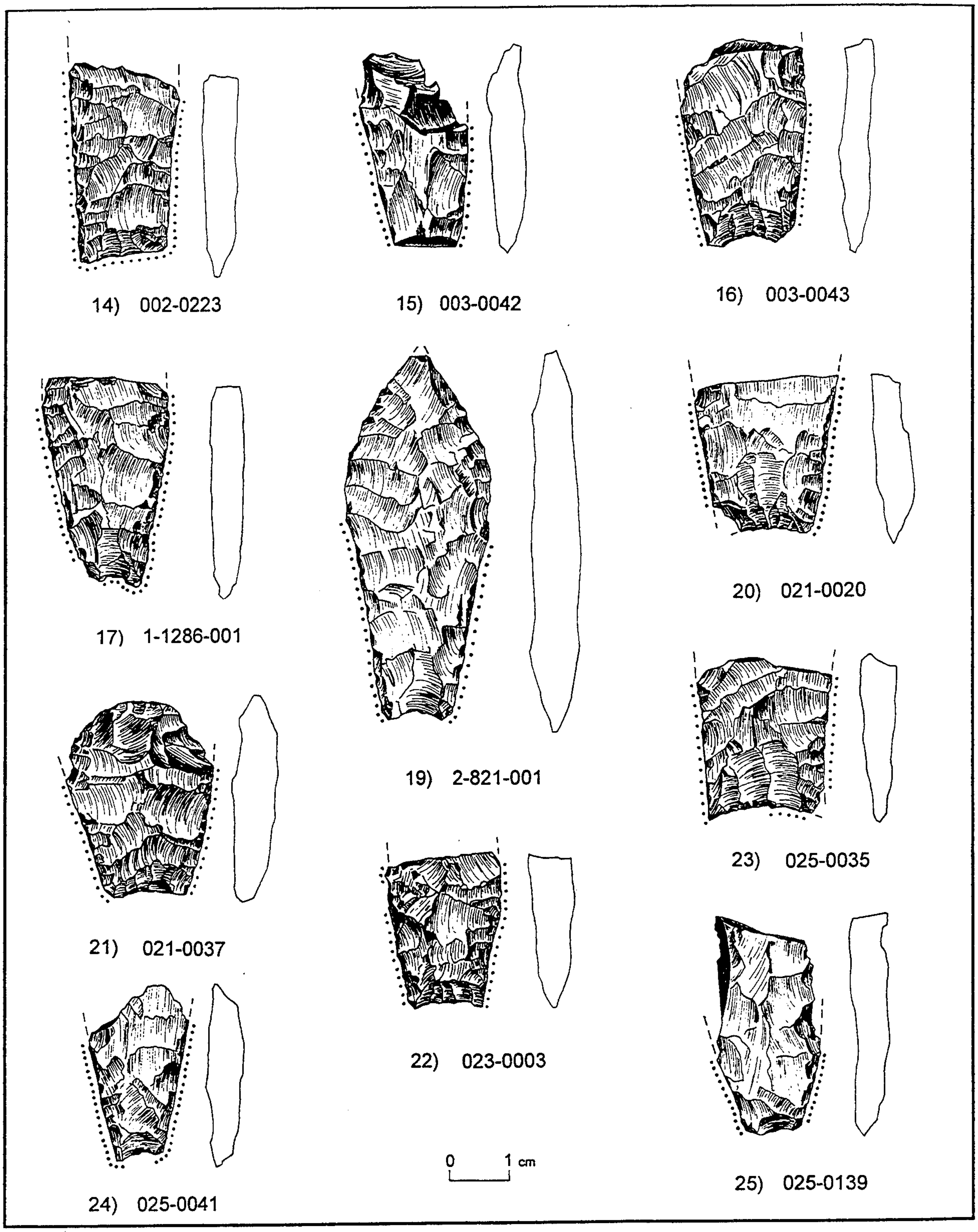
14) 002-0223
15) 003-0042
16) 003-0043
17) 1-1286-001
19) 2-821-001
20) 021-0020
23) 025-0035
21) 021-0037
22) 023-0003
24) 025-0041
0 1 cm
25) 025-0139

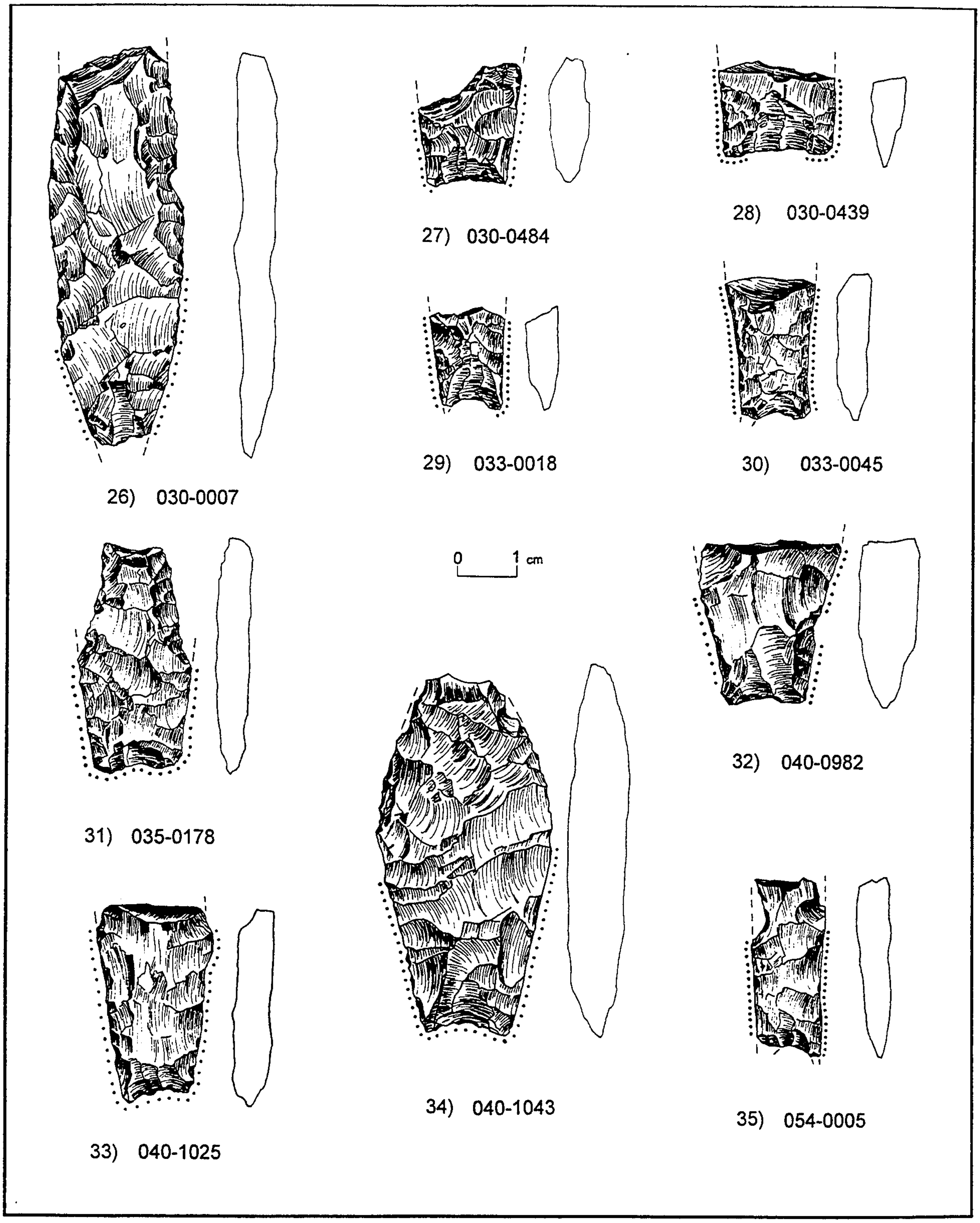

26) 030-0007
27) 030-0484
28) 030-0439
29) 033-0018
30) 033-0045
31) 035-0178
32) 040-0982
33) 040-1025
34) 040-1043
35) 054-0005

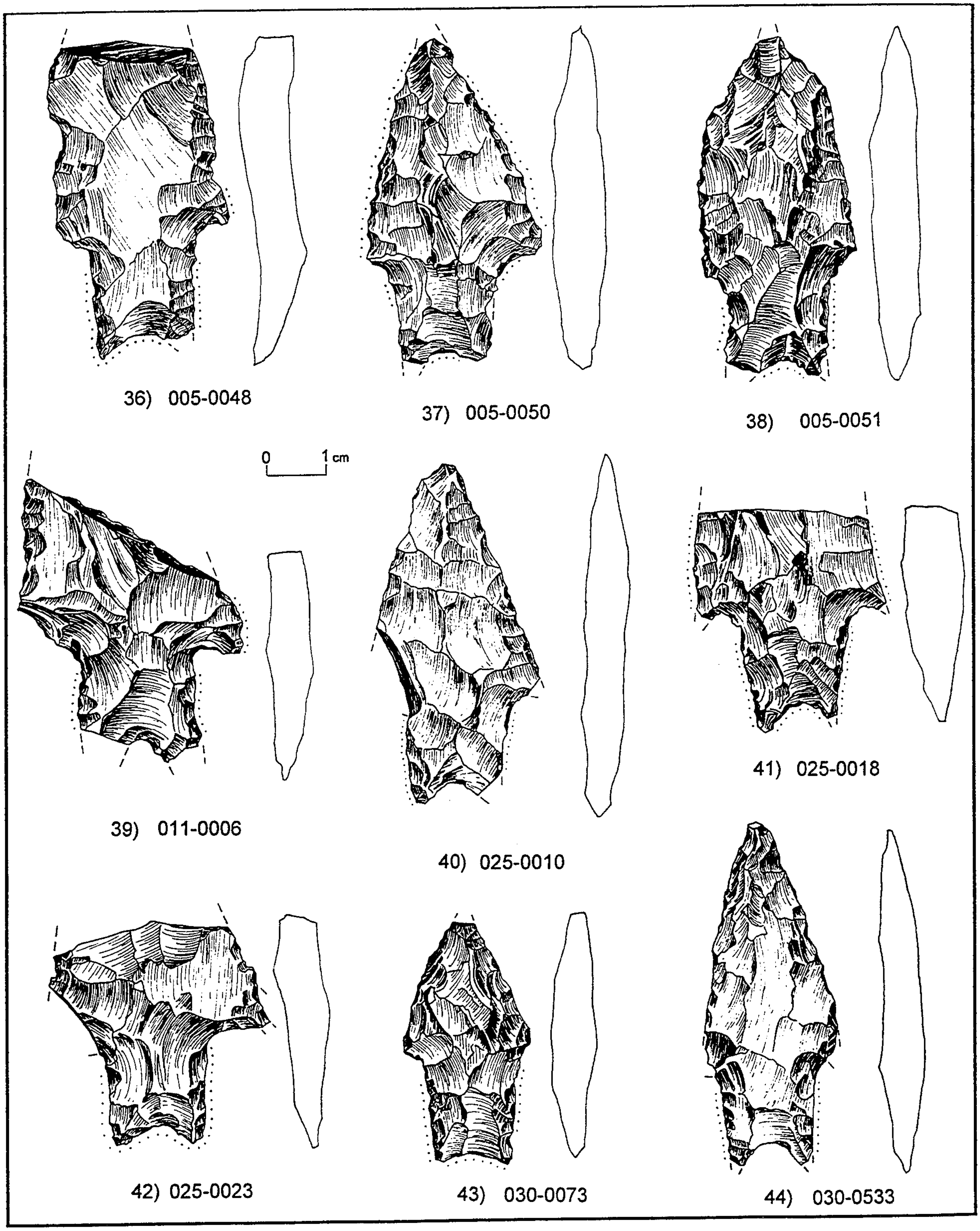
36) 005-0048
37) 005-0050
38) 005-0051
0 1 cm
39) 011-0006
40) 025-0010
41) 025-0018
42) 025-0023
43) 030-0073
44) 030-0533

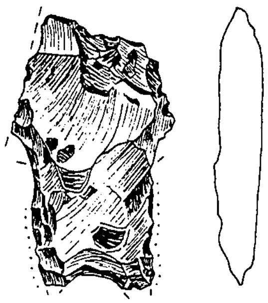

46) 030-1997

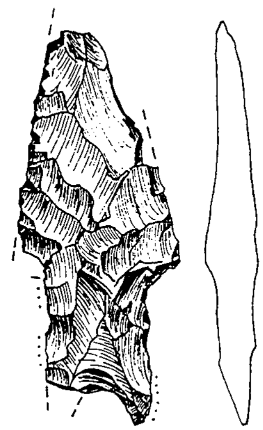

47) 030-1999

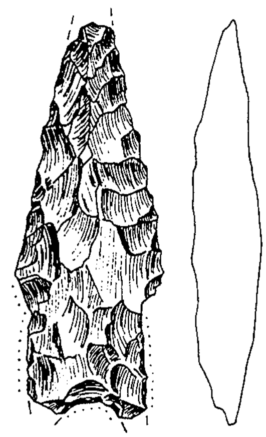

48) 030-2000

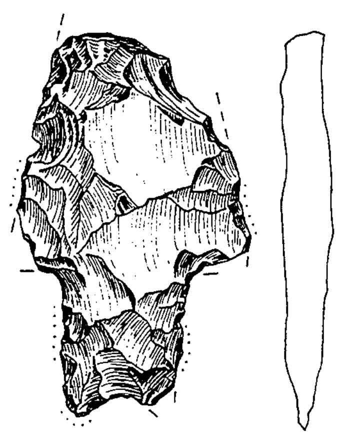

49) 030-2012

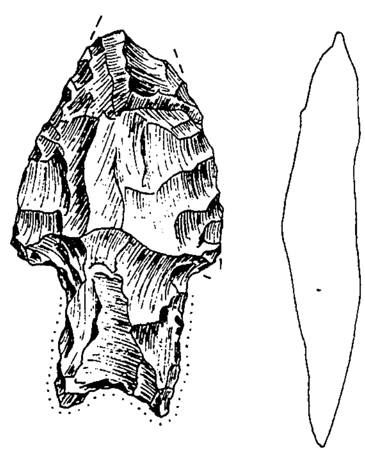

50) 030-2090

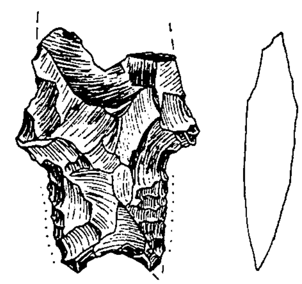

51) 035-2204

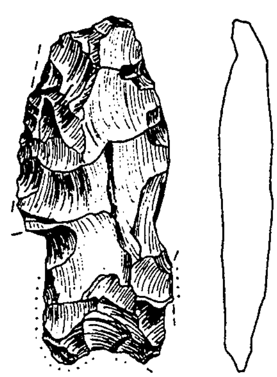

52) 035-2205

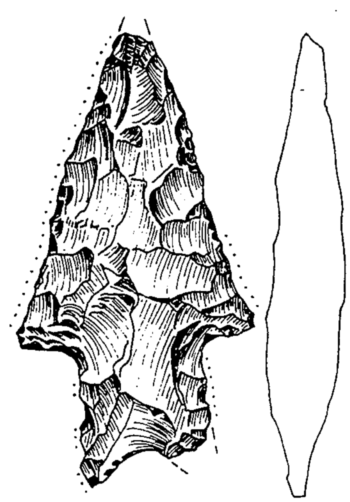

53) 035-2384

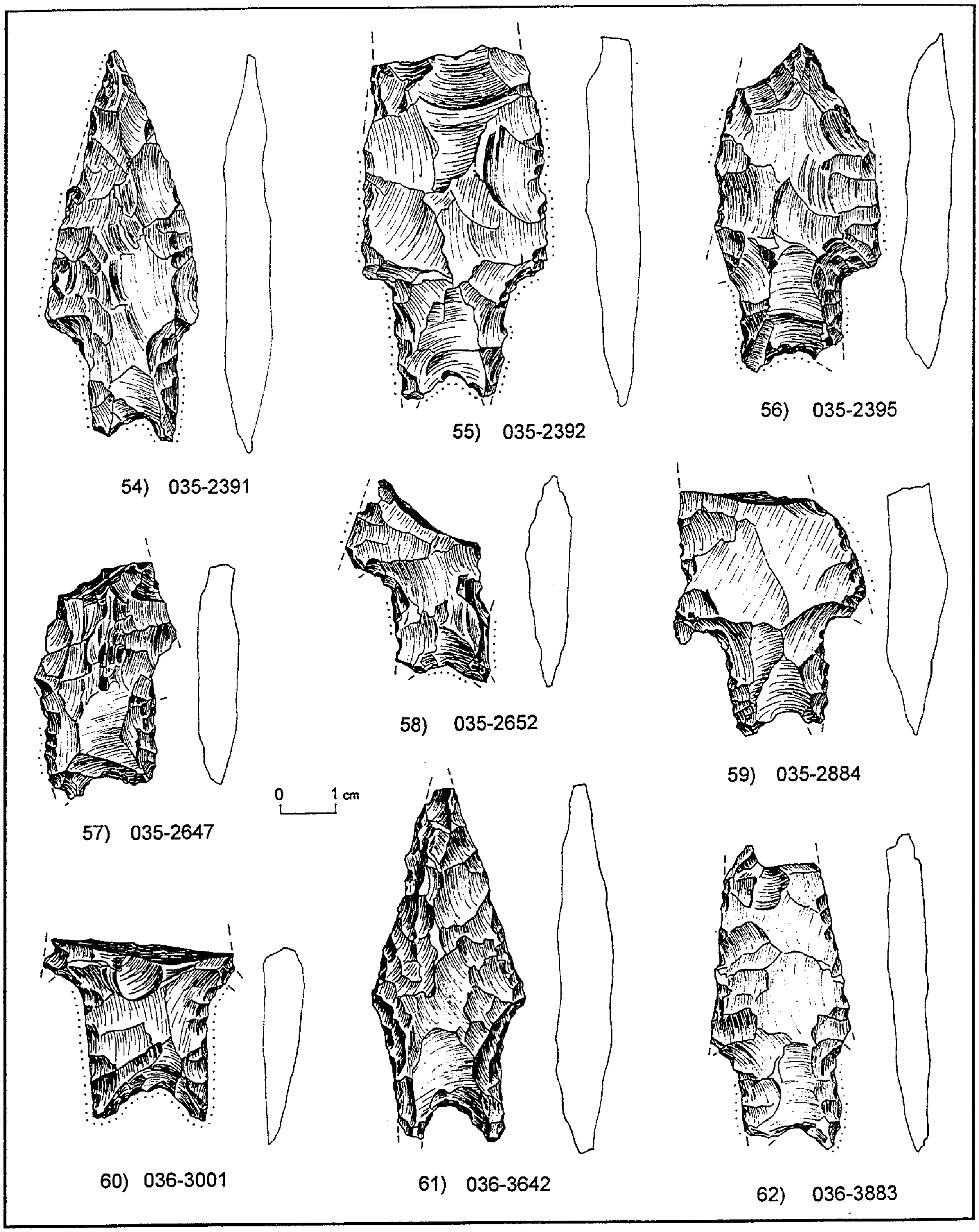
54) 035-2391
55) 035-2392
56) 035-2395
57) 035-2647
58) 035-2652
59) 035-2884
0 1 cm
60) 036-3001
61) 036-3642
62) 036-3883

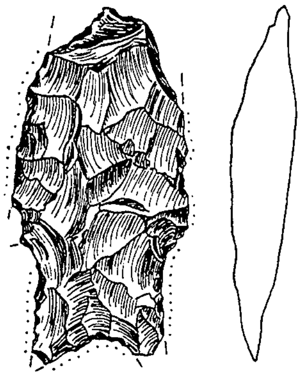

63) 037-0669

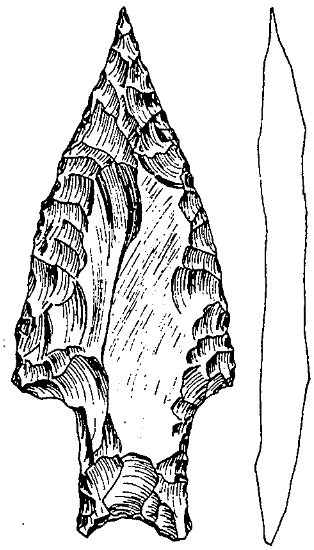

65) 038-0098

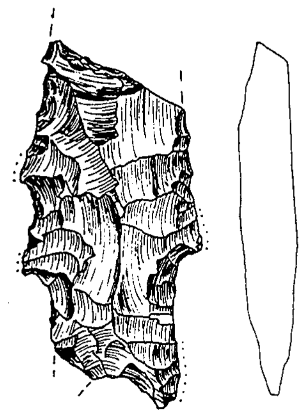

66) 038-0733

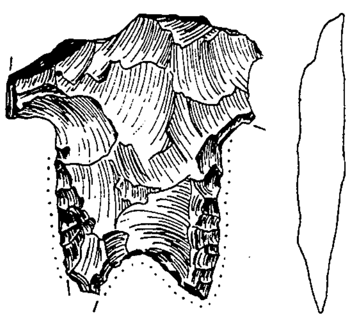

67) 038-0816

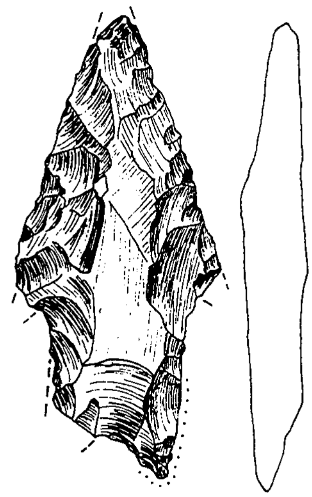

68) 044-1253M

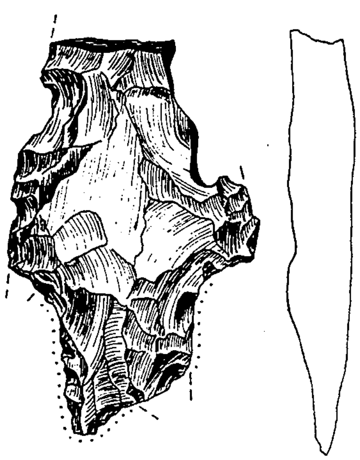

69) 044-1443M

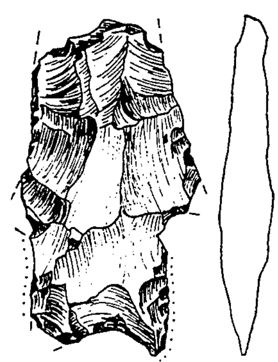

70) 044-1614M

0 1 cm

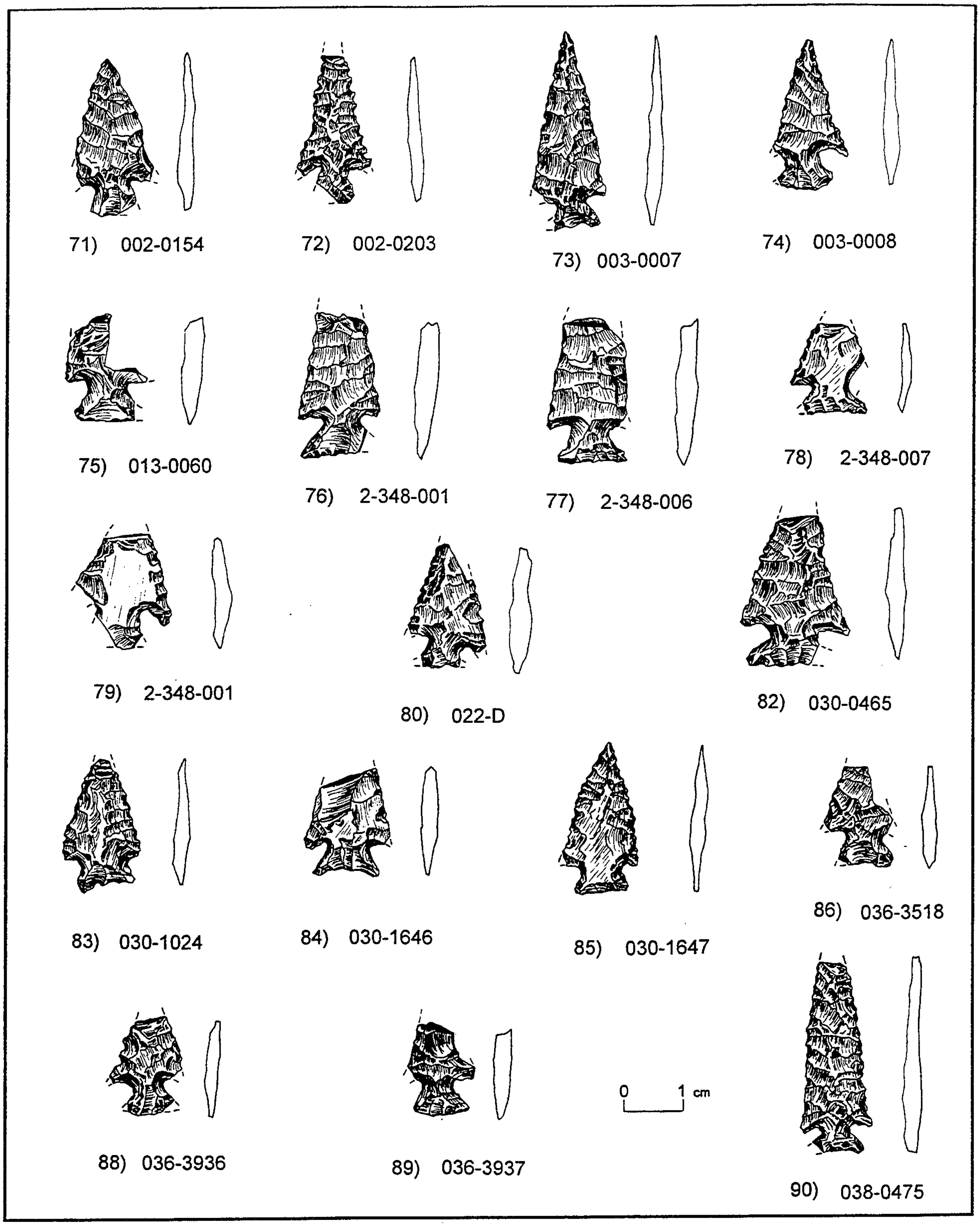

71) 002-0154
72) 002-0203
73) 003-0007
74) 003-0008
75) 013-0060
76) 2-348-001
77) 2-348-006
78) 2-348-007
79) 2-348-001
80) 022-D
82) 030-0465
83) 030-1024
84) 030-1646
85) 030-1647
86) 036-3518
88) 036-3936
89) 036-3937
0 1 cm
90) 038-0475

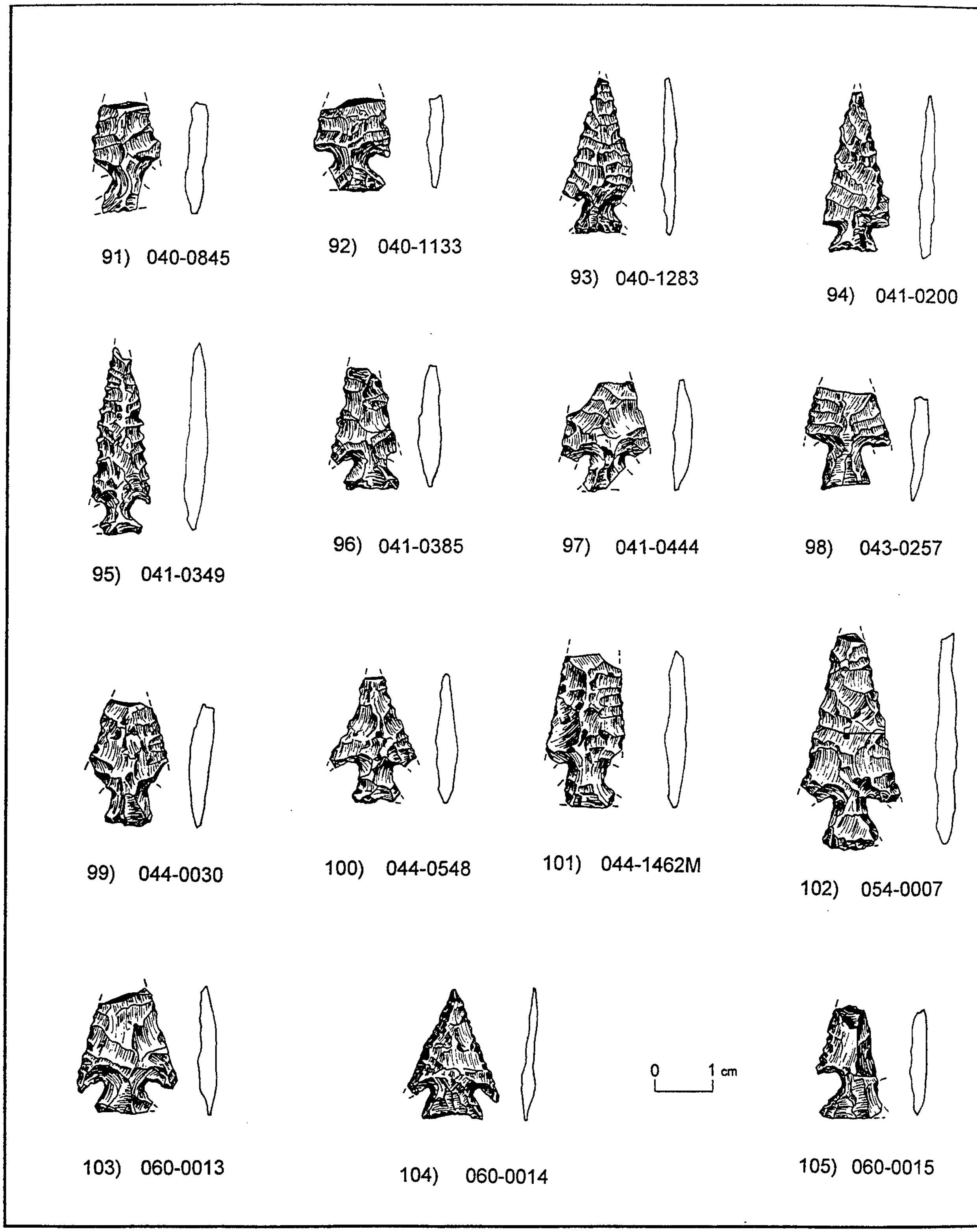

91) 040-0845

92) 040-1133

93) 040-1283

94) 041-0200

95) 041-0349

96) 041-0385

97) 041-0444

98) 043-0257

99) 044-0030

100) 044-0548

101) 044-1462M

102) 054-0007

103) 060-0013

104) 060-0014

105) 060-0015

APPENDIX C

Morphological Measurements for the 105 Artifacts Used in this Study

Table C-1 Projectile Point Metrics - Paleoindian.

Specimen No.	Accession Number	Total Length	Blade Width	Blade Thickness	Blade Angle (°)	Blade Serration	Haft Length	Haft Width (max)	Haft Thickness	Haft Angle (°)	Neck Width	Neck Grinding	Neck Angle (°)	Base Width	Base Grinding	Basal Thinning	Weight (g)	Base Depth
Plainview/Barber																		
1	003-0028	66.0	25.0	7.0	92°	No	20.8	22.5	6.2	82°	NA	None	NA	19.8	None	Yes	13.0	2.5
2	003-0041	NA	NA	NA	NA	NA	25.2	21.2	6.1	88.5°	NA	Heavy	NA	20.3	Moderate	Yes	NA	5.4
3	030-0403	NA	NA	NA	NA	NA	NA	NA	5.2	88.5°	NA	Heavy	NA	28.8	Heavy	Yes	NA	8.3
4	030-0444	NA	NA	NA	NA	NA	NA	NA	4.8	88.5°	NA	Heavy	NA	24.1	Heavy	Yes	NA	4.5
5	030-0772	NA	NA	NA	NA	NA	25.7	25.4	6.4	87°	NA	Heavy	NA	23.6	Heavy	Yes	NA	4.4
6	30-1559	NA	NA	NA	NA	NA	NA	NA	20.3	15.7	NA	Heavy	NA	NA	No	Appears Reworked	NA	
7	035-2881	NA	NA	NA	NA	NA	NA	NA	5.0	87°	NA	Heavy	NA	21.9	Moderate	Yes	NA	8.1
8	035-2882	NA	NA	NA	NA	NA	28.7	25.0	7.0	89°	NA	Heavy	NA	23.5	Moderate	Yes	NA	8.0
9	036-3107	NA	NA	NA	NA	NA	NA	NA	5.2	88.5°	NA	Heavy	NA	22.0	Heavy	Yes	NA	6.0
10	44-0553	NA	NA	NA	NA	NA	NA	NA	24.4	15.8	NA	Heavy	NA	NA	Heavy	Yes	NA	
Golondrina																		
11	003-0026	NA	NA	NA	NA	NA	NA	NA	7.0	93°	NA	Moderate	NA	32.0	Moderate	Yes	NA	3.2
12	004-0002	NA	NA	NA	NA	NA	NA	NA	6.5	86°	NA	Heavy	NA	25.0	Heavy	Yes	NA	5.2
13	013-0014	NA	NA	NA	NA	NA	NA	NA	7.0	90.5°	NA	Heavy	NA	28.0	Moderate	Yes	NA	3.4
Angostura																		
14	002-0223	NA	NA	NA	NA	NA	NA	NA	6.5	86°	NA	Heavy	NA	15.3	Heavy	Yes	NA	0
15	003-0042	NA	NA	NA	NA	NA	NA	NA	6.5	81.5°	NA	Heavy	NA	12.0	Heavy	Yes	NA	0
16	003-0043	NA	NA	NA	NA	NA	24.3	22.4	5.2	82°	NA	Heavy	NA	16.1	Heavy	Yes	NA	1.3
17	1-1286-001	NA	NA	NA	NA	NA	NA	NA	5.8	77.5°	NA	Heavy	NA	10.2	Moderate	Yes	NA	1.3
18	013-0010	52.4	20.5	7.2	110°	No	25.5	19.5	7.2	83°	NA	Heavy	NA	14.9	Heavy	Yes	9.6	1.2
19	2-821-001	60.5	26.1	8.2	107°	No	34.4	24.3	8.2	79.5°	NA	Heavy	NA	13.2	Moderate	Yes	13.7	1.2
20	021-0020	NA	NA	NA	NA	NA	NA	NA	6.6	81°	NA	Heavy	NA	18.5	Light	Yes	NA	1.0
21	021-0037	NA	NA	NA	NA	NA	NA	NA	6.6	73°	NA	Heavy	NA	14.4	Moderate	Yes	NA	0.
22	023-0003	NA	NA	NA	NA	NA	NA	20.5	8.0	78.5°	NA	Moderate	NA	13.0	Light	Yes	NA	1.0
23	025-0035	NA	NA	NA	NA	NA	NA	NA	6.1	85°	NA	Heavy	NA	20.3	Light	Yes	NA	2.0
24	025-0041	NA	NA	NA	NA	NA	NA	NA	6.5	77.5°	NA	Heavy	NA	8.8	Moderate	Yes	NA	1.0
25	025-0139	NA	NA	NA	NA	NA	NA	NA	6.0	72°	NA	Heavy	NA	10.0	Heavy	No	NA	0
26	030-0007	NA	23.0	6.3	92°	No	16.4	19.0	5.5	71°	NA	Heavy	NA	10.2	NA	Yes	NA	NA
27	030-0484	NA	NA	NA	NA	NA	NA	NA	6.9	81.5°	NA	Heavy	NA	15.2	Heavy	Yes	NA	1.0
28	030-0439	NA	NA	NA	NA	NA	NA	NA	5.9	86.5°	NA	Moderate	NA	19.5	Moderate	Yes	NA	1.3
29	033-0018	NA	NA	NA	NA	NA	NA	NA	5.5	85°	NA	Very Heavy	NA	11.0	Heavy	Yes	NA	1.8
30	033-0045	NA	NA	NA	NA	NA	NA	NA	6.0	86°	NA	Heavy	NA	13.0	Heavy	Yes	NA	1.8
31	035-0178	NA	NA	NA	NA	NA	16.5	19.8	5.2	81.5°	NA	Heavy	NA	15.2	Heavy	Yes	NA	1.0
32	040-0982	NA	NA	NA	NA	NA	NA	NA	8.8	78°	NA	Moderate	NA	16.6	Moderate	Yes	NA	0
33	040-1025	NA	NA	NA	NA	NA	29.0	21.0	6.2	83°	NA	Moderate	NA	13.5	Moderate	Yes	NA	1.0
34	040-1043	NA	30.9	10.5	109°	No	27.2	29.2	10.3	77°	NA	Heavy	NA	15.8	Heavy	Yes	NA	1.0
35	054-0005	NA	NA	NA	NA	NA	NA	NA	6.5	87°	NA	Heavy	NA	11.7	Moderate	Yes	NA	1.9

Table C-2 Projectile Point Metrics - Middle Archaic.

Specimen No.	Accession Number	Total Length	Blade Width	Blade Thickness	Blade Angle (°)	Blade Serration	Haft Length	Haft Width (max)	Haft Thickness	Haft Angle (°)	Neck Width	Neck Grinding	Neck Angle (°)	Base Width	Base Grinding	Basal Thinning	Weight (g)	Base Depth
Pedernales																		
36	005-0048	NA	28.7	9.6	93°	No	16.8	18.7	6.4	87.5°	18.7	Light	129°	17.5	Light	Yes	NA	3.7
37	005-0050	54.6	30.6	9.5	108°	No	16.0	19.3	7.1	83.5°	19.3	Light	116°	16.2	Moderate	Yes	13.7	1.8
38	005-0051	56.3	22.1	8.1	95.5°	No	12.0	18.5	5.8	90°	18.5	Light	136°	16.6	Light	Yes	12.7	2.0
39	011-0006	NA	NA	10.5	102°	No	NA	20.9	6.0	NA	19.0	Light	119°	NA	NA	Yes	NA	NA
40	025-0010	59.2	NA	7.8	109.5°	No	17.0	18.2	7.2	83.5°	18.2	Light	NA	16.3	No	Yes	NA	3.2
41	025-0018	NA	32.6	10.1	96.5°	No	18.0	19.3	8.0	77°	19.3	Light	126°	15.5	Light	Yes	NA	3.9
42	025-0023	NA	NA	7.9	107.5°	No	18.0	18.3	5.5	86.5°	18.3	Light	NA	15.5	Light	Yes	NA	3.0
43	030-0073	40.9	22.0	8.0	112°	No	16.7	16.9	6.4	83.5°	16.9	Light	120°	15.5	Light	Yes	6.4	2.0
44	030-0533	57.7	23.3	8.0	104.5°	No	15.0	17.2	6.0	85°	15.0	Light	139°	14.9	No	Yes	10.0	4.2
45	030-0689	65.7	25.0	6.5	96.5°	No	18.2	16.3	6.5	87.5°	16.3	No	104°	14.0	No	Yes	10.2	3.0
46	030-1997	NA	22.5	7.0	108.5°	No	19.3	17.3	7.5	86.5°	17.0	Light	148°	16.0	No	Yes	NA	1.9
47	030-1999	NA	21.0	6.2	101°	No	20.0	14.7	6.0	90°	13.6	Light	128°	NA	No	Yes	NA	4.9
48	030-2000	51.7	20.8	9.4	101.5°	No	15.9	16.6	8.2	91.5°	16.2	Light	144°	16.6	Light	Yes	8.6	2.3
49	030-2012	NA	30.5	8.3	103°	No	18.2	18.0	6.3	86°	18.0	Light	115°	15.8	No	Yes	NA	3.3
50	030-2090	NA	28.3	10.1	106°	No	18.0	16.9	8.5	87°	16.4	Light	118°	15.8	Light	Yes	NA	2.8
51	035-2204	NA	23.0	6.9	103.5°	No	15.0	16.5	6.6	81°	16.5	Light	129°	14.6	No	Yes	NA	2.5
52	035-2205	NA	NA	7.1	97.5°	No	15.5	17.0	6.8	91.5°	16.5	Light	NA	16.0	Light	Yes	NA	2.0
53	035-2384	NA	31.75	10.25	109°	No	18.1	18.65	8.3	100°	17.8	Light	109°	NA	Light	Yes	NA	
54	035-2391	66.0	21.8	7.8	110°	No	19.2	11.3	8.2	86.5°	11.3	Light	118°	15.0	Light	Yes	12.5	3.5
55	035-2392	NA	32.0	9.7	93°	No	19.4	20.8	7.0	83°	20.8	Light	118°	16.0	Light	Yes	NA	4.0
56	035-2395	NA	28.1	7.6	98°	No	15.6	17.2	6.3	87°	17.0	Moderate	108°	17.2	Light	Yes	NA	3.8
57	035-2647	NA	NA	7.0	103°	No	18.8	20.2	6.7	84°	20.2	Light	NA	19.7	No	Yes	NA	2.8
58	035-2652	NA	NA	6.6	NA	NA	18.4	16.5	6.0	90°	15.9	Light	NA	NA	Light	Yes	NA	4.9
59	035-2884	NA	33.3	9.6	101.5°	No	17.0	17.6	8.2	82.5°	17.6	No	120°	16.7	No	Yes	NA	4.0
60	036-3001	NA	33.2	7.1	104.5°	NA	22.1	21.8	7.0	87.5°	21.8	Light	108.5°	19.8	Light	Yes	NA	4.7
61	036-3642	58.8	27.0	8.9	107°	No	16.2	20.5	8.3	84°	20.5	Moderate	148°	19.5	Light	Yes	13.0	5.3
62	036-3883	NA	24.0	6.1	97.5°	No	17.3	17.0	6.0	87°	16.8	Light	132°	16.8	No	Yes	NA	3.2
63	037-0669	NA	24.6	9.0	96.5°	No	14.4	17.7	6.0	93°	17.0	Light	132°	17.7	Light	Yes	NA	3.0
64	038-0021	NA	36.0	8.0	108.5°	No	16.3	17.0	6.1	87°	17.0	No	102°	16.1	Light	Yes	NA	4.1
65	038-0098	71.0	30.3	7.25	107°	No	20.2	16.7	6.8	90°	15.6	Light	90°	16.6	No	Yes		2.7
66	038-0733	NA	26.0	7.0	96°	No	19.0	18.0	6.6	90°	18.0	No	140°	NA	Light	Yes	NA	4.3
67	038-0816	NA	NA	NA	NA	NA	22.1	22.9	6.7	86°	22.9	Light	153°	20.4	Light	Yes	NA	5.3
68	044M-1253	60.2	28.0	7.2	108.5°	No	22.4	19.6	6.8	87.5°	18.0	Light	113°	NA	No	Yes	NA	5.3
69	044M-1443	NA	34.5	8.5	103°	No	17.7	18.4	7.1	83.5°	17.7	Light	118°	NA	Light	Yes	NA	3.8
70	044M-1614	NA	24.7	7.1	102°	No	16.0	18.1	6.5	91°	17.9	Light	141°	17.9	No	Yes	NA	3.0

Table C-3 Projectile Point Metrics - Late Prehistoric.

Specimen No.	Accession Number	Total Length	Blade Width	Blade Thickness	Blade Angle (°)	Blade Serration	Haft Length	Haft Width (max)	Haft Thickness	Haft Angle (°)	Neck Width	Neck Grinding	Neck Angle (°)	Base Width	Base Grinding	Basal Thinning	Weight (g)	Base Depth
Scallorn																		
71	002-0154	26.0	14.1	2.9	107.5°	No	5.0	8.5	3.1	108°	6.5	No	109°	8.5	No	Yes	0.9	1.0
72	002-0203	NA	12.6	2.7	102°	Yes	6.2	NA	2.2	108.5°	5.0	No	110°	NA	No	Yes	NA	0
73	003-0007	32.3	13.4	2.8	102°	No	5.0	NA	2.2	123°	5.6	No	115°	NA	No	Yes	1.1	0
74	003-0008	25.2	12.6	4.0	106°	No	6.7	9.5	2.5	134°	6.0	No	103°	9.5	No	Yes	0.9	0
75	013-0060	NA	15.5	4.0	92°	No	8.5	11.0	3.1	125°	7.6	No	91°	11.0	No	Yes	NA	0
76	2-348-001	NA	13.8	4.2	96.5°	No	6.4	12.0	2.6	125°	6.2	No	102.5°	12.0	No	Yes	NA	0
77	2-348-006	NA	14.6	3.8	98°	No	6.5	NA	2.3	131°	6.8	No	125°	NA	No	Yes	NA	0
78	2-348-007	NA	NA	2.0	110°	Yes	5.2	NA	1.8	132.5°	6.6	No	NA	NA	No	Yes	NA	0
79	2-384-001	NA	NA	4.0	107°	No	6.2	NA	2.6	98°	7.9	No	NA	NA	No	NA	NA	0
80	22-D	NA	14.3	4.0	106°	Yes	4.2	7.3	2.8	112°	6.3	No	94°	7.3	No	Yes	NA	0
81	023-0031	NA	16.0	3.3	103°	Yes	7.0	9.8	2.5	117°	5.4	No	72°	9.8	No	Yes	NA	0
82	030-0465	NA	18	4.0	107.5°	Yes	5.9	NA	2.5	146°	8.0	No	102°	NA	No	Yes	NA	0
83	030-1024	NA	13.8	3.0	017.5°	Yes	4.0	10.0	1.8	112.5°	8.6	No	110°	10.0	No	Yes	1.0	0
84	030-1646	NA	15.0	3.0	104.5°	No	5.0	11.0	2.0	118.5°	7.9	No	90°	11.0	No	Yes	No	0.5
85	030-1647	25.4	13.2	3.0	94°	Yes	3.6	10.2	2.2	123°	7.1	No	97°	10.2	No	Yes	0.8	0
86	036-3518	NA	NA	2.9	104°	No	5.8	NA	2.5	114.5°	6.5	No	128°	NA	No	Yes	NA	0
87	036-3529	NA	14.6	3.3	103.5°	No	7.8	11.2	3.2	129.5°	6.3	No	85°	11.2	No	Yes	NA	0
88	036-3936	NA	NA	2.8	109.5°	Yes	5.7	7.9	2.3	123°	5.3	No	112°	7.9	No	Yes	NA	0
89	036-3937	NA	NA	3.1	105°	No	6.1	9.7	2.5	115.5°	5.1	No	108°	9.7	No	Yes	NA	0
90	038-0475	NA	11.5	2.8	96°	Yes	4.9	NA	2.0	134°	5.5	No	115°	NA	No	Yes	NA	0
91	040-0845	NA	11.8	3.0	103.5°	Yes	6.5	NA	3.0	113°	6.0	No	169°	NA	No	Yes	NA	0
92	040-1133	NA	12.8	3.0	99°	No	6.0	NA	2.6	136°	5.6	No	109°	NA	No	Yes	NA	0
93	040-1283	NA	12.0	3.0	111.5°	No	5.5	8.1	2.5	115°	5.0	No	102°	8.1	No	Yes	NA	0
94	041-0200	NA	12.2	2.8	102°	No	4.3	9.2	2.0	116.5°	6.6	No	127°	9.2	No	Yes	0.8	0
95	041-0349	NA	11.0	3.8	97.5°	Yes	5.0	7.0	2.5	141°	4.3	No	117°	7.0	No	No	NA	0
96	041-0385	NA	11.3	4.0	102°	Yes	5.5	9.5	3.1	125.5°	6.0	No	120°	9.5	No	Yes	NA	0
97	041-0444	NA	10.3	4.0	101.5°	No	6.0	NA	3.0	103°	5.8	No	65°	NA	No	Yes	NA	0
98	043-0257	NA	NA	3.0	108°	Yes	8.0	9.0	2.5	105.5°	6.0	No	NA	9.0	No	Yes	NA	0
99	044-0030	NA	NA	3.6	105.5°	No	5.6	8.9	3.0	105°	6.1	No	NA	8.9	No	Yes	NA	0
100	044-0548	NA	14.5	3.5	111°	No	6.2	8.5	2.5	108°	5.9	No	82.5°	8.5	No	Yes	NA	0
101	044M-1462	NA	12.9	4.0	97.5°	No	7.3	NA	2.5	141°	6.7	No	115°	NA	No	Yes	NA	0
102	054-0007	NA	16.9	3.8	102°	No	9.0	10.0	3.0	113°	6.3	No	80°	10.0	No	Yes	NA	0
103	060-0013	NA	17.2	3.8	108°	No	5.9	10.0	2.5	116.5°	6.9	No	85°	10.0	No	Yes	NA	0
104	060-0014	21.4	16.0	2.0	114°	No	5.2	10.5	1.5	118.5°	7.9	No	79°	10.5	No	Yes	0.6	0.5
105	060-0015	NA	NA	3.8	105°	Yes	7.0	NA	3.2	130°	6.9	No	NA	NA	No	Yes	NA	0

APPENDIX D

Supporting Information for INAA Analysis

Chemical Characterization of Chert from the Edwards Formation in Texas

Using Instrumental Neutron Activation Analysis

Table D-1 Element Concentrations in Edwards Formation Chert and Projectile Points (ppm).

Anid	Cs	Eu	Fe	Hf	Rb	Sb	Sc	Sr	Ta	Tb	Th
EFC001	0.0164	0.0021	229.7	0.0699	0.4702	0.0161	0.0951	7.69	0.0150	0.0019	0.1212
EFC002	0.0167	0.0023	222.1	0.0798	0.5818	0.0125	0.1092	8.01	0.0164	0.0000	0.1516
EFC003	0.0146	0.0019	165.5	0.0669	0.5410	0.0069	0.0846	8.59	0.0133	0.0000	0.1192
EFC004	0.0142	0.0018	186.7	0.0768	0.5394	0.0111	0.0888	7.82	0.0151	0.0000	0.1294
EFC005	0.0142	0.0021	163.8	0.0695	0.5802	0.0094	0.0976	6.28	0.0141	0.0000	0.1292
EFC006	0.0132	0.0024	173.0	0.0705	0.4693	0.0081	0.1020	6.31	0.0146	0.0014	0.1313
EFC007	0.0152	0.0020	202.6	0.0705	0.4962	0.0104	0.0849	6.97	0.0138	0.0000	0.1094
EFC008	0.0154	0.0023	193.9	0.0677	0.3797	0.0101	0.0789	10.59	0.0139	0.0017	0.1161
EFC009	0.0184	0.0021	219.1	0.0784	0.5886	0.0099	0.1089	7.39	0.0163	0.0000	0.1443
EFC010	0.0216	0.0030	766.5	0.0883	0.6264	0.0174	0.0963	31.66	0.0179	0.0015	0.1566
EFC011	0.0129	0.0020	192.0	0.0715	0.5142	0.0133	0.1108	7.05	0.0153	0.0000	0.1266
EFC012	0.0153	0.0045	288.8	0.0886	0.5654	0.0112	0.1025	7.60	0.0177	0.0024	0.1400
EFC013	0.0151	0.0024	223.6	0.0795	0.5672	0.0107	0.1127	6.48	0.0161	0.0000	0.1423
EFC014	0.0127	0.0023	164.8	0.0618	0.4786	0.0103	0.0848	6.13	0.0133	0.0000	0.1103
EFC015	0.0137	0.0019	160.4	0.0642	0.3549	0.0097	0.0797	9.90	0.0136	0.0000	0.1236
EFC016	0.0178	0.0028	203.2	0.0772	0.5906	0.0106	0.1107	6.34	0.0164	0.0000	0.1421
EFC017	0.0142	0.0025	184.6	0.0732	0.5305	0.0103	0.0968	5.95	0.0151	0.0000	0.1322
EFC019	0.0166	0.0024	280.4	0.0744	0.5216	0.0120	0.0979	6.99	0.0154	0.0000	0.1324
EFC020	0.0147	0.0022	188.6	0.0721	0.5406	0.0098	0.0892	6.51	0.0146	0.0000	0.1237
EFC021	0.0179	0.0022	227.8	0.0834	0.6548	0.0118	0.1057	8.28	0.0175	0.0012	0.1450
EFC022	0.0085	0.0022	353.3	0.0525	0.2911	0.0090	0.1062	14.87	0.0112	0.0015	0.1172
EFC023	0.0048	0.0017	287.9	0.0534	0.2641	0.0063	0.0982	11.10	0.0094	0.0012	0.1010
EFC024	0.0075	0.0018	163.4	0.0543	0.2909	0.0076	0.0934	12.22	0.0121	0.0000	0.1152
EFC025	0.0015	0.0011	119.9	0.0218	0.1941	0.0045	0.0397	3.58	0.0034	0.0000	0.0371
EFC026	0.0074	0.0016	200.2	0.0354	0.2128	0.0057	0.0604	10.06	0.0055	0.0000	0.0668
EFC027	0.0104	0.0017	312.9	0.0598	0.4958	0.0080	0.0923	10.11	0.0109	0.0000	0.1087
EFC028	0.0073	0.0018	274.6	0.0550	0.3571	0.0087	0.1083	9.03	0.0123	0.0000	0.1193
EFC029	0.0065	0.0022	440.8	0.0557	0.3349	0.0073	0.0916	14.50	0.0101	0.0000	0.0950
EFC030	0.0068	0.0018	349.7	0.0517	0.5059	0.0081	0.0913	10.99	0.0098	0.0000	0.0968
EFC031	0.0036	0.0014	170.4	0.0375	0.3267	0.0076	0.0574	6.09	0.0072	0.0000	0.0670
EFC032	0.0048	0.0014	132.5	0.0373	0.2174	0.0068	0.0648	5.22	0.0067	0.0021	0.0675
EFC033	0.0085	0.0017	219.6	0.0587	0.2787	0.0092	0.1056	8.62	0.0120	0.0000	0.1179
EFC034	0.0038	0.0017	210.8	0.0309	0.2009	0.0058	0.0543	6.87	0.0054	0.0000	0.0587
EFC035	0.0069	0.0027	396.0	0.0390	0.2390	0.0050	0.0689	19.69	0.0066	0.0018	0.0749
EFC036	0.0050	0.0018	313.2	0.0494	0.2331	0.0077	0.0921	9.28	0.0102	0.0000	0.1017
EFC037	0.0054	0.0019	237.8	0.0381	0.2920	0.0064	0.0626	6.64	0.0074	0.0000	0.0704
EFC038	0.0079	0.0024	453.2	0.0575	0.3441	0.0074	0.1055	14.89	0.0110	0.0000	0.1132
EFC039	0.0062	0.0015	189.6	0.0392	0.2743	0.0060	0.0543	6.05	0.0065	0.0000	0.0724
EFC040	0.0050	0.0020	189.0	0.0330	0.3255	0.0049	0.0569	9.99	0.0063	0.0000	0.0682
EFC041	0.0082	0.0018	294.9	0.0596	0.4471	0.0082	0.0948	9.77	0.0111	0.0000	0.1093
EFC042	0.0061	0.0017	278.1	0.0540	0.3044	0.0087	0.0960	8.39	0.0107	0.0000	0.1129
EFC043	0.0000	0.0320	281.7	0.0320	0.2367	0.0146	0.0632	0.00	0.0049	0.0246	0.0570

Anid	Cs	Eu	Fe	Hf	Rb	Sb	Sc	Sr	Ta	Tb	Th
EFC044	0.0020	0.0057	358.0	0.0405	0.1771	0.0104	0.0632	5.42	0.0070	0.0043	0.0708
EFC045	0.0040	0.0054	302.2	0.0341	0.2608	0.0128	0.0598	2.26	0.0057	0.0047	0.0536
EFC046	0.0042	0.0103	219.8	0.0453	0.3134	0.0120	0.0673	5.00	0.0084	0.0086	0.0784
EFC047	0.0000	0.0170	198.5	0.0312	0.2563	0.0152	0.0524	2.12	0.0058	0.0130	0.0528
EFC048	0.0000	0.0110	158.4	0.0312	0.1571	0.0085	0.0561	1.59	0.0059	0.0088	0.0548
EFC049	0.0028	0.0076	267.4	0.0465	0.3638	0.0121	0.0897	4.40	0.0094	0.0077	0.0867
EFC050	0.0000	0.0144	63.2	0.0184	0.1282	0.0111	0.0405	0.00	0.0024	0.0088	0.0328
EFC051	0.0000	0.0596	167.6	0.0357	0.2003	0.0110	0.0642	1.42	0.0051	0.0400	0.0566
EFC052	0.0030	0.0063	251.9	0.0470	0.3204	0.0133	0.0855	2.57	0.0090	0.0054	0.0851
EFC053	0.0000	0.0732	217.9	0.0295	0.2764	0.0124	0.0543	1.20	0.0053	0.0530	0.0507
EFC054	0.0000	0.0205	217.0	0.0298	0.2980	0.0129	0.0571	0.00	0.0052	0.0167	0.0555
EFC055	0.0000	0.0173	158.7	0.0309	0.0000	0.0121	0.0488	1.82	0.0051	0.0121	0.0482
EFC056	0.0000	0.0031	311.6	0.0551	0.3271	0.0169	0.0900	4.82	0.0101	0.0000	0.0967
EFC057	0.0000	0.0089	224.1	0.0264	0.1699	0.0125	0.0512	3.19	0.0043	0.0059	0.0480
EFC058	0.0000	0.0083	54.4	0.0158	0.0578	0.0097	0.0339	2.10	0.0025	0.0044	0.0321
EFC059	0.0056	0.0034	76.1	0.0323	0.2139	0.0087	0.0501	0.00	0.0052	0.0026	0.0475
EFC060	0.0059	0.0888	501.3	0.0531	0.3627	0.0184	0.0914	3.59	0.0108	0.0524	0.0952
EFC061	0.0057	0.0129	199.2	0.0403	0.3379	0.0094	0.0600	4.17	0.0062	0.0080	0.0620
EFC062	0.0039	0.0683	405.3	0.0531	0.2258	0.0157	0.0968	1.99	0.0098	0.0401	0.0897
EFC063	0.0056	0.0021	36.6	0.0203	0.2237	0.0162	0.0115	2.97	0.0000	0.0013	0.0153
EFC064	0.0028	0.0023	28.7	0.0080	0.1482	0.0054	0.0159	1.31	0.0017	0.0017	0.0169
EFC065	0.0000	0.0012	44.9	0.0144	0.1910	0.0093	0.0203	1.45	0.0024	0.0000	0.0351
EFC066	0.0028	0.0026	84.6	0.0149	0.1098	0.0166	0.0208	0.63	0.0019	0.0015	0.0225
EFC067	0.0121	0.0022	39.2	0.0208	0.2626	0.0051	0.0099	2.62	0.0021	0.0015	0.0144
EFC068	0.0000	0.0008	15.5	0.0084	0.0653	0.0046	0.0125	0.70	0.0000	0.0000	0.0126
EFC069	0.0000	0.0011	16.5	0.0057	0.0903	0.0035	0.0134	0.00	0.0000	0.0005	0.0128
EFC070	0.0000	0.0049	79.3	0.0215	0.0858	0.0074	0.0384	1.62	0.0039	0.0035	0.0427
EFC071	0.0068	0.0047	136.3	0.0202	0.2627	0.0067	0.0122	2.69	0.0011	0.0033	0.0158
EFC072	0.0000	0.0011	28.9	0.0084	0.0539	0.0056	0.0225	0.76	0.0014	0.0000	0.0204
EFC073	0.0035	0.0032	58.5	0.0110	0.1562	0.0093	0.0295	3.15	0.0027	0.0030	0.0478
EFC074	0.0027	0.0018	97.8	0.0143	0.1093	0.0118	0.0189	2.34	0.0015	0.0000	0.0217
EFC075	0.0026	0.0009	21.0	0.0084	0.0000	0.0049	0.0154	1.61	0.0011	0.0000	0.0165
EFC076	0.0035	0.0016	105.2	0.0114	0.2212	0.0128	0.0142	1.01	0.0011	0.0013	0.0136
EFC077	0.0018	0.0018	22.1	0.0092	0.1238	0.0055	0.0214	1.30	0.0026	0.0014	0.0224
EFC078	0.0000	0.0011	19.9	0.0048	0.0000	0.0042	0.0131	0.94	0.0008	0.0000	0.0129
EFC079	0.0030	0.0011	24.2	0.0083	0.0000	0.0058	0.0162	0.80	0.0000	0.0000	0.0131
EFC080	0.0083	0.0012	41.9	0.0173	0.3012	0.0044	0.0090	3.75	0.0013	0.0006	0.0147
EFC081	0.0000	0.0010	24.5	0.0070	0.0947	0.0047	0.0142	1.09	0.0010	0.0000	0.0142
EFC082	0.0071	0.0039	124.1	0.0210	0.2841	0.0058	0.0117	2.25	0.0020	0.0024	0.0161
EFC083	0.0000	0.0019	61.0	0.0272	0.1762	0.0057	0.0594	0.00	0.0042	0.0000	0.0480
EFC084	0.0000	0.0020	77.7	0.0253	0.1936	0.0100	0.0596	2.27	0.0039	0.0010	0.0472
EFC085	0.0000	0.0123	77.9	0.0295	0.1934	0.0107	0.0747	0.00	0.0042	0.0073	0.0546
EFC086	0.0000	0.0018	74.1	0.0238	0.2018	0.0117	0.0577	0.91	0.0049	0.0014	0.0498

Anid	Cs	Eu	Fe	Hf	Rb	Sb	Sc	Sr	Ta	Tb	Th
EFC087	0.0000	0.0078	88.6	0.0269	0.2570	0.0066	0.0685	9.40	0.0044	0.0047	0.0490
EFC088	0.0039	0.0024	62.1	0.0236	0.1138	0.0158	0.0529	1.06	0.0040	0.0000	0.0447
EFC089	0.0000	0.0018	53.0	0.0231	0.1721	0.0061	0.0625	0.00	0.0038	0.0000	0.0454
EFC090	0.0000	0.0016	81.2	0.0232	0.1634	0.0126	0.0593	1.60	0.0046	0.0000	0.0484
EFC091	0.0028	0.0025	62.9	0.0238	0.2428	0.0048	0.0467	0.89	0.0033	0.0000	0.0384
EFC092	0.0000	0.0167	53.6	0.0243	0.1939	0.0060	0.0603	1.22	0.0038	0.0109	0.0443
EFC093	0.0000	0.0027	96.6	0.0266	0.1750	0.0074	0.0639	1.63	0.0040	0.0013	0.0516
EFC094	0.0000	0.0017	68.5	0.0229	0.1597	0.0095	0.0610	0.00	0.0038	0.0016	0.0494
EFC095	0.0032	0.0266	102.6	0.0346	0.2837	0.0057	0.0515	0.91	0.0055	0.0175	0.0479
EFC096	0.0035	0.0175	76.5	0.0270	0.2098	0.0074	0.0540	2.26	0.0035	0.0097	0.0465
EFC097	0.0000	0.0021	101.3	0.0249	0.1252	0.0086	0.0600	2.01	0.0044	0.0010	0.0475
EFC098	0.0039	0.0108	50.9	0.0255	0.1912	0.0054	0.0522	1.44	0.0041	0.0092	0.0426
EFC099	0.0000	0.0278	67.7	0.0266	0.1897	0.0106	0.0718	1.45	0.0043	0.0213	0.0524
EFC100	0.0000	0.0019	82.8	0.0273	0.1386	0.0092	0.0613	0.64	0.0041	0.0000	0.0472
EFC101	0.0000	0.0032	74.4	0.0308	0.2347	0.0073	0.0644	1.30	0.0047	0.0016	0.0560
EFC102	0.0000	0.0205	72.7	0.0308	0.2487	0.0092	0.0715	1.50	0.0061	0.0136	0.0589
EFC103	0.0074	0.0028	46.6	0.0360	0.2630	0.0090	0.0279	3.18	0.0037	0.0033	0.0358
EFC104	0.0041	0.0013	42.8	0.0263	0.2650	0.0050	0.0342	2.23	0.0044	0.0000	0.0379
EFC105	0.0072	0.0040	38.5	0.0293	0.2565	0.0032	0.0219	4.37	0.0036	0.0032	0.0307
EFC106	0.0080	0.0012	29.8	0.0266	0.3680	0.0046	0.0265	2.29	0.0049	0.0000	0.0334
EFC107	0.0028	0.0014	44.1	0.0231	0.1585	0.0039	0.0335	3.03	0.0036	0.0000	0.0316
EFC108	0.0028	0.0019	43.5	0.0197	0.1213	0.0039	0.0313	2.36	0.0035	0.0008	0.0278
EFC109	0.0000	0.0016	127.5	0.0305	0.2074	0.0077	0.0517	4.34	0.0048	0.0000	0.0508
EFC110	0.0046	0.0013	40.6	0.0182	0.1847	0.0061	0.0253	2.32	0.0033	0.0000	0.0247
EFC111	0.0061	0.0015	24.5	0.0181	0.2812	0.0037	0.0177	2.50	0.0025	0.0000	0.0231
EFC112	0.0053	0.0028	37.6	0.0302	0.2319	0.0039	0.0351	2.33	0.0050	0.0030	0.0364
EFC113	0.0048	0.0020	67.9	0.0367	0.3443	0.0056	0.0503	2.10	0.0074	0.0009	0.0567
EFC114	0.0033	0.0022	79.1	0.0329	0.2222	0.0060	0.0624	6.71	0.0055	0.0012	0.0646
EFC115	0.0042	0.0023	61.5	0.0254	0.2424	0.0056	0.0501	0.00	0.0056	0.0025	0.0468
EFC116	0.0044	0.0026	33.6	0.0347	0.2814	0.0038	0.0376	1.80	0.0048	0.0017	0.0365
EFC117	0.0041	0.0019	35.7	0.0224	0.3010	0.0048	0.0252	2.59	0.0036	0.0016	0.0270
EFC118	0.0023	0.0017	43.5	0.0260	0.2393	0.0049	0.0424	1.66	0.0054	0.0000	0.0460
EFC119	0.0029	0.0016	44.1	0.0226	0.2573	0.0038	0.0403	1.74	0.0043	0.0000	0.0461
EFC121	0.0039	0.0020	58.5	0.0334	0.2394	0.0050	0.0385	2.57	0.0052	0.0000	0.0414
CDF001	0.0093	0.0079	236.7	0.0447	0.3090	0.0458	0.0688	3.18	0.0073	0.0025	0.0608
CDF002	0.0088	0.0048	354.3	0.0487	0.3182	0.0298	0.0323	9.29	0.0000	0.0031	0.0401
CDF003	0.0157	0.0033	132.6	0.0657	0.4790	0.0000	0.0916	4.52	0.0142	0.0012	0.1208
CDF004	0.0278	0.0073	188.7	0.0425	0.4874	0.0000	0.0866	0.00	0.0056	0.0043	0.0824
CDF005	0.0076	0.0041	74.4	0.0177	0.1910	0.0000	0.0261	1.72	0.0018	0.0016	0.0468
CDF007	0.0120	0.0067	292.2	0.0539	0.3351	0.0000	0.0930	4.23	0.0107	0.0036	0.0744
CDF008	0.0139	0.0062	349.1	0.0327	0.3143	0.0553	0.0458	2.18	0.0062	0.0020	0.0586
CDF009	0.0113	0.0406	182.5	0.0224	0.2319	0.0000	0.0261	1.37	0.0025	0.0223	0.1096
CDF010	0.0137	0.0098	123.3	0.0749	0.4689	0.0094	0.0986	4.84	0.0144	0.0049	0.1349

Anid	Cs	Eu	Fe	Hf	Rb	Sb	Sc	Sr	Ta	Tb	Th
CDF011	0.0120	0.0118	311.6	0.0269	0.3116	0.0141	0.0584	2.36	0.0050	0.0059	0.0636
CDF012	0.0090	0.0027	65.4	0.0426	0.1879	0.0066	0.0246	1.13	0.0019	0.0014	0.0382
CDF013	0.0136	0.0131	375.5	0.0251	0.2780	0.0268	0.0502	11.81	0.0024	0.0049	0.0753
CDF014	0.0169	0.0040	157.2	0.0353	0.4799	0.0088	0.0426	1.66	0.0042	0.0024	0.0475
CDF015	0.0187	0.0072	291.6	0.0703	0.4804	0.0178	0.0936	7.15	0.0134	0.0033	0.1385
CDF016	0.0140	0.0123	84.9	0.0137	0.4533	0.0108	0.0195	6.40	0.0047	0.0060	0.0322
CDF017	0.0126	0.0160	313.0	0.0489	0.4396	0.0198	0.0252	4.57	0.0000	0.0083	0.0453
CDF018	0.0000	0.0166	231.7	0.0434	0.3500	0.0140	0.0422	7.90	0.0056	0.0094	0.1081
CDF019	0.0472	0.0059	430.1	0.0900	0.9757	0.0137	0.0749	21.89	0.0094	0.0030	0.0909
CDF020	0.0457	0.0196	86.9	0.0904	0.6144	0.0204	0.0144	6.12	0.0000	0.0096	0.0319
CDF022	0.0202	0.0056	150.3	0.0171	0.3206	0.0142	0.0199	2.04	0.0000	0.0031	0.0346
CDF023	0.0073	0.0991	622.8	0.0550	0.3257	0.0240	0.0836	0.00	0.0114	0.0617	0.1020
CDF024	0.0198	0.0082	57.1	0.0643	0.4303	0.0152	0.0260	10.14	0.0000	0.0037	0.0335
CDF025	0.0167	0.0083	185.3	0.0733	0.5937	0.0210	0.0870	9.28	0.0158	0.0058	0.1858
CDF026	0.0201	0.0059	199.2	0.0663	0.6422	0.0306	0.0863	0.00	0.0059	0.0032	0.0947
CDF027	0.0330	0.0068	74.7	0.1088	0.5712	0.0136	0.0114	3.73	0.0000	0.0040	0.0230
CDF028	0.0084	0.0235	56.0	0.0200	0.2557	0.0065	0.0235	3.78	0.0000	0.0109	0.0423
CDF029	0.0108	0.0110	121.5	0.0363	0.4135	0.0092	0.0389	4.15	0.0034	0.0045	0.0788
CDF030	0.0075	0.0093	111.5	0.0261	0.1718	0.0077	0.0362	2.31	0.0046	0.0033	0.0444
CDF031	0.0266	0.0053	80.3	0.0416	0.3863	0.0187	0.0232	5.84	0.0000	0.0025	0.0471
CDF032	0.0093	0.0027	144.6	0.0402	0.1821	0.0214	0.0489	1.85	0.0065	0.0000	0.0593
CDF033	0.0089	0.0024	95.8	0.0230	0.2081	0.0248	0.0269	0.00	0.0000	0.0000	0.0283
CDF034	0.0092	0.0000	101.0	0.0233	0.2840	0.0219	0.0299	4.72	0.0028	0.0000	0.0391
CDF035	0.0060	0.0025	83.0	0.0208	0.0000	0.0074	0.0312	0.00	0.0040	0.0000	0.0316
CDF037	0.0075	0.0279	110.2	0.0339	0.4667	0.0093	0.0259	7.59	0.0000	0.0120	0.1074
CDF038	0.0154	0.0026	107.7	0.0245	0.3891	0.0176	0.0403	102.71	0.0040	0.0000	0.0368
CDF039	0.0078	0.0074	357.7	0.0486	0.3657	0.0129	0.0764	15.55	0.0082	0.0000	0.0951
CDF040	0.0000	0.0030	324.5	0.0418	0.2783	0.0163	0.0645	7.37	0.0059	0.0000	0.0644
CDF041	0.0057	0.0080	213.9	0.0438	0.3295	0.0092	0.0621	31.23	0.0088	0.0041	0.0677
CDF042	0.0000	0.0021	89.9	0.0493	0.4825	0.0122	0.1012	0.00	0.0088	0.0000	0.0555
CDF043	0.0126	0.0255	363.1	0.0630	0.4934	0.0143	0.0255	7.27	0.0046	0.0130	0.0903
CDF044	0.0108	0.0015	102.1	0.0131	0.0000	0.0176	0.0204	0.00	0.0000	0.0000	0.0242
CDF045	0.0000	0.0042	299.4	0.0380	0.1859	0.0206	0.0648	5.75	0.0043	0.0000	0.0713
CDF046	0.0086	0.0061	42.0	0.0232	0.2369	0.0062	0.0324	2.72	0.0028	0.0036	0.0379
CDF047	0.0030	0.0034	220.2	0.0356	0.1861	0.0308	0.0865	0.00	0.0043	0.0000	0.0747
CDF048	0.0133	0.0000	86.6	0.0677	0.6094	0.0169	0.0173	4.43	0.0000	0.0000	0.0174
CDF049	0.0422	0.0139	237.2	0.0827	1.1030	0.0187	0.1929	26.38	0.0153	0.0112	0.1337
CDF050	0.0054	0.0039	74.9	0.0321	0.2716	0.0162	0.0656	0.00	0.0048	0.0033	0.0409
CDF051	0.0000	0.0021	91.7	0.0182	0.1605	0.0148	0.0395	1.01	0.0024	0.0000	0.0286
CDF052	0.0163	0.0000	65.1	0.0081	0.2665	0.0172	0.0140	5.96	0.0000	0.0007	0.0174
CDF053	0.0066	0.0059	551.2	0.0451	0.2941	0.0206	0.1031	11.15	0.0097	0.0044	0.0933
CDF054	0.0204	0.0043	352.5	0.0576	0.5014	0.0117	0.1013	8.62	0.0114	0.0000	0.1164
CDF055	0.0062	0.0040	47.4	0.0215	0.3339	0.0051	0.0210	2.97	0.0000	0.0000	0.0305

Anid	Cs	Eu	Fe	Hf	Rb	Sb	Sc	Sr	Ta	Tb	Th
CDF056	0.0082	0.0080	498.4	0.0420	0.3356	0.0105	0.0709	16.72	0.0076	0.0047	0.0732
CDF057	0.0040	0.0344	165.1	0.0318	0.2450	0.0109	0.0681	1.18	0.0055	0.0242	0.0561
CDF058	0.0045	0.0156	357.5	0.0332	0.2150	0.0130	0.0710	4.08	0.0059	0.0183	0.0626
CDF059	0.0056	0.0106	48.4	0.0142	0.2221	0.0052	0.0235	6.14	0.0023	0.0075	0.0286
CDF060	0.0181	0.0044	210.0	0.0793	0.5657	0.0087	0.1126	6.59	0.0155	0.0023	0.1351
CDF061	0.0059	0.0038	241.5	0.0274	0.2414	0.0186	0.0462	4.41	0.0046	0.0026	0.0524
CDF062	0.0027	0.0024	118.7	0.0268	0.2595	0.0130	0.0408	4.61	0.0039	0.0000	0.0616
CDF063	0.0078	0.0018	102.0	0.0270	0.2314	0.0093	0.0427	3.62	0.0046	0.0000	0.0485
CDF064	0.0064	0.0040	52.9	0.0302	0.2803	0.0052	0.0269	2.89	0.0030	0.0023	0.0260
CDF065	0.0000	0.0047	197.9	0.0417	0.2673	0.0125	0.0777	2.64	0.0071	0.0039	0.0791
CDF066	0.0000	0.0038	235.1	0.0228	0.0815	0.0193	0.0468	0.00	0.0037	0.0022	0.0377
CDF067	0.0068	0.0018	107.6	0.0402	0.3774	0.0154	0.0718	0.00	0.0076	0.0000	0.0628
CDF068	0.0146	0.0024	46.1	0.0499	0.3515	0.0082	0.0109	3.44	0.0000	0.0017	0.0175
CDF069	0.0124	0.0046	91.2	0.0393	0.3973	0.0196	0.0296	3.57	0.0034	0.0024	0.0355
CDF070	0.0000	0.0014	136.7	0.0137	0.1629	0.0325	0.0239	0.71	0.0029	0.0000	0.0295
CDF071	0.0050	0.0039	364.2	0.0367	0.3631	0.0078	0.0706	8.18	0.0096	0.0000	0.0951
CDF072	0.0078	0.0071	131.8	0.0414	0.2998	0.0118	0.0419	7.30	0.0045	0.0028	0.0464
CDF073	0.0000	0.0103	537.4	0.0563	0.3467	0.0219	0.0846	2.47	0.0085	0.0034	0.0977
CDF074	0.0151	0.0062	301.9	0.0410	0.5064	0.0170	0.0455	10.80	0.0056	0.0000	0.0521
CDF075	0.0078	0.0018	67.1	0.0816	0.7251	0.0644	0.0247	7.29	0.0005	0.0000	0.0192
CDF076	0.0073	0.0044	97.0	0.0391	0.8520	0.0159	0.0252	4.79	0.0000	0.0024	0.0180
CDF077	0.0137	0.0033	64.6	0.0414	0.4752	0.0085	0.0165	8.02	0.0000	0.0016	0.0178
CDF078	0.0134	0.0109	361.2	0.0709	0.6105	0.0219	0.0514	7.78	0.0085	0.0056	0.0660
CDF079	0.0087	0.0047	58.9	0.0455	0.5181	0.0096	0.0413	2.74	0.0029	0.0000	0.0389
CDF080	0.0138	0.0066	723.3	0.0287	0.4520	0.0235	0.0327	7.20	0.0025	0.0000	0.0633
CDF081	0.0062	0.0025	51.9	0.0292	0.2367	0.0105	0.0494	0.00	0.0000	0.0000	0.0424
CDF082	0.0205	0.0074	912.2	0.0708	0.5610	0.0397	0.1004	4.94	0.0093	0.0000	0.1292
CDF083	0.0168	0.0041	336.1	0.0279	0.0000	0.0358	0.0486	0.00	0.0000	0.0000	0.0472
CDF084	0.0078	0.0047	88.9	0.0199	0.4305	0.0178	0.0136	3.38	0.0000	0.0023	0.0251
CDF085	0.0000	0.0170	56.8	0.0391	0.2826	0.0091	0.0478	0.00	0.0000	0.0065	0.0495
CDF086	0.0000	0.0033	260.9	0.0312	0.1702	0.0117	0.0359	5.74	0.0046	0.0000	0.0437
CDF087	0.0155	0.0029	141.9	0.0704	0.5766	0.0064	0.1200	0.00	0.0161	0.0000	0.1356
CDF088	0.0115	0.0050	223.0	0.0543	0.6003	0.0342	0.0217	4.61	0.0000	0.0000	0.0248
CDF089	0.0120	0.0336	508.6	0.0333	0.5535	0.0214	0.0424	0.00	0.0000	0.0159	0.0478
CDF090	0.0197	0.0022	115.6	0.0940	0.5922	0.0109	0.0141	7.39	0.0000	0.0000	0.0178
CDF091	0.0096	0.0034	138.6	0.0150	0.1365	0.0178	0.0298	1.95	0.0000	0.0011	0.0244
CDF092	0.0079	0.0053	110.2	0.0861	0.3599	0.0147	0.0270	11.89	0.0037	0.0026	0.0260
CDF093	0.0081	0.0033	105.8	0.0437	0.3836	0.0150	0.0384	3.10	0.0045	0.0019	0.0596
CDF094	0.0097	0.0039	158.6	0.0707	0.3940	0.0227	0.0232	5.87	0.0000	0.0000	0.0317
CDF095	0.0095	0.0092	485.2	0.0574	0.4892	0.0270	0.0891	6.65	0.0101	0.0055	0.0994
CDF096	0.0080	0.0081	181.7	0.0323	0.3351	0.0117	0.0220	5.65	0.0029	0.0070	0.0434
CDF097	0.0089	0.0081	132.8	0.0733	0.6983	0.0204	0.0261	5.85	0.0042	0.0033	0.0277
CDF098	0.0086	0.0016	54.9	0.0352	1.2496	0.0222	0.0088	8.58	0.0000	0.0000	0.0154

Anid	Cs	Eu	Fe	Hf	Rb	Sb	Sc	Sr	Ta	Tb	Th
CDF099	0.0066	0.0121	275.2	0.0436	0.3278	0.0130	0.0618	4.39	0.0073	0.0059	0.0719
CDF100	0.0094	0.0075	81.4	0.0287	0.3829	0.0125	0.0162	2.53	0.0035	0.0035	0.0254
CDF101	0.0131	0.0032	97.3	0.0472	0.6557	0.0123	0.0378	2.57	0.0000	0.0000	0.0554
CDF102	0.0107	0.0079	215.5	0.0536	0.4862	0.0209	0.0152	3.07	0.0029	0.0043	0.0605
CDF103	0.2037	0.1573	1137.9	0.1254	1.7293	0.1914	0.4504	152.97	0.0337	0.0944	0.3966
CDF104	0.0034	0.0105	629.2	0.0449	0.2464	0.0382	0.0395	5.74	0.0023	0.0044	0.0660
CDF105	0.0058	0.0019	66.0	0.0159	0.3083	0.0075	0.0427	6.78	0.0024	0.0000	0.0477
CDF106	0.0134	0.0036	196.3	0.0574	0.4965	0.0081	0.0988	13.20	0.0107	0.0048	0.0796
CDF107	0.1209	0.0789	813.1	0.0799	1.7001	0.2179	0.1885	8.65	0.0194	0.0444	0.2290
CDF108	0.0196	0.0009	51.7	0.0168	0.2699	0.0094	0.0201	3.71	0.0000	0.0000	0.0156

Anid	Zn	Zr	Al	Ca	Dy	K	Mn	Na	V
EFC001	0.59	5.12	2033.9	992.0	0.0000	496.2	0.4487	428.3	2.129
EFC002	0.72	6.19	2714.4	0.0	0.0000	337.6	0.2474	448.5	3.433
EFC003	0.31	6.43	2074.1	0.0	0.0000	0.0	0.3030	391.7	1.468
EFC004	0.33	5.32	2490.5	784.2	0.0000	431.2	0.3957	421.2	2.791
EFC005	0.60	6.46	2202.8	850.4	0.0000	425.1	0.5053	354.4	2.971
EFC006	0.41	6.02	1995.1	1054.4	0.0000	315.5	0.1851	411.3	3.762
EFC007	0.72	5.23	2048.6	613.5	0.0000	413.7	0.2256	415.4	1.924
EFC008	0.60	5.41	2219.7	795.0	0.0000	434.0	0.2342	374.7	2.019
EFC009	0.50	6.16	2182.5	0.0	0.0000	524.2	0.2913	456.5	3.668
EFC010	0.79	4.24	2683.2	2996.7	0.0000	275.6	0.6311	439.0	3.381
EFC011	0.52	6.86	2173.0	659.0	0.0000	336.6	2.2211	409.6	2.434
EFC012	0.89	6.51	2786.4	0.0	0.0000	388.2	0.2122	493.7	4.251
EFC013	0.75	7.32	2357.2	785.2	0.0000	531.3	0.6300	447.7	3.346
EFC014	0.57	4.81	2213.0	1718.2	0.0000	371.1	0.8056	330.0	2.221
EFC015	0.30	4.78	2134.9	824.1	0.0000	394.9	0.3160	386.3	2.392
EFC016	0.43	6.35	1995.3	0.0	0.0000	355.4	0.5131	420.5	2.582
EFC017	0.42	5.97	2066.4	717.2	0.0000	483.1	0.8828	441.8	2.368
EFC019	0.66	5.76	2297.2	0.0	0.0000	348.5	0.3861	426.4	2.791
EFC020	0.59	5.61	2345.0	627.3	0.0000	517.5	0.3872	457.2	2.787
EFC021	0.87	5.81	2581.1	665.0	0.0000	469.3	0.2894	497.4	4.333
EFC022	1.82	6.86	2168.2	3399.7	0.0000	0.0	8.4946	399.3	1.670
EFC023	1.43	7.29	1743.2	4095.5	0.0000	327.3	2.1286	428.3	1.865
EFC024	0.56	6.15	2004.7	1679.5	0.0000	388.0	1.0501	383.2	1.490
EFC025	0.27	5.25	1777.3	0.0	0.0000	372.1	0.3117	255.0	1.164
EFC026	0.83	5.76	1823.6	4192.7	0.0000	0.0	1.1154	306.9	1.677
EFC027	1.32	5.92	2016.9	2797.3	0.0000	0.0	0.9441	390.2	0.000
EFC028	1.20	6.03	1977.3	1841.1	0.0000	428.3	1.1514	352.8	1.891
EFC029	1.40	6.10	1672.6	8165.8	0.0000	0.0	5.5516	350.1	2.675
EFC030	1.28	6.50	1758.6	6487.5	0.0000	0.0	3.9864	333.0	1.287
EFC031	0.36	6.00	1970.4	2632.7	0.0000	211.8	1.0781	279.5	0.000
EFC032	0.41	5.88	1572.6	1306.2	0.0000	0.0	0.9160	312.6	1.701
EFC033	1.00	5.23	1807.5	5333.0	0.0000	0.0	1.1420	361.3	0.000

Anid	Zn	Zr	Al	Ca	Dy	K	Mn	Na	V
EFC034	0.46	4.36	1793.5	3357.8	0.0000	290.3	0.7904	229.6	1.348
EFC035	1.95	5.07	1228.6	0.0	0.2372	0.0	0.5357	148.6	0.000
EFC036	0.87	4.59	1754.8	5229.9	0.0000	0.0	4.5212	340.7	2.140
EFC037	0.45	4.69	1885.6	3022.7	0.0000	222.2	1.4326	265.2	0.759
EFC038	2.78	7.31	2019.9	8601.0	0.0000	240.5	6.8669	387.7	0.000
EFC039	0.40	4.44	1955.5	0.0	0.0000	0.0	0.1683	336.0	0.888
EFC040	0.63	3.97	1857.3	1269.0	0.0000	251.4	0.5688	329.0	1.245
EFC041	0.87	4.92	2012.0	3435.8	0.0000	242.8	1.9542	380.2	0.000
EFC042	0.97	5.52	1853.1	0.0	0.0000	0.0	0.4175	392.6	0.000
EFC043	0.49	5.52	1463.1	0.0	0.0863	0.0	2.2173	205.3	2.988
EFC044	0.82	4.17	1609.0	20631.0	0.0000	131.6	6.1765	248.4	4.957
EFC045	0.63	4.99	1610.3	0.0	0.0472	312.9	3.2394	224.7	2.374
EFC046	0.71	5.06	1825.6	745.0	0.0000	0.0	0.8119	297.4	2.542
EFC047	0.37	5.52	1401.1	7765.9	0.0568	0.0	1.7985	197.3	1.659
EFC048	0.62	4.61	1183.2	0.0	0.0653	266.3	1.3496	213.9	2.592
EFC049	0.93	5.72	2095.4	0.0	0.0554	227.9	2.6283	306.4	2.167
EFC050	0.31	3.21	1248.7	0.0	0.0000	115.2	0.3653	152.2	0.000
EFC051	0.90	5.83	1654.5	0.0	0.1062	332.2	0.9612	283.1	1.702
EFC052	0.62	6.05	1710.5	0.0	0.0000	237.1	1.5227	285.6	2.746
EFC053	0.74	6.43	1327.7	3983.7	0.1459	0.0	2.9007	194.5	2.694
EFC054	0.51	4.49	1364.2	0.0	0.0856	153.3	2.4894	214.7	2.857
EFC055	0.82	4.52	1377.8	0.0	0.0000	0.0	0.8998	188.0	2.642
EFC056	0.60	6.24	2044.3	9957.3	0.0000	0.0	2.6296	322.8	3.101
EFC057	0.48	5.95	1069.3	10797.1	0.0000	0.0	3.0279	176.9	3.123
EFC058	0.21	3.80	1234.5	291.7	0.0000	0.0	0.2104	133.9	0.000
EFC059	0.27	7.53	1424.4	0.0	0.0000	0.0	0.2054	205.2	1.543
EFC060	1.46	6.71	1852.2	14765.3	0.2719	354.8	9.4000	283.5	2.778
EFC061	0.50	4.84	1674.8	1456.6	0.0000	0.0	0.8187	246.5	2.461
EFC062	0.68	6.22	1733.3	0.0	0.2662	0.0	3.3883	267.9	2.529
EFC063	0.13	17.11	1727.8	697.4	0.0000	0.0	0.1342	152.8	0.000
EFC064	0.19	7.81	1200.6	0.0	0.0000	0.0	0.0000	111.0	0.000
EFC065	0.12	9.99	2828.5	575.4	0.0000	0.0	0.9626	158.4	0.000
EFC066	0.12	12.02	1074.4	0.0	0.0000	0.0	0.0785	114.2	0.000
EFC067	0.11	14.49	2012.2	0.0	0.0000	307.1	0.1986	181.2	0.000
EFC068	0.09	5.23	1141.3	0.0	0.0000	0.0	0.0000	107.4	0.000
EFC069	0.08	6.13	1032.4	0.0	0.0000	0.0	0.0000	119.1	0.000
EFC070	0.25	3.54	1400.5	0.0	0.0000	0.0	0.2334	153.9	0.974
EFC071	0.11	12.16	1633.8	0.0	0.0000	0.0	0.2588	204.3	2.452
EFC072	0.16	5.22	1281.1	0.0	0.0000	0.0	0.2697	118.3	0.000
EFC073	0.15	6.94	1270.8	0.0	0.0000	0.0	0.1254	131.6	0.000
EFC074	0.21	10.26	1206.8	0.0	0.0000	0.0	0.3759	128.2	1.360
EFC075	0.00	7.84	1063.9	0.0	0.0000	0.0	0.0963	111.0	0.000
EFC076	0.12	9.92	1228.3	0.0	0.0000	126.5	0.3468	127.0	2.048

Anid	Zn	Zr	Al	Ca	Dy	K	Mn	Na	V
EFC077	0.00	6.43	1074.4	0.0	0.0000	0.0	0.0000	121.4	0.000
EFC078	0.05	3.16	1072.7	0.0	0.0000	0.0	0.3217	113.6	0.000
EFC079	0.09	7.07	1019.7	0.0	0.0000	0.0	0.0000	109.1	0.000
EFC080	0.06	12.06	1761.2	0.0	0.0000	0.0	0.3366	160.4	0.000
EFC081	0.28	3.64	1315.1	0.0	0.0000	0.0	0.1169	113.5	0.000
EFC082	0.10	12.70	1416.7	375.3	0.0000	0.0	0.3087	164.3	0.000
EFC083	0.33	16.09	1684.8	0.0	0.0000	0.0	0.1365	169.1	0.000
EFC084	0.37	13.94	1175.2	2857.4	0.0000	297.2	0.6936	150.5	0.000
EFC085	0.51	16.00	1252.1	0.0	0.0000	0.0	0.4262	156.1	0.000
EFC086	0.41	11.71	1115.3	0.0	0.0000	93.4	0.3390	102.1	0.000
EFC087	0.50	15.81	1486.6	4431.4	0.0798	0.0	2.6226	166.6	0.000
EFC088	0.41	11.58	1203.9	0.0	0.0000	0.0	0.4033	141.4	1.725
EFC089	0.58	14.84	1258.2	1436.3	0.0000	0.0	0.5260	147.8	0.000
EFC090	0.52	10.43	1345.6	0.0	0.0000	146.4	0.2697	155.9	0.000
EFC091	0.33	19.89	1367.4	0.0	0.0000	174.0	0.3448	155.4	0.709
EFC092	0.36	16.41	1109.1	0.0	0.1419	0.0	0.2401	142.7	0.000
EFC093	0.58	11.45	1600.2	0.0	0.0000	291.8	0.5481	178.1	0.000
EFC094	0.55	13.95	1325.9	0.0	0.0000	0.0	0.2794	142.3	0.000
EFC095	0.40	18.21	1893.6	12137.0	0.0000	0.0	6.9798	375.0	2.231
EFC096	0.37	16.53	1564.7	0.0	0.0000	0.0	0.2411	188.0	0.000
EFC097	0.60	12.70	1129.1	758.7	0.0000	0.0	0.5945	153.9	1.197
EFC098	0.33	16.62	1159.4	256.3	0.0000	0.0	1.3596	155.1	0.000
EFC099	0.42	14.09	1343.4	1556.3	0.0873	0.0	0.7291	151.8	0.000
EFC100	0.67	11.30	1446.9	0.0	0.0000	0.0	0.2270	130.1	0.000
EFC101	0.37	15.60	1460.8	0.0	0.0000	0.0	0.2159	174.6	0.000
EFC102	0.45	12.70	1483.1	0.0	0.1352	0.0	0.3239	174.9	0.000
EFC103	0.15	13.18	1881.9	568.0	0.0000	172.0	0.0000	231.1	0.000
EFC104	0.15	8.09	1732.0	0.0	0.0000	0.0	0.0000	242.0	1.434
EFC105	0.12	13.26	2316.1	565.4	0.0000	336.2	0.1537	309.3	0.000
EFC106	0.19	13.49	2010.7	0.0	0.0000	450.7	0.3801	197.6	0.000
EFC107	0.27	6.13	1329.2	689.8	0.0000	150.9	0.0000	146.7	0.000
EFC108	0.26	5.48	1384.3	0.0	0.0000	0.0	0.2514	158.4	1.123
EFC109	0.52	5.65	1645.3	1750.0	0.0000	0.0	0.6369	274.5	1.300
EFC110	0.09	11.55	1553.1	0.0	0.0000	0.0	0.1703	205.7	0.000
EFC111	0.22	9.85	1176.9	0.0	0.0000	0.0	0.2254	144.2	0.000
EFC112	0.13	9.36	1742.5	0.0	0.0000	275.3	0.3425	227.1	0.000
EFC113	0.32	6.30	1667.4	0.0	0.0000	0.0	0.4927	211.9	1.178
EFC114	0.43	6.89	1501.0	967.2	0.0000	0.0	0.4565	243.7	1.289
EFC115	0.24	6.25	1361.0	0.0	0.0000	0.0	0.3154	195.3	0.000
EFC116	0.16	10.81	1930.2	0.0	0.0000	0.0	0.3407	241.6	0.000
EFC117	0.20	7.69	1524.2	0.0	0.0000	237.6	0.6061	188.5	0.000
EFC118	0.28	5.92	1279.9	0.0	0.0000	0.0	0.6576	212.7	0.000
EFC119	0.15	5.96	1650.7	0.0	0.0000	232.5	0.1591	191.7	0.000

Anid	Zn	Zr	Al	Ca	Dy	K	Mn	Na	V
EFC121	0.31	6.29	1619.5	1974.5	0.0000	0.0	0.9506	237.1	0.000
CDF001	2.20	15.19	1873.0	0.0	0.0000	251.5	4.7557	289.6	5.564
CDF002	1.58	42.33	1567.7	412.6	0.0000	0.0	2.2062	250.7	5.435
CDF003	2.36	4.24	1924.9	1476.4	0.0000	323.9	1.6132	383.9	2.110
CDF004	0.95	11.40	1492.8	814.0	0.0000	318.9	2.3043	282.1	0.000
CDF005	0.91	29.83	1161.2	362.9	0.0000	0.0	6.4612	159.0	0.000
CDF007	1.23	4.18	1892.1	1728.9	0.0000	334.0	1.4513	307.0	2.129
CDF008	1.29	5.96	1620.2	4223.3	0.0000	220.9	6.7709	173.6	1.651
CDF009	1.83	5.70	1395.7	818.1	0.1049	0.0	4.0132	139.4	2.123
CDF010	0.73	4.42	2055.4	1315.2	0.0558	375.9	1.1922	369.3	1.992
CDF011	1.45	3.23	1689.4	646.6	0.0000	243.6	1.0720	263.2	0.000
CDF012	0.95	10.19	1685.0	431.1	0.0000	0.0	3.6689	208.5	0.000
CDF013	2.45	7.78	1915.6	466.5	0.0000	0.0	11.2273	261.8	0.000
CDF014	0.68	4.02	1573.5	473.0	0.0538	341.7	3.1855	284.1	0.000
CDF015	1.73	5.86	1924.4	1498.1	0.0000	415.4	2.3279	374.9	2.457
CDF016	1.40	46.15	1922.6	577.2	0.0000	391.5	1.4994	203.8	1.657
CDF017	1.64	65.35	2126.6	361.0	0.0000	316.3	3.7020	222.6	0.000
CDF018	1.40	10.88	1921.6	1800.9	0.0000	275.6	4.2035	244.9	2.300
CDF019	0.70	5.14	2208.7	3381.8	0.0000	582.4	32.4627	330.6	0.000
CDF020	1.04	50.24	2150.7	0.0	0.0000	494.3	1.6970	233.9	0.000
CDF022	0.51	73.03	1590.3	580.0	0.0000	195.9	3.5088	181.7	0.000
CDF023	2.29	11.48	1486.3	1403.3	0.3245	0.0	20.0834	263.2	1.773
CDF024	0.98	27.38	1800.2	508.1	0.0000	0.0	2.0675	221.2	0.000
CDF025	1.40	15.16	1922.6	3374.2	0.0000	346.0	3.1896	347.0	5.051
CDF026	0.67	39.63	1388.8	403.9	0.0000	252.6	2.3693	252.5	2.207
CDF027	0.46	53.92	2422.8	561.6	0.0000	355.9	0.9397	219.6	0.000
CDF028	0.54	10.72	1614.9	589.4	0.0000	292.5	1.5943	183.2	0.000
CDF029	0.74	33.46	1643.3	1269.0	0.0398	269.7	1.9562	221.7	2.211
CDF030	0.34	10.60	1454.3	738.6	0.0000	279.7	2.2599	173.8	0.000
CDF031	1.36	77.93	1789.2	1031.7	0.0000	243.9	1.3573	249.7	0.000
CDF032	0.74	25.03	1337.7	0.0	0.0000	122.4	2.2767	200.2	0.000
CDF033	0.65	36.04	1186.3	302.4	0.0000	186.1	1.9305	169.7	0.000
CDF034	1.02	59.84	1671.4	523.2	0.0000	244.3	1.2596	211.9	2.406
CDF035	0.37	6.02	1218.6	239.9	0.0000	0.0	0.4104	115.3	1.228
CDF037	0.91	8.15	1817.0	1766.5	0.1100	141.4	4.0891	204.8	0.000
CDF038	0.93	47.11	1632.8	1641.5	0.0000	0.0	3.6422	193.8	2.007
CDF039	1.76	8.65	1575.2	8412.7	0.0000	414.8	7.4413	292.2	2.566
CDF040	1.64	6.69	1483.5	3119.2	0.0000	0.0	5.0060	260.8	3.008
CDF041	0.83	9.48	1774.1	4639.0	0.0000	0.0	4.0858	230.3	1.548
CDF042	0.82	34.84	1430.1	0.0	0.0000	281.6	8.7494	254.9	0.000
CDF043	1.50	8.41	1750.1	2654.9	0.0000	0.0	1.3020	259.7	0.835
CDF044	0.97	7.14	1242.4	0.0	0.0000	0.0	1.4567	139.4	1.754
CDF045	1.16	6.85	1214.7	5150.7	0.0000	0.0	3.8879	215.5	1.712

Anid	Zn	Zr	Al	Ca	Dy	K	Mn	Na	V
CDF046	0.98	16.60	2045.2	845.2	0.0000	0.0	0.5566	198.2	0.000
CDF047	1.70	20.90	1281.5	0.0	0.0000	237.4	2.1830	211.1	3.371
CDF048	1.11	46.29	2038.7	620.9	0.0000	465.6	0.5679	289.4	1.204
CDF049	1.69	17.83	2320.2	11900.9	0.0000	732.5	3.4420	483.9	2.081
CDF050	1.24	16.87	1570.5	0.0	0.0000	0.0	0.5807	234.2	1.149
CDF051	0.69	10.36	1622.0	0.0	0.0000	0.0	0.7253	176.4	3.531
CDF052	1.35	81.50	1552.3	322.7	0.0000	217.3	0.5171	160.5	2.494
CDF053	1.91	9.21	1429.7	31983.4	0.0000	0.0	18.4023	227.1	2.689
CDF054	1.34	9.80	1808.9	6938.3	0.0000	306.3	4.6871	319.4	0.000
CDF055	0.36	63.37	1640.6	279.1	0.0000	0.0	1.0559	162.2	1.940
CDF056	1.81	6.98	1303.6	18460.0	0.0000	0.0	13.3539	266.2	2.189
CDF057	0.57	6.94	1072.1	0.0	0.0932	214.4	2.4975	214.3	1.503
CDF058	0.99	6.92	1277.8	10825.7	0.0000	0.0	9.8489	201.8	2.438
CDF059	0.39	6.84	1375.7	735.8	0.0000	0.0	1.8709	167.0	0.000
CDF060	0.72	6.78	2260.7	797.9	0.0000	101.5	1.2014	357.7	2.059
CDF061	1.00	6.91	1099.5	27141.2	0.0000	0.0	19.1291	184.5	1.761
CDF062	0.76	7.76	1155.4	6913.8	0.0000	0.0	5.9930	191.6	1.577
CDF063	1.07	7.19	1540.3	399.9	0.0000	0.0	0.8739	184.1	0.000
CDF064	0.40	9.70	1391.1	0.0	0.0000	273.6	1.3045	179.8	1.821
CDF065	0.71	6.04	1729.2	8705.7	0.0000	0.0	11.9663	282.5	2.305
CDF066	0.54	7.45	1277.3	0.0	0.0000	0.0	1.3081	149.7	1.573
CDF067	0.90	35.17	1895.6	0.0	0.0000	258.6	0.4872	250.7	1.012
CDF068	0.57	52.39	2115.8	465.6	0.0000	149.0	0.4049	184.0	0.000
CDF069	0.81	29.43	1872.0	587.3	0.0000	280.8	1.4166	218.7	0.000
CDF070	0.64	23.86	1213.7	1761.1	0.0000	0.0	4.3830	134.5	3.853
CDF071	1.46	7.72	1295.0	1842.9	0.0000	145.4	1.0249	213.5	0.000
CDF072	0.62	28.11	1536.2	800.5	0.0000	239.2	1.7909	184.7	0.000
CDF073	1.52	5.75	1853.1	2035.4	0.0000	325.7	9.3165	295.8	0.000
CDF074	0.60	4.53	1845.5	502.8	0.0000	295.7	1.5867	233.2	2.492
CDF075	0.24	48.13	2188.9	399.0	0.0000	388.8	0.3898	192.3	0.000
CDF076	0.37	60.53	1782.5	878.7	0.0000	0.0	1.1989	167.9	1.081
CDF077	0.29	50.94	2234.2	508.7	0.0000	362.4	1.1142	173.3	0.000
CDF078	0.86	4.81	2188.4	497.0	0.0000	519.1	0.9120	207.6	1.579
CDF079	0.65	17.54	1901.1	661.4	0.0000	249.8	1.2764	181.8	0.000
CDF080	1.04	6.51	1479.4	834.1	0.0000	0.0	2.9247	153.5	3.072
CDF081	1.15	35.50	1525.3	0.0	0.0000	270.3	1.0769	163.9	0.000
CDF082	1.09	6.52	1740.0	14071.7	0.0326	0.0	18.4430	312.4	4.224
CDF083	0.76	8.64	1306.2	402.7	0.0000	0.0	2.4513	183.1	1.822
CDF084	1.25	5.11	1673.0	0.0	0.0000	0.0	3.5408	188.0	0.000
CDF085	1.02	21.09	1436.4	0.0	0.0340	361.2	1.0507	218.1	0.000
CDF086	0.38	3.58	1386.8	11390.4	0.0000	0.0	4.4221	131.5	2.154
CDF087	0.71	8.44	2102.3	439.6	0.0000	460.9	0.7483	380.2	0.000
CDF088	0.77	28.42	2285.0	0.0	0.0000	0.0	2.7804	303.3	0.000

Anid	Zn	Zr	Al	Ca	Dy	K	Mn	Na	V
CDF089	0.37	9.61	1575.3	0.0	0.1142	306.3	1.9684	183.9	2.438
CDF090	0.49	27.97	2282.2	807.3	0.0000	415.6	1.2448	188.3	0.000
CDF091	0.28	7.55	1162.6	0.0	0.0000	0.0	0.6717	151.8	0.000
CDF092	0.71	22.67	1823.3	0.0	0.0000	451.7	0.8591	239.9	0.000
CDF093	0.32	35.17	1711.1	0.0	0.0000	412.8	1.5673	203.8	0.000
CDF094	0.61	17.39	2122.7	0.0	0.0000	471.1	1.4498	185.3	0.000
CDF095	1.02	5.56	1529.5	8989.0	0.0000	0.0	5.6806	273.2	2.170
CDF096	1.37	14.25	1968.7	819.4	0.0000	0.0	2.1950	194.3	1.696
CDF097	1.39	45.26	2344.9	0.0	0.0000	483.5	2.5047	202.3	0.000
CDF098	0.57	21.75	2527.6	0.0	0.0000	826.5	1.9559	381.4	0.000
CDF099	0.70	4.82	1644.1	0.0	0.0000	0.0	1.8631	183.8	2.004
CDF100	0.84	13.76	1717.2	1074.4	0.0000	0.0	2.1264	111.2	0.000
CDF101	0.40	45.34	1761.5	0.0	0.0000	334.5	0.7260	175.7	1.547
CDF102	0.42	19.45	2277.4	649.6	0.0000	0.0	2.1843	145.9	0.000
CDF103	12.96	19.69	3338.2	30126.4	0.5477	909.3	14.4198	492.9	7.014
CDF104	3.41	34.96	1745.1	729.3	0.0000	0.0	12.3336	127.1	2.661
CDF105	2.86	30.82	1687.8	0.0	0.0000	304.9	0.7022	180.5	0.000
CDF106	8.41	6.43	1669.2	3862.3	0.0000	466.8	2.5461	339.5	1.711
CDF107	20.22	14.15	2869.4	3202.2	0.3118	619.3	26.7981	303.4	5.485
CDF108	2.63	51.02	1562.4	0.0	0.0000	0.0	1.4050	219.1	1.841

Anid	As	Ba	La	Lu	Nd	Sm	U	Yb	Ce	Co	Cr
EFC001	0.000	16.06	0.2700	0.0000	0.224	0.0905	1.123	0.0113	0.321	0.0188	1.074
EFC002	0.000	15.90	0.2990	0.0000	0.251	0.0938	1.200	0.0049	0.369	0.0180	1.544
EFC003	0.000	16.44	0.2739	0.0000	0.220	0.0949	1.270	0.0030	0.355	0.0103	1.121
EFC004	0.000	13.68	0.2562	0.0045	0.205	0.0774	0.980	0.0081	0.285	0.0205	1.137
EFC005	0.000	14.58	0.2893	0.0000	0.155	0.0901	1.185	0.0125	0.326	0.0186	1.317
EFC006	0.000	12.73	0.2772	0.0042	0.219	0.0907	1.215	0.0064	0.340	0.0171	1.223
EFC007	0.000	16.57	0.2806	0.0040	0.243	0.0796	1.025	0.0075	0.309	0.0157	1.202
EFC008	0.000	13.13	0.2811	0.0043	0.135	0.0811	1.019	0.0064	0.295	0.0195	1.066
EFC009	0.000	13.31	0.2933	0.0040	0.000	0.0899	1.116	0.0077	0.345	0.0204	1.405
EFC010	0.000	18.01	0.2445	0.0041	0.158	0.0690	0.765	0.0059	0.304	0.0473	1.572
EFC011	0.000	11.55	0.3961	0.0052	0.280	0.1240	1.619	0.0068	0.407	0.0398	1.221
EFC012	0.000	17.65	0.4329	0.0050	0.453	0.1186	1.295	0.0102	0.597	0.0214	1.309
EFC013	0.000	17.72	0.3356	0.0049	0.269	0.1019	1.254	0.0067	0.368	0.0541	1.457
EFC014	0.000	11.08	0.2432	0.0035	0.263	0.0772	0.977	0.0000	0.288	0.0190	1.150
EFC015	0.000	15.99	0.2599	0.0048	0.232	0.0798	1.001	0.0000	0.315	0.0163	1.189
EFC016	0.000	13.17	0.4928	0.0048	0.338	0.0998	1.178	0.0083	0.391	0.0150	1.438
EFC017	0.000	11.40	0.3029	0.0033	0.215	0.0843	1.047	0.0119	0.327	0.0191	1.233
EFC019	0.000	13.04	0.3080	0.0009	0.220	0.0871	1.072	0.0045	0.362	0.0259	1.247
EFC020	0.000	16.22	0.2795	0.0036	0.399	0.0781	0.978	0.0083	0.300	0.0172	1.156
EFC021	0.000	17.19	0.3193	0.0038	0.179	0.0849	0.998	0.0102	0.331	0.0207	1.472
EFC022	0.000	11.87	0.3738	0.0053	0.467	0.1137	1.477	0.0077	0.354	0.0307	0.983

Anid	As	Ba	La	Lu	Nd	Sm	U	Yb	Ce	Co	Cr
EFC023	0.000	11.33	0.3784	0.0058	0.164	0.1077	1.435	0.0000	0.302	0.0215	0.875
EFC024	0.000	7.49	0.3431	0.0048	0.238	0.0953	1.274	0.0000	0.309	0.0154	1.015
EFC025	0.000	14.11	0.3260	0.0000	0.156	0.0953	1.267	0.0000	0.252	0.0107	0.661
EFC026	0.000	12.30	0.3061	0.0000	0.307	0.0879	1.164	0.0032	0.258	0.0155	0.745
EFC027	0.000	17.71	0.2926	0.0036	0.205	0.0862	1.081	0.0000	0.277	0.0234	0.864
EFC028	0.000	11.13	0.3756	0.0000	0.206	0.0989	1.268	0.0052	0.305	0.0198	0.968
EFC029	0.000	8.86	0.3592	0.0048	0.284	0.1091	1.357	0.0051	0.339	0.0349	0.965
EFC030	0.000	10.98	0.3988	0.0035	0.292	0.1185	1.505	0.0000	0.336	0.0342	0.819
EFC031	0.000	14.22	0.3097	0.0000	0.188	0.0871	1.161	0.0000	0.255	0.0168	0.680
EFC032	0.160	10.33	0.1490	0.0068	0.318	0.0805	1.122	0.0036	0.321	0.0196	0.738
EFC033	0.164	10.28	0.1365	0.0063	0.133	0.0761	0.917	0.0082	0.297	0.0263	0.935
EFC034	0.108	10.80	0.1236	0.0055	0.186	0.0662	0.880	0.0026	0.263	0.0173	0.618
EFC035	0.216	10.07	0.1536	0.0074	0.294	0.0823	1.017	0.0083	0.340	0.0174	0.760
EFC036	0.162	7.68	0.1390	0.0063	0.208	0.0738	0.954	0.0060	0.285	0.0290	0.908
EFC037	0.154	15.12	0.1284	0.0064	0.146	0.0694	0.917	0.0053	0.262	0.0224	0.694
EFC038	0.216	10.32	0.1920	0.0093	0.319	0.1049	1.391	0.0071	0.424	0.0336	1.000
EFC039	0.000	17.08	0.1270	0.0060	0.303	0.0687	0.927	0.0081	0.255	0.0170	0.699
EFC040	0.000	10.75	0.1213	0.0050	0.219	0.0615	0.784	0.0050	0.260	0.0147	0.658
EFC041	0.000	11.41	0.1151	0.0057	0.192	0.0596	0.763	0.0062	0.243	0.0292	0.900
EFC042	0.181	10.26	0.1558	0.0000	0.241	0.0787	1.032	0.0069	0.313	0.0278	0.938
EFC043	0.362	24.59	1.9629	0.0141	1.438	0.2133	0.977	0.0487	1.241	0.0238	0.697
EFC044	0.324	40.99	0.4569	0.0068	0.380	0.0837	0.806	0.0221	0.425	0.0236	0.697
EFC045	0.352	29.18	0.4156	0.0078	0.319	0.0923	0.955	0.0141	0.439	0.0244	0.569
EFC046	0.416	48.67	0.7350	0.0076	0.486	0.1049	0.806	0.0253	0.513	0.0335	0.923
EFC047	0.352	29.20	1.2088	0.0087	0.846	0.1460	0.935	0.0351	0.750	0.0213	0.723
EFC048	0.307	28.01	0.7299	0.0084	0.600	0.1103	0.868	0.0281	0.477	0.0195	0.644
EFC049	0.347	43.97	0.8420	0.0092	0.451	0.1150	1.095	0.0254	0.462	0.0206	0.701
EFC050	0.160	21.60	0.4508	0.0058	0.498	0.1168	0.661	0.0144	0.682	0.0109	0.595
EFC051	0.277	34.81	3.0221	0.0132	2.757	0.3493	1.019	0.0621	1.774	0.0193	0.709
EFC052	0.358	38.76	0.6289	0.0089	0.357	0.0986	0.977	0.0157	0.448	0.0280	0.633
EFC053	0.331	24.70	3.5223	0.0198	3.264	0.4110	1.061	0.0824	3.299	0.0242	0.673
EFC054	0.000	22.58	0.8659	0.0101	0.827	0.1583	0.880	0.0308	0.814	0.0195	0.693
EFC055	0.221	29.27	0.7480	0.0081	0.695	0.1393	0.875	0.0283	0.617	0.0181	0.634
EFC056	0.324	34.19	0.1849	0.0062	0.240	0.0865	1.122	0.0061	0.326	0.0247	0.650
EFC057	0.286	21.08	0.6576	0.0072	0.463	0.1221	1.128	0.0132	0.541	0.0139	0.633
EFC058	0.121	20.11	0.2582	0.0032	0.380	0.0855	0.698	0.0069	0.444	0.0065	0.479
EFC059	0.182	21.95	0.3411	0.0000	0.370	0.1236	1.563	0.0048	0.406	0.0058	0.496
EFC060	0.000	35.25	5.3176	0.0192	3.461	0.4592	1.565	0.0928	2.914	0.0391	0.830
EFC061	0.591	46.29	0.8906	0.0063	0.722	0.1230	0.876	0.0188	0.690	0.0144	0.680
EFC062	0.421	25.80	3.0606	0.0164	3.288	0.3735	0.903	0.0855	2.449	0.0343	0.771
EFC063	0.000	31.16	0.5341	0.0000	0.616	0.2837	4.017	0.0027	0.775	0.0030	0.267
EFC064	0.000	13.84	0.3116	0.0000	0.404	0.1373	1.925	0.0039	0.405	0.0029	0.256
EFC065	0.000	17.01	0.3124	0.0000	0.416	0.1560	2.161	0.0000	0.423	0.0053	0.345

Anid	As	Ba	La	Lu	Nd	Sm	U	Yb	Ce	Co	Cr
EFC066	0.116	15.03	0.3925	0.0000	0.601	0.1942	2.642	0.0024	0.530	0.0039	0.423
EFC067	0.000	39.12	0.5101	0.0000	0.694	0.2504	3.558	0.0038	0.681	0.0063	0.163
EFC068	0.000	7.23	0.1770	0.0000	0.405	0.0845	1.182	0.0000	0.237	0.0015	0.271
EFC069	0.000	8.16	0.2158	0.0000	0.443	0.1066	1.499	0.0000	0.296	0.0025	0.359
EFC070	0.000	14.63	0.2941	0.0035	0.229	0.0641	0.588	0.0065	0.268	0.0080	0.656
EFC071	0.000	31.29	0.4696	0.0000	0.520	0.2162	2.854	0.0040	0.585	0.0032	0.429
EFC072	0.000	10.43	0.2093	0.0000	0.194	0.0910	1.257	0.0000	0.254	0.0110	0.433
EFC073	0.000	11.59	0.2884	0.0000	0.391	0.1201	1.476	0.0062	0.354	0.0065	0.507
EFC074	0.000	16.81	0.3863	0.0000	0.458	0.1717	2.360	0.0041	0.487	0.0062	0.413
EFC075	0.000	11.66	0.2822	0.0000	0.385	0.1348	1.857	0.0000	0.354	0.0017	0.312
EFC076	0.000	18.03	0.3955	0.0000	0.446	0.1676	2.353	0.0000	0.455	0.0032	0.404
EFC077	0.000	11.22	0.3000	0.0000	0.338	0.1206	1.564	0.0037	0.335	0.0035	0.342
EFC078	0.000	9.67	0.1163	0.0030	0.108	0.0544	0.712	0.0026	0.147	0.0019	0.283
EFC079	0.000	13.11	0.3126	0.0000	0.332	0.1265	1.682	0.0000	0.331	0.0021	0.355
EFC080	0.000	33.65	0.5363	0.0000	0.744	0.2224	3.055	0.0000	0.581	0.0026	0.164
EFC081	0.320	9.98	0.1670	0.0000	0.177	0.0707	0.909	0.0000	0.196	0.0025	0.505
EFC082	0.000	33.00	0.6086	0.0000	0.548	0.2414	3.160	0.0045	0.597	0.0049	0.366
EFC083	0.000	17.43	0.7073	0.0000	0.751	0.2907	3.862	0.0000	0.771	0.0065	0.474
EFC084	0.000	14.99	0.6118	0.0000	0.586	0.2525	3.306	0.0061	0.674	0.0149	0.472
EFC085	0.000	19.12	1.2364	0.0000	1.078	0.3290	3.912	0.0152	0.988	0.0104	0.527
EFC086	0.000	14.70	0.5181	0.0000	0.597	0.2032	2.777	0.0049	0.584	0.0079	0.495
EFC087	0.000	19.34	1.0536	0.0000	1.653	0.3161	3.972	0.0119	1.054	0.0131	0.537
EFC088	0.000	14.61	0.5250	0.0000	0.519	0.1513	2.173	0.0000	0.584	0.0144	0.437
EFC089	0.000	15.37	0.6647	0.0000	0.000	0.2312	2.751	0.0000	0.768	0.0135	0.475
EFC090	0.000	10.45	0.4664	0.0000	0.000	0.2155	1.954	0.0000	0.489	0.0176	0.869
EFC091	0.000	27.22	0.8842	0.0000	0.000	0.4337	3.537	0.0000	0.953	0.0145	0.406
EFC092	0.000	20.32	1.2326	0.0127	0.858	0.2735	3.021	0.0000	1.211	0.0167	0.430
EFC093	0.000	14.12	0.5710	0.0000	0.000	0.1267	2.169	0.0000	0.600	0.0164	0.527
EFC094	0.000	17.01	0.7000	0.0000	0.000	0.2507	2.744	0.0000	0.681	0.0136	0.524
EFC095	0.000	26.27	1.9561	0.0130	1.591	0.3266	3.488	0.0000	1.990	0.0246	0.423
EFC096	0.000	20.67	1.1583	0.0112	1.070	0.3714	3.144	0.0000	1.082	0.0203	0.476
EFC097	0.000	14.30	0.5992	0.0023	0.000	0.2930	2.341	0.0000	0.611	0.0260	0.556
EFC098	0.000	21.83	1.3706	0.0000	0.000	0.3743	3.309	0.0000	1.075	0.0193	0.376
EFC099	0.000	15.29	1.7974	0.0132	1.136	0.3132	2.610	0.0599	1.050	0.0185	0.458
EFC100	0.000	14.99	0.5521	0.0000	0.000	0.1664	2.249	0.0000	0.581	0.0275	0.509
EFC101	0.000	19.01	0.7771	0.0000	0.000	0.1388	2.758	0.0000	0.748	0.0173	0.505
EFC102	0.000	16.34	1.5039	0.0104	0.000	0.2293	2.440	0.0000	1.241	0.0191	0.618
EFC103	0.000	27.91	0.7210	0.0000	0.000	0.1252	2.350	0.0000	0.617	0.0113	0.417
EFC104	0.000	20.42	0.3811	0.0000	0.000	0.1171	1.536	0.0000	0.355	0.0112	0.500
EFC105	0.000	34.76	0.7056	0.0000	0.000	0.2235	2.374	0.0057	0.625	0.0129	0.390
EFC106	0.000	24.62	0.6719	0.0000	0.000	0.2076	2.446	0.0000	0.611	0.0110	0.336
EFC107	0.000	17.11	0.3248	0.0040	0.000	0.1040	1.314	0.0000	0.339	0.0120	0.573
EFC108	0.000	15.68	0.3127	0.0035	0.000	0.0996	1.203	0.0000	0.306	0.0131	0.540

Anid	As	Ba	La	Lu	Nd	Sm	U	Yb	Ce	Co	Cr
EFC109	0.000	17.79	0.1915	0.0000	0.000	0.0591	1.094	0.0000	0.283	0.0154	0.573
EFC110	0.000	20.63	0.6270	0.0000	0.000	0.2024	2.314	0.0000	0.605	0.0117	0.335
EFC111	0.000	19.16	0.5221	0.0000	0.000	0.0874	1.827	0.0000	0.494	0.0116	0.293
EFC112	0.000	19.72	0.7570	0.0047	0.000	0.1471	1.745	0.0000	0.500	0.0117	0.466
EFC113	0.000	21.09	0.3972	0.0000	0.000	0.0738	1.294	0.0000	0.313	0.0156	0.709
EFC114	0.000	7.19	0.3671	0.0041	0.000	0.0603	1.283	0.0000	0.414	0.0176	0.721
EFC115	0.000	15.66	0.3738	0.0019	0.000	0.0601	1.243	0.0000	0.327	0.0154	0.597
EFC116	0.000	21.81	0.6057	0.0000	0.000	0.1144	1.816	0.0000	0.484	0.0113	0.427
EFC117	0.000	22.89	0.4698	0.0000	0.000	0.0905	1.519	0.0000	0.380	0.0121	0.419
EFC118	0.000	16.06	0.4287	0.0000	0.000	0.0949	1.278	0.0000	0.393	0.0136	0.465
EFC119	0.000	13.88	0.6165	0.0000	0.000	0.0513	1.191	0.0000	0.838	0.0120	0.492
EFC121	0.000	12.84	0.3361	0.0027	0.000	0.0663	1.251	0.0000	0.313	0.0204	0.614
CDF001	0.665	75.16	0.5889	0.0171	0.844	0.2692	3.596	0.0150	1.117	0.0635	0.690
CDF002	0.672	182.85	1.1410	0.0477	2.044	0.7307	10.733	0.0113	2.301	0.1357	0.505
CDF003	0.337	9.55	0.1873	0.0055	0.232	0.0763	0.878	0.0057	0.422	0.0676	0.922
CDF004	0.082	14.50	0.4958	0.0158	0.818	0.2177	2.773	0.0184	0.803	0.1391	1.059
CDF005	0.076	52.32	0.8952	0.0336	1.629	0.5327	7.801	0.0058	1.751	0.0446	0.146
CDF007	0.309	8.25	0.2752	0.0052	0.319	0.0757	0.689	0.0100	0.372	0.0738	1.004
CDF008	0.212	15.77	0.3193	0.0075	0.354	0.1153	1.341	0.0139	0.526	0.0867	0.687
CDF009	0.000	12.14	1.1402	0.0177	1.399	0.2618	1.158	0.0845	1.530	0.0839	0.672
CDF010	0.141	10.34	0.4052	0.0070	0.377	0.0976	0.780	0.0177	0.631	0.0366	1.116
CDF011	0.171	17.45	0.4797	0.0049	0.463	0.0963	0.594	0.0170	0.308	0.0800	0.979
CDF012	0.000	15.76	0.3041	0.0102	0.470	0.1648	2.336	0.0031	0.521	0.0341	0.386
CDF013	0.336	30.64	0.5752	0.0092	0.766	0.1783	1.791	0.0154	0.451	0.2174	0.561
CDF014	0.230	8.96	0.2562	0.0048	0.261	0.0717	0.789	0.0089	0.348	0.0868	0.677
CDF015	0.388	12.12	0.4823	0.0081	0.488	0.1136	1.158	0.0098	0.739	0.0523	1.174
CDF016	0.000	59.65	1.6707	0.0490	2.650	0.8539	11.813	0.0096	2.717	0.0552	0.368
CDF017	0.464	110.52	1.4608	0.0000	3.310	0.8178	18.016	0.0438	2.705	0.1548	0.509
CDF018	0.000	136.25	0.6303	0.0115	1.034	0.1951	2.521	0.0270	1.150	0.0835	0.897
CDF019	0.000	453.90	0.2518	0.0027	0.434	0.0457	0.507	0.0183	0.426	0.1846	1.048
CDF020	0.322	69.53	1.3748	0.0000	2.870	0.6439	13.882	0.0377	2.065	0.0536	0.166
CDF022	0.303	66.76	1.2663	0.0000	3.357	0.8437	20.812	0.0000	2.699	0.0554	0.327
CDF023	0.000	35.07	4.4751	0.0271	4.944	0.5558	1.794	0.1908	1.609	0.3211	0.949
CDF024	0.000	40.29	0.6512	0.0000	1.429	0.3317	7.466	0.0104	1.190	0.0400	0.215
CDF025	0.000	21.38	0.4250	0.0000	0.623	0.1926	3.849	0.0162	0.850	0.1095	1.965
CDF026	0.000	32.81	0.8016	0.0000	1.921	0.4763	11.584	0.0278	1.660	0.0986	0.878
CDF027	0.168	65.46	1.0593	0.0000	2.090	0.6215	14.460	0.0050	1.951	0.0294	0.206
CDF028	0.000	17.58	0.7507	0.0118	1.272	0.2215	2.835	0.0282	1.052	0.0453	0.423
CDF029	0.195	117.08	0.8142	0.0000	1.433	0.4203	9.375	0.0321	1.635	0.0789	0.702
CDF030	0.000	18.75	0.5022	0.0089	0.813	0.1358	2.273	0.0114	0.562	0.0414	0.802
CDF031	0.000	73.23	1.5002	0.0000	3.216	0.9228	22.166	0.0000	3.030	0.0391	0.388
CDF032	0.257	16.30	0.4970	0.0000	1.233	0.2777	6.473	0.0119	0.930	0.0462	0.850
CDF033	0.234	30.83	0.6585	0.0000	1.293	0.4146	9.977	0.0106	1.269	0.0380	0.453

Anid	As	Ba	La	Lu	Nd	Sm	U	Yb	Ce	Co	Cr
CDF034	0.000	63.96	1.0798	0.0000	2.698	0.7055	16.992	0.0000	2.183	0.0427	0.415
CDF035	0.000	6.10	0.1731	0.0048	0.305	0.0719	1.561	0.0036	0.287	0.0656	0.714
CDF037	0.000	24.87	0.7752	0.0111	1.250	0.1991	1.842	0.0392	1.298	0.1286	0.641
CDF038	0.393	124.48	0.9632	0.0000	2.308	0.5475	13.842	0.0000	1.760	0.0580	0.458
CDF039	0.339	17.29	0.4966	0.0078	0.601	0.1228	1.989	0.0186	0.603	0.0709	0.889
CDF040	0.000	34.75	0.1605	0.0047	0.000	0.0734	1.358	0.0061	0.329	0.0595	1.480
CDF041	0.000	261.18	0.8178	0.0072	0.610	0.1241	1.993	0.0207	0.475	0.0404	0.812
CDF042	0.189	28.54	0.7556	0.0000	1.220	0.4061	9.832	0.0073	1.291	0.0273	0.604
CDF043	0.420	50.49	1.0161	0.0094	1.581	0.2018	1.965	0.0329	0.903	0.0710	0.782
CDF044	0.000	22.62	0.1742	0.0000	0.355	0.0820	2.025	0.0000	0.286	0.0409	0.360
CDF045	0.000	11.03	0.2780	0.0054	0.350	0.0805	1.487	0.0107	0.403	0.0432	0.892
CDF046	0.000	26.64	0.4807	0.0147	0.756	0.2374	3.451	0.0059	0.738	0.0737	0.963
CDF047	0.477	27.82	0.4625	0.0198	0.796	0.2813	4.365	0.0053	0.923	0.1104	0.637
CDF048	0.118	55.22	0.8749	0.0426	1.578	0.6748	10.652	0.0000	1.894	0.0771	0.178
CDF049	0.477	30.55	0.5300	0.0231	0.777	0.2874	3.626	0.0402	1.190	0.1272	1.130
CDF050	0.187	14.08	0.3974	0.0162	0.754	0.2411	3.623	0.0149	0.762	0.0567	0.442
CDF051	0.192	34.15	0.2418	0.0097	0.394	0.1535	2.325	0.0050	0.481	0.0493	0.549
CDF052	0.214	79.38	1.6269	0.0748	3.128	1.1892	19.238	0.0000	3.409	0.0520	0.236
CDF053	0.303	20.05	0.2795	0.0113	0.431	0.1367	1.702	0.0167	0.571	0.0956	1.172
CDF054	0.000	11.69	0.2246	0.0083	0.268	0.1096	1.479	0.0165	0.452	0.1019	1.047
CDF055	0.000	64.56	1.3522	0.0575	2.340	0.9261	14.723	0.0000	2.683	0.0140	0.134
CDF056	0.214	10.83	0.3947	0.0101	0.534	0.1305	1.483	0.0154	0.576	0.0811	0.840
CDF057	0.159	15.17	0.7987	0.0113	1.055	0.2362	1.165	0.0399	0.913	0.0325	0.696
CDF058	0.111	9.68	0.7334	0.0110	0.708	0.1599	1.304	0.0328	1.136	0.0599	0.960
CDF059	0.197	15.06	0.5743	0.0082	0.542	0.1349	1.379	0.0135	0.546	0.0164	0.271
CDF060	0.332	26.18	0.5683	0.0071	0.441	0.0958	1.147	0.0100	0.369	0.0281	1.266
CDF061	0.000	22.12	0.2422	0.0088	0.323	0.1166	1.542	0.0131	0.454	0.0330	0.717
CDF062	0.000	15.37	0.1977	0.0071	0.403	0.1152	1.668	0.0054	0.413	0.0369	0.701
CDF063	0.000	19.32	0.1883	0.0081	0.252	0.1025	1.479	0.0037	0.345	0.0420	0.702
CDF064	0.000	32.03	0.3340	0.0094	0.487	0.1578	2.223	0.0049	0.494	0.0127	0.282
CDF065	0.320	38.97	0.2959	0.0083	0.230	0.1029	1.274	0.0115	0.418	0.0210	0.741
CDF066	0.000	11.03	0.1996	0.0073	0.298	0.0969	1.316	0.0090	0.291	0.0220	0.727
CDF067	0.206	27.38	0.8075	0.0295	1.250	0.5237	8.033	0.0000	1.508	0.0130	0.865
CDF068	0.000	63.12	1.2370	0.0446	2.043	0.8164	12.348	0.0000	2.203	0.0122	0.325
CDF069	0.205	42.93	0.8327	0.0254	1.260	0.4656	6.840	0.0065	1.277	0.0212	0.262
CDF070	0.459	24.50	0.5807	0.0204	0.789	0.3634	5.627	0.0000	1.050	0.0217	0.365
CDF071	0.184	8.75	0.2384	0.0083	0.412	0.1227	1.649	0.0081	0.457	0.0377	1.006
CDF072	0.306	101.98	0.8906	0.0247	1.146	0.4418	6.564	0.0105	1.482	0.0239	0.492
CDF073	0.352	24.63	0.7087	0.0081	0.488	0.1111	0.896	0.0118	0.688	0.0977	0.669
CDF074	0.362	98.07	0.1961	0.0056	0.000	0.0751	0.760	0.0126	0.366	0.0286	0.677
CDF075	0.000	65.20	0.9440	0.0000	2.655	0.7365	9.049	0.0000	2.390	0.0111	0.400
CDF076	0.000	105.36	1.2629	0.0000	3.076	0.9392	11.503	0.0000	2.899	0.0185	0.331
CDF077	0.000	55.31	1.0712	0.0000	3.009	0.8123	9.993	0.0000	2.520	0.0149	0.633

Anid	As	Ba	La	Lu	Nd	Sm	U	Yb	Ce	Co	Cr
CDF078	0.000	55.20	0.6375	0.0064	0.781	0.0950	0.650	0.0251	1.119	0.0249	0.787
CDF079	0.000	38.56	0.4404	0.0000	0.788	0.2780	3.229	0.0000	0.915	0.0166	0.249
CDF080	0.000	31.11	0.2969	0.0000	0.408	0.0974	1.012	0.0115	0.469	0.0370	1.305
CDF081	0.000	47.38	0.7601	0.0000	1.677	0.5740	6.974	0.0000	1.692	0.0075	0.205
CDF082	0.371	28.55	0.3639	0.0076	0.289	0.0987	0.907	0.0160	0.584	0.1133	1.156
CDF083	0.000	23.22	0.2345	0.0099	0.000	0.1051	1.165	0.0000	0.486	0.0663	0.809
CDF084	0.000	32.76	0.2305	0.0067	0.000	0.0964	0.929	0.0092	0.368	0.0290	0.432
CDF085	0.000	31.88	1.4311	0.0000	1.555	0.3673	3.733	0.0271	2.269	0.0188	0.471
CDF086	0.000	28.36	0.1391	0.0000	0.000	0.0578	0.563	0.0073	0.233	0.0278	0.897
CDF087	0.000	15.61	0.1972	0.0000	0.000	0.0912	1.024	0.0000	0.371	0.0256	1.192
CDF088	0.212	43.92	0.7646	0.0000	1.488	0.4809	5.322	0.0000	1.493	0.0362	0.391
CDF089	0.400	39.29	2.5764	0.0147	1.914	0.3059	1.581	0.0622	1.959	0.0390	0.724
CDF090	0.000	50.84	0.6093	0.0000	1.324	0.4079	4.948	0.0000	1.261	0.0196	0.233
CDF091	0.000	23.79	0.2480	0.0000	0.000	0.1129	1.270	0.0000	0.437	0.0232	0.548
CDF092	0.000	59.19	0.6555	0.0000	0.974	0.3694	4.278	0.0000	1.185	0.0176	0.404
CDF093	0.000	71.53	0.9509	0.0000	1.587	0.5491	6.490	0.0000	1.791	0.0215	0.304
CDF094	0.000	48.09	0.5658	0.0000	1.091	0.2786	3.154	0.0000	0.966	0.0180	0.598
CDF095	0.000	28.53	0.7947	0.0115	0.660	0.0942	0.835	0.0251	0.614	0.0448	1.041
CDF096	0.000	63.25	0.4753	0.0000	0.742	0.2356	2.496	0.0070	0.926	0.0340	0.409
CDF097	0.000	69.35	1.2898	0.0000	2.875	0.7411	8.610	0.0114	2.336	0.0323	0.769
CDF098	0.000	50.32	0.5993	0.0000	1.043	0.3652	4.261	0.0000	1.127	0.0274	1.036
CDF099	0.000	18.02	0.7514	0.0090	0.972	0.1099	0.736	0.0223	0.706	0.0393	0.796
CDF100	0.000	24.85	0.5332	0.0000	0.990	0.2461	2.643	0.0080	1.006	0.0753	0.607
CDF101	0.000	57.38	1.1765	0.0000	2.129	0.7129	8.597	0.0000	2.128	0.0161	0.460
CDF102	0.000	29.31	0.6683	0.0000	1.301	0.3320	3.636	0.0000	1.092	0.0556	0.978
CDF103	1.261	26.24	4.0298	0.0530	4.608	0.8345	2.947	0.2657	4.021	0.5775	11.721
CDF104	0.341	63.88	1.1805	0.0000	1.614	0.6249	6.090	0.0274	1.716	0.1186	1.161
CDF105	0.066	63.45	0.8482	0.0000	1.228	0.5060	5.284	0.0099	1.359	0.0176	0.252
CDF106	0.000	5.88	3.7576	0.0044	2.156	0.0705	0.591	0.0088	7.004	0.0545	1.319
CDF107	0.945	30.98	2.0901	0.0286	2.466	0.5370	1.890	0.0955	1.695	0.1386	6.804
CDF108	0.150	52.96	1.3689	0.0000	1.981	0.8644	9.088	0.0000	2.064	0.0161	0.123

Table D-2 Principal Components Analysis Based on Edwards Formation Source Specimens.

Simultaneous R-Q Factor Analysis Based on Variance-Covariance Matrix

Eigenvalues and Percentage of Variance Explained:

Eigenvalue	%Variance	Cum. %Var.
0.8886	50.3112	50.3112
0.4228	23.9406	74.2518
0.1381	7.8183	82.0701
0.0874	4.9456	87.0157
0.0653	3.6945	90.7102
0.0437	2.4749	93.1851
0.0320	1.8118	94.9969
0.0225	1.2762	96.2731
0.0135	0.7655	97.0386
0.0108	0.6090	97.6476
0.0098	0.5574	98.2050
0.0071	0.4013	98.6063
0.0061	0.3434	98.9498
0.0046	0.2582	99.2079
0.0043	0.2458	99.4537
0.0032	0.1814	99.6351
0.0023	0.1327	99.7678
0.0017	0.0956	99.8634
0.0012	0.0692	99.9326
0.0007	0.0393	99.9718
0.0005	0.0282	100.0000

Table D-2 (Continued)

Eigenvectors (largest to smallest):

BA	-0.0026	-0.1727	0.0750	-0.0499	-0.3332	0.1145	-0.2339	-0.5745	0.1785	-0.4298	0.1422	0.1921	-0.1739	0.0599	-0.2150	-0.1573	-0.2114	0.0439	0.1648	-0.0167	0.0228
LA	0.0003	-0.4614	0.1993	0.0903	-0.0361	0.1574	0.0635	0.0773	0.2057	-0.0998	-0.6646	0.1149	-0.2372	0.1231	0.2467	0.0046	0.2408	-0.0321	-0.0656	-0.0154	-0.0056
SM	-0.0556	-0.2867	0.1539	0.2655	-0.0102	-0.2734	-0.0170	0.1159	-0.0372	0.0637	-0.0230	0.2989	0.3184	0.1304	-0.6671	0.1628	0.0875	-0.1018	-0.1592	-0.0554	0.0181
U	-0.1003	-0.1099	0.1929	0.4718	0.0218	-0.1997	-0.0219	0.0448	-0.0880	0.0009	0.2313	-0.0761	-0.1431	0.1903	0.2177	0.0241	-0.0139	0.1549	0.2272	0.3887	0.5260
CE	-0.0050	-0.3453	0.1521	0.0816	-0.0163	-0.0461	0.0815	0.0482	-0.0286	0.1545	-0.1001	-0.0451	0.1927	-0.7011	0.0344	-0.2496	-0.4259	0.0163	0.1669	0.0352	0.0020
CO	0.2995	-0.0826	0.0653	0.0945	0.2737	0.2635	0.1331	-0.5541	-0.5098	0.1628	-0.1829	-0.2308	0.1318	0.1038	-0.1060	0.0260	0.0618	-0.0136	0.0141	0.0243	0.0565
CR	0.1878	0.0802	0.1013	-0.1481	0.0826	-0.0125	-0.0550	0.2208	-0.0047	0.1119	-0.2521	0.0583	0.0370	0.4790	-0.0592	-0.0124	-0.6469	0.3163	0.1727	-0.0535	-0.0462
EU	0.1289	-0.5914	0.0210	-0.5006	-0.1631	-0.0197	0.2901	0.1219	-0.0987	0.0575	0.4108	-0.1424	0.0104	0.1865	0.0678	0.0811	0.0718	0.0546	-0.0016	0.0171	0.0028
FE	0.3716	-0.0180	-0.0882	-0.1060	-0.1782	-0.4668	-0.3414	-0.1876	-0.0163	0.5145	-0.0766	0.1875	-0.2907	-0.0936	0.0629	0.0305	0.1554	0.0547	0.0637	0.0445	-0.0613
HF	0.2669	0.0397	0.2426	0.0631	-0.1022	0.1208	-0.0978	-0.0535	0.0153	-0.0302	0.1410	0.1666	0.0465	-0.1017	0.2872	0.3940	-0.3046	-0.1196	-0.6235	-0.0469	0.1726
RB	0.1675	0.0601	0.2223	0.1448	-0.3401	0.2043	-0.1600	0.1064	0.3392	0.2300	0.0099	-0.6645	-0.0373	0.0502	-0.2725	-0.0575	0.0399	-0.0704	-0.0733	0.0207	-0.0099
SB	0.0982	-0.0827	0.0522	-0.1585	0.0077	-0.2952	-0.5435	0.1676	-0.3326	-0.4692	-0.1545	-0.3097	0.2363	-0.0043	0.1131	-0.0207	0.0549	-0.1443	0.0009	0.0342	-0.0182
SC	0.2759	-0.0006	0.1399	-0.0079	0.3471	0.0379	0.0309	0.1794	-0.0337	-0.1149	0.1520	0.1124	-0.3853	0.0112	-0.1842	-0.3914	-0.0654	-0.2874	-0.1996	0.4309	-0.2258
SR	0.2928	0.2578	0.0073	0.1312	-0.4933	-0.3065	0.5681	0.0432	-0.2062	-0.2892	-0.1731	-0.0342	-0.0642	-0.0344	-0.0299	-0.0283	-0.0182	-0.0236	0.0132	0.0194	-0.0543
TA	0.3199	0.0808	0.2322	0.0045	0.0700	0.2636	-0.0581	0.1668	0.0521	-0.1637	0.0849	0.1450	0.0283	-0.2391	-0.0843	0.5027	0.1953	0.1992	0.4487	0.1791	-0.2118
TH	0.2955	0.0671	0.1839	-0.0269	0.1425	0.0690	-0.0296	0.1953	-0.0566	-0.0938	0.1121	0.0951	-0.1445	-0.1129	-0.0982	-0.3176	0.2055	0.1903	0.0210	-0.6067	0.4300
ZN	0.3219	-0.0457	-0.0767	0.0395	0.4051	-0.3698	0.1857	-0.2376	0.5919	-0.1718	0.0310	-0.1613	0.2688	0.0417	0.1079	0.0164	0.0121	-0.0010	0.0224	-0.0397	0.0106
ZR	-0.0737	-0.1231	0.2190	0.4269	0.0484	-0.1170	-0.0284	-0.0338	-0.1283	0.0097	0.2712	-0.0774	-0.1232	0.1302	0.2442	-0.0203	-0.0369	0.0329	0.0481	-0.4171	-0.6036
AL	0.0723	0.0486	0.0897	0.0470	-0.1551	0.0987	-0.0650	-0.0229	0.0171	0.0150	0.0460	0.1540	0.4168	0.0444	0.1374	-0.3954	0.2492	0.5668	-0.2815	0.2668	-0.1805
MN	0.3205	-0.2548	-0.7466	0.3769	-0.0794	0.2335	-0.1166	0.1937	-0.0221	-0.0827	0.0532	0.0176	-0.0010	0.0124	-0.0065	0.0010	-0.0870	0.0397	-0.0179	-0.0289	0.0028
NA	0.1723	0.0803	0.1009	0.0290	-0.1862	0.1723	-0.0266	0.0491	0.0528	0.1649	0.0788	0.2746	0.3955	0.2187	0.2546	-0.2324	0.0545	-0.5772	0.3336	-0.0279	0.0499

Scaled Factor Loading Matrix (largest to smallest component):

BA	-0.0025	-0.1123	0.0279	-0.0147	-0.0851	0.0239	-0.0418	-0.0863	0.0208	-0.0446	0.0141	0.0162	-0.0135	0.0040	-0.0142	-0.0089	-0.0102	0.0018	0.0058	-0.0004	0.0005
LA	0.0002	-0.3000	0.0741	0.0267	-0.0092	0.0329	0.0114	0.0116	0.0239	-0.0104	-0.0659	0.0097	-0.0185	0.0083	0.0163	0.0003	0.0117	-0.0013	-0.0023	-0.0004	-0.0001
SM	-0.0524	-0.1864	0.0572	0.0785	-0.0026	-0.0572	-0.0030	0.0174	-0.0043	0.0066	-0.0023	0.0252	0.0248	0.0088	-0.0440	0.0092	0.0042	-0.0042	-0.0056	-0.0015	0.0004
U	-0.0945	-0.0715	0.0717	0.1394	0.0056	-0.0417	-0.0039	0.0067	-0.0102	0.0001	0.0229	-0.0064	-0.0111	0.0129	0.0143	0.0014	-0.0007	0.0064	0.0079	0.0102	0.0117
CE	-0.0047	-0.2245	0.0565	0.0241	-0.0042	-0.0096	0.0146	0.0072	-0.0033	0.0160	-0.0099	-0.0038	0.0150	-0.0473	0.0023	-0.0141	-0.0206	0.0007	0.0058	0.0009	0.0000
CO	0.2824	-0.0537	0.0243	0.0279	0.0699	0.0551	0.0238	-0.0832	-0.0593	0.0169	-0.0181	-0.0194	0.0103	0.0070	-0.0070	0.0015	0.0030	-0.0006	0.0005	0.0006	0.0013
CR	0.1771	0.0521	0.0376	-0.0438	0.0211	-0.0026	-0.0098	0.0332	-0.0006	0.0116	-0.0250	0.0049	0.0029	0.0323	-0.0039	-0.0007	-0.0313	0.0130	0.0060	-0.0014	-0.0010
EU	0.1215	-0.3846	0.0078	-0.1479	-0.0417	-0.0041	0.0519	0.0183	-0.0115	0.0060	0.0408	-0.0120	0.0008	0.0126	0.0045	0.0046	0.0035	0.0022	-0.0001	0.0005	0.0001
FE	0.3503	-0.0117	-0.0328	-0.0313	-0.0455	-0.0976	-0.0611	-0.0282	-0.0019	0.0534	-0.0076	0.0158	-0.0226	-0.0063	0.0041	0.0017	0.0075	0.0022	0.0022	0.0012	-0.0014
HF	0.2516	0.0258	0.0902	0.0187	-0.0261	0.0253	-0.0175	-0.0080	0.0018	-0.0031	0.0140	0.0140	0.0036	-0.0069	0.0189	0.0223	-0.0147	-0.0049	-0.0218	-0.0012	0.0039
RB	0.1579	0.0391	0.0826	0.0428	-0.0869	0.0427	-0.0286	0.0160	0.0394	0.0239	0.0010	-0.0560	-0.0029	0.0034	-0.0180	-0.0033	0.0019	-0.0029	-0.0026	0.0005	-0.0002
SB	0.0925	-0.0538	0.0194	-0.0468	0.0020	-0.0617	-0.0972	0.0252	-0.0387	-0.0487	-0.0153	-0.0261	0.0184	-0.0003	0.0075	-0.0012	0.0027	-0.0059	0.0000	0.0009	-0.0004
SC	0.2601	-0.0004	0.0520	-0.0023	0.0887	0.0079	0.0055	0.0269	-0.0039	-0.0119	0.0151	0.0095	-0.0300	0.0008	-0.0121	-0.0222	-0.0032	-0.0118	-0.0070	0.0113	-0.0050
SR	0.2760	0.1676	0.0027	0.0388	-0.1260	-0.0641	0.1016	0.0065	-0.0240	-0.0300	-0.0172	-0.0029	-0.0050	-0.0023	-0.0020	-0.0016	-0.0009	-0.0010	0.0005	0.0005	-0.0012
TA	0.3016	0.0525	0.0863	0.0013	0.0179	0.0551	-0.0104	0.0250	0.0061	-0.0170	0.0084	0.0122	0.0022	-0.0161	-0.0056	0.0284	0.0095	0.0082	0.0157	0.0047	-0.0047
TH	0.2786	0.0437	0.0683	-0.0079	0.0364	0.0144	-0.0053	0.0293	-0.0066	-0.0097	0.0111	0.0080	-0.0113	-0.0076	-0.0065	-0.0180	0.0099	0.0078	0.0007	-0.0160	0.0096
ZN	0.3034	-0.0297	-0.0285	0.0117	0.1035	-0.0773	0.0332	-0.0357	0.0688	-0.0178	0.0031	-0.0136	0.0209	0.0028	0.0071	0.0009	0.0006	-0.0000	0.0008	-0.0010	0.0002
ZR	-0.0694	-0.0800	0.0814	0.1262	0.0124	-0.0245	-0.0051	-0.0051	-0.0149	0.0010	0.0269	-0.0065	-0.0096	0.0088	0.0161	-0.0011	-0.0018	0.0014	0.0017	-0.0110	-0.0135
AL	0.0682	0.0316	0.0333	0.0139	-0.0396	0.0206	-0.0116	-0.0034	0.0020	0.0016	0.0046	0.0130	0.0325	0.0030	0.0091	-0.0224	0.0121	0.0233	-0.0098	0.0070	-0.0040
MN	0.3021	-0.1657	-0.2774	0.1114	-0.0203	0.0488	-0.0209	0.0291	-0.0026	-0.0086	0.0053	0.0015	-0.0001	0.0008	-0.0004	0.0001	-0.0042	0.0016	-0.0006	-0.0008	0.0001
NA	0.1625	0.0522	0.0375	0.0086	-0.0476	0.0360	-0.0048	0.0074	0.0061	0.0171	0.0078	0.0231	0.0308	0.0148	0.0168	-0.0132	0.0026	-0.0237	0.0117	-0.0007	0.0011

Table D-3 Mahalanobis Distance Calculation and Posterior Classification for Two or More Groups.

Groups are:

1.000	PC-F1
2.000	PC-F2
3.000	PC-F3
4.000	PC-F4
5.000	PC-F5
6.000	PC-F6

Variables used are: PC01 PC02 PC03 PC04 PC05

Probabilities are jackknifed for specimens included in each group.

	Probabilities:							
ID. NO.	PC-F1	PC-F2	PC-F3	PC-F4	PC-F5	PC-F6	From:	Into:
EFC001	95.493	1.118	3.516	0.000	0.005	0.215	1	1
EFC002	80.620	0.406	0.542	0.000	0.001	0.045	1	1
EFC004	23.744	9.938	2.101	0.000	0.004	0.042	1	1
EFC005	37.125	9.569	0.939	0.000	0.011	0.385	1	1
EFC006	6.645	0.682	0.465	0.000	0.008	0.099	1	1
EFC007	77.211	1.225	1.516	0.000	0.006	0.101	1	1
EFC008	91.761	1.943	2.031	0.000	0.005	0.083	1	1
EFC009	86.904	2.630	0.648	0.000	0.002	0.058	1	1
EFC013	9.302	0.413	0.350	0.000	0.001	0.166	1	1
EFC014	7.985	4.231	8.851	0.000	0.015	1.142	1	3
EFC015	42.396	5.985	2.951	0.000	0.005	0.051	1	1
EFC016	0.241	0.021	1.450	0.000	0.008	0.442	1	3
EFC017	67.596	1.706	4.896	0.000	0.012	0.696	1	1
EFC019	72.462	0.176	1.642	0.000	0.003	0.200	1	1
EFC020	99.610	1.831	2.756	0.000	0.006	0.166	1	1
EFC021	39.741	0.487	0.813	0.000	0.001	0.039	1	1

				Probabilities:				
ID. NO.	PC-F1	PC-F2	PC-F3	PC-F4	PC-F5	PC-F6	From:	Into:
EFC022	0.028	53.300	1.427	0.000	0.004	0.039	2	2
EFC023	0.206	80.134	0.699	0.000	0.022	0.515	2	2
EFC024	1.391	50.206	1.321	0.000	0.029	0.604	2	2
EFC026	0.504	88.470	4.026	0.000	0.037	2.339	2	2
EFC027	6.399	54.993	4.035	0.000	0.006	0.268	2	2
EFC028	5.192	30.345	1.375	0.000	0.012	0.828	2	2
EFC029	0.075	68.754	3.141	0.000	0.006	0.087	2	2
EFC030	0.058	72.015	0.729	0.000	0.010	0.149	2	2
EFC031	0.188	43.563	1.064	0.000	0.037	1.888	2	2
EFC032	0.057	9.954	1.513	0.000	0.066	6.157	2	2

ID. NO.	PC-F1	PC-F2	PC-F3	PC-F4	PC-F5	PC-F6	From:	Into:
EFC033	0.236	53.971	2.822	0.000	0.008	0.674	2	2
EFC034	0.262	37.174	32.067	0.000	0.001	0.873	2	2
EFC036	0.038	31.794	7.624	0.000	0.006	0.275	2	2
EFC037	1.415	53.794	41.742	0.000	0.003	0.485	2	2
EFC038	0.020	70.584	1.410	0.000	0.001	0.042	2	2
EFC039	1.498	41.816	4.550	0.000	0.003	0.071	2	2
EFC040	1.656	48.356	36.589	0.000	0.001	0.090	2	2
EFC041	0.103	5.264	14.065	0.000	0.002	0.086	2	3
EFC042	1.000	24.818	1.429	0.000	0.008	0.342	2	2

Probabilities:

ID. NO.	PC-F1	PC-F2	PC-F3	PC-F4	PC-F5	PC-F6	From:	Into:
EFC043	0.000	0.000	96.101	0.018	0.190	0.000	3	3
EFC044	0.000	0.000	7.938	0.004	0.003	0.009	3	3
EFC045	0.000	0.000	80.934	0.033	0.020	0.029	3	3
EFC046	0.000	0.000	32.728	0.002	0.033	0.044	3	3
EFC047	0.000	0.000	92.412	0.096	0.043	0.001	3	3
EFC048	0.000	0.000	51.069	0.166	0.033	0.003	3	3
EFC049	0.000	0.000	79.411	0.005	0.106	0.027	3	3
EFC051	0.000	0.000	57.314	0.006	1.578	0.000	3	3
EFC052	0.000	0.000	58.009	0.007	0.223	0.085	3	3
EFC053	0.000	0.000	38.315	0.000	1.705	0.000	3	3
EFC054	0.000	0.000	82.575	0.048	0.015	0.000	3	3
EFC055	0.000	0.000	45.361	0.109	0.021	0.001	3	3
EFC056	0.353	0.003	33.924	0.000	0.018	0.747	3	3
EFC057	0.000	0.000	35.830	0.177	0.007	0.004	3	3
EFC060	0.000	0.000	6.554	0.001	0.028	0.000	3	3
EFC061	0.000	0.000	7.186	0.020	0.012	0.016	3	3
EFC062	0.000	0.000	35.445	0.002	0.265	0.000	3	3

Probabilities:

ID. NO.	PC-F1	PC-F2	PC-F3	PC-F4	PC-F5	PC-F6	From:	Into:
EFC063	0.000	0.000	0.000	58.587	0.000	15.535	4	4
EFC064	0.000	0.000	0.000	82.860	0.000	1.808	4	4
EFC065	0.000	0.015	0.000	11.019	0.000	9.088	4	4
EFC066	0.000	0.000	0.001	11.076	0.000	0.633	4	4
EFC067	0.000	0.000	0.000	74.395	0.000	7.739	4	4
EFC068	0.000	0.000	0.000	62.967	0.000	0.066	4	4
EFC069	0.000	0.002	0.000	88.978	0.000	0.077	4	4
EFC071	0.000	0.000	0.000	20.592	0.000	0.145	4	4
EFC072	0.000	0.000	0.004	51.899	0.000	0.531	4	4
EFC074	0.000	0.000	0.001	69.092	0.000	11.760	4	4

ID. NO.	PC-F1	PC-F2	PC-F3	PC-F4	PC-F5	PC-F6	From:	Into:
EFC075	0.000	0.002	0.000	35.940	0.000	0.225	4	4
EFC076	0.000	0.000	0.000	73.129	0.000	1.393	4	4
EFC077	0.000	0.000	0.002	90.279	0.000	4.811	4	4
EFC078	0.000	0.002	0.003	7.341	0.000	0.001	4	4
EFC079	0.000	0.000	0.000	63.090	0.000	0.694	4	4
EFC080	0.000	0.000	0.000	28.759	0.000	0.037	4	4
EFC081	0.000	0.000	0.014	8.859	0.000	0.114	4	4
EFC082	0.000	0.000	0.000	62.489	0.000	0.937	4	4

Probabilities:

ID. NO.	PC-F1	PC-F2	PC-F3	PC-F4	PC-F5	PC-F6	From:	Into:
EFC083	0.000	0.000	0.000	1.204	31.809	0.129	5	5
EFC084	0.000	0.000	0.000	2.236	88.756	0.165	5	5
EFC085	0.000	0.000	0.002	4.547	84.559	0.003	5	5
EFC086	0.000	0.000	0.000	3.852	72.537	0.069	5	5
EFC087	0.000	0.000	0.001	1.217	3.410	0.017	5	5
EFC088	0.000	0.000	0.002	6.590	10.899	0.029	5	5
EFC089	0.000	0.000	0.000	2.086	47.082	0.003	5	5
EFC090	0.000	0.000	0.001	0.164	70.729	0.134	5	5
EFC091	0.000	0.000	0.000	4.189	22.752	0.007	5	5
EFC092	0.000	0.000	0.002	1.115	51.663	0.000	5	5
EFC093	0.000	0.000	0.005	1.109	60.313	0.161	5	5
EFC094	0.000	0.000	0.000	0.816	91.723	0.166	5	5
EFC096	0.000	0.000	0.002	3.416	61.084	0.001	5	5
EFC097	0.000	0.000	0.001	1.006	62.947	0.016	5	5
EFC098	0.000	0.000	0.000	0.147	53.744	0.000	5	5
EFC099	0.000	0.000	0.024	0.117	53.223	0.000	5	5
EFC100	0.000	0.000	0.000	0.892	21.915	0.002	5	5
EFC101	0.000	0.000	0.001	0.947	81.953	0.052	5	5
EFC102	0.000	0.000	0.027	0.977	26.984	0.000	5	5
EFC095	0.000	0.000	0.002	0.002	4.998	0.000	5	5

Probabilities:

ID. NO.	PC-F1	PC-F2	PC-F3	PC-F4	PC-F5	PC-F6	From:	Into:
EFC103	0.000	0.000	0.000	2.869	0.078	61.779	6	6
EFC104	0.000	0.272	0.001	0.151	0.025	52.846	6	6
EFC105	0.000	0.000	0.000	1.810	0.013	8.004	6	6
EFC106	0.000	0.007	0.000	1.744	1.066	3.467	6	6
EFC107	0.000	0.059	0.011	0.214	0.009	80.567	6	6
EFC108	0.000	0.001	0.043	0.895	0.002	49.328	6	6
EFC110	0.000	0.004	0.000	8.172	0.018	65.852	6	6
EFC111	0.000	0.009	0.000	15.518	0.002	61.482	6	6

ID. NO.	PC-F1	PC-F2	PC-F3	PC-F4	PC-F5	PC-F6	From:	Into:
EFC112	0.000	0.000	0.001	3.955	0.121	74.539	6	6
EFC113	0.004	0.012	0.160	0.008	0.435	76.070	6	6
EFC114	0.023	0.704	0.403	0.001	0.386	16.257	6	6
EFC115	0.001	0.001	0.242	0.026	0.050	80.417	6	6
EFC116	0.000	0.001	0.001	2.178	0.270	85.612	6	6
EFC117	0.000	0.018	0.002	4.174	0.002	20.491	6	6
EFC118	0.000	0.002	0.019	0.590	0.195	37.103	6	6
EFC119	0.000	0.000	0.009	0.133	0.036	31.547	6	6
EFC121	0.002	0.070	0.177	0.050	0.070	46.782	6	6

Summary of Classification Success: Classified Into Group:

From Group:	PC-F1	PC-F2	PC-F3	PC-F4	PC-F5	PC-F6	Total
PC-F1	14	0	2	0	0	0	16
PC-F2	0	18	1	0	0	0	19
PC-F3	0	0	17	0	0	0	17
PC-F4	0	0	0	18	0	0	18
PC-F5	0	0	0	0	20	0	20
PC-F6	0	0	0	0	0	17	17
Total	14	18	20	18	20	17	107